

Analysis and Design of Developable Surfaces for Shipbuilding

by

Julie Steele Chalfant

B.S., Mechanical Engineering
United States Naval Academy, 1988

Submitted to the Department of Ocean Engineering
and the Department of Mechanical Engineering
in partial fulfillment of the requirements for the degrees of
Master of Science in Naval Architecture and Marine Engineering
and

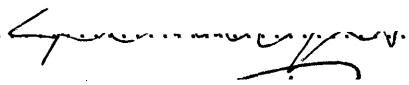
Master of Science in Mechanical Engineering

at the

MASSACHUSETTS INSTITUTE OF TECHNOLOGY

June 1997

© Massachusetts Institute of Technology 1997. All rights reserved.

Author..........
Department of Ocean Engineering
May 9, 1997

Certified by
Nicholas M. Patrikalakis
Professor of Ocean Engineering
Thesis Co-Supervisor

Certified by
Takashi Maekawa
Lecturer and Research Scientist
Thesis Co-Supervisor

Certified by
David C. Gossard
Professor of Mechanical Engineering
Thesis Reader

Accepted by.....
J. Kim Vandiver
Chairman, Departmental Committee on Graduate Students
Department of Ocean Engineering

Accepted by.....
Ain Sonin
Chairman, Departmental Committee on Graduate Students
Department of Mechanical Engineering

MASSACHUSETTS INSTITUTE OF TECHNOLOGY

JUL 15 1997 ENG.

1

1

Analysis and Design of Developable Surfaces for Shipbuilding

by
Julie Steele Chalfant

Submitted to the Department of Ocean Engineering
and the Department of Mechanical Engineering
on May 9, 1997, in partial fulfillment of the
requirements for the degrees of
Master of Science in Naval Architecture and Marine Engineering
and
Master of Science in Mechanical Engineering

Abstract

A developable surface can be formed by bending or rolling a planar surface without stretching or tearing; in other words, it can be developed or unrolled isometrically onto a plane. Developable surfaces are widely used in manufacturing with materials that are not amenable to stretching. A ship hull design entirely composed of developable surfaces would greatly reduce production costs of that hull.

This thesis describes a new, user-friendly method of designing developable surfaces with a B-spline representation. First, it expands the work of Aumann in designing developable B-spline strip surfaces whose directrices lie on parallel planes. The computer program developed can assist in designing surfaces from curves of any degree with any number of segments, and includes a test for regularity. Second, a new method is developed which permits the design of developable surfaces with general three-dimensional space curves as directrices. The computer program permits design of degree (3-1) B-spline developable surfaces with two patches using a minimization process. The basis is provided to extend this to surfaces with more patches and higher degrees. A test is provided to ensure that the minimization process results in a developable or nearly developable surface. This method is extended to include special interesting cases such as triangular degenerate patches and surfaces with a planar resulting directrix.

This thesis also treats common differential geometry properties such as lines of curvature and geodesics that are useful in the design and manufacturing process. Lines of curvature are vital in the forming process, since the planar shape must be placed so the rollers are parallel to the lines of zero curvature. As an inflection line greatly affects the forming process, a method is described to determine the inflection line in advance; several properties of developable surfaces related to inflection lines are also described.

Straight lines on a plane map to geodesics on a developable surface. This fact is of assistance in many aspects of the use of developable surfaces, including layout and quality control. A method is described to calculate geodesics on a developable surface as an initial value problem instead of the more complicated boundary value problem.

Engineering examples are provided for each topic, and a small boat hull is designed using the methods described. In addition, recommendations for further research are made.

Thesis Co-Supervisor: Nicholas M. Patrikalakis, Professor of Ocean Engineering

Thesis Co-Supervisor: Takashi Maekawa, Lecturer and Research Scientist

Thesis Reader: David C. Gossard, Professor of Mechanical Engineering

Acknowledgements

I would like to express my sincere appreciation for the guidance provided by Dr. Takashi Maekawa and Prof. N. M. Patrikalakis. I would additionally like to thank Prof. D. C. Gosard for his assistance, Mr. Stephen Abrams and Mr. Fred Baker for their assistance with computer work, Dr. Xiuzi Ye for his feedback, and the members of the Design Laboratory including Dr. Wonjoon Cho, Mr. Todd Jackson, Mr. Guoling Shen and Mr. Guoxin Yu for their support.

Special thanks to LT Allan Andrew, LT Kurt Crake, LT Tom Laverghetta, LT Chris Levesque, LT Casey Moton, and LT Tom Trapp for their camaraderie and support, and to LCDR Mark Welsh and CAPT Alan Brown.

This work was funded by the United States Navy.

Contents

Abstract	3
Acknowledgements	4
Contents	5
List of Figures	7
List of Tables	9
1 Introduction	11
1.1 Background and Motivation	11
1.2 Research Objective	12
1.3 Thesis Organization	12
2 Review of Curves and Surfaces	13
2.1 Introduction	13
2.2 Basic Theory of Curves	13
2.3 Basic Theory of Surfaces	18
3 Curve and Surface Representation	25
3.1 Introduction	25
3.2 Bézier Curves and Surfaces	25
3.3 B-Spline Curves and Surfaces	29
4 Review of Differential Geometry Properties of Developable Surfaces	37
4.1 Introduction	37
4.2 Ruled and Developable Surfaces	37
5 Design With B-Spline Developable Surfaces	47
5.1 Introduction and Literature Review	47
5.1.1 Developable Bézier Strips	47
5.1.2 Duality Between Points and Planes	48
5.1.3 Nonlinear Representation	48
5.1.4 Development	48
5.2 B-Spline Developable Surfaces with Directrices in Parallel Planes	49
5.3 Developable Surfaces with 3D Directrices	54
5.3.1 Developable $(n, 1)$ Bézier Surfaces	54
5.3.2 B-Spline Developable Surfaces	59

5.3.3	Accuracy of Resulting Developable Surfaces	62
5.3.4	Developable Surfaces Constrained by Planes	63
5.3.5	Degenerate Developable Surfaces	64
5.4	Development of a Developable Surface onto a Plane	66
5.5	Examples	68
5.5.1	Example of a Developable B-Spline Strip Surface	68
5.5.2	Example of a Developable B-Spline Surface with 3D Directrices	69
6	Geodesics on Developable Surfaces	73
6.1	Introduction	73
6.2	Formulation	73
6.3	Examples	77
7	Lines of Curvature on Developable Surfaces	81
7.1	Introduction	81
7.2	Inflection Line	81
8	Engineering Example	89
9	Conclusions and Recommendations	95
9.1	Conclusions	95
9.2	Future Work	95
	Contents	97

List of Figures

2-1	Tangent Vector	14
2-2	Osculating Plane	15
2-3	Space Curve	17
2-4	Curvature Vectors	20
3-1	A Cubic Bézier Curve with Control Polygon	26
3-2	The deCasteljau Algorithm	27
3-3	A Bézier Surface with Control Net	28
3-4	Continuity Conditions	29
3-5	A Cubic B-spline Curve Segment with Control Polygon	30
3-6	Convex Hull Property for a Cubic B-Spline Curve	31
3-7	The deBoor Algorithm	32
3-8	Knot Removal	34
4-1	A Ruled Surface	38
4-2	A Developable Surface with Tangent Plane along a Ruling	38
4-3	An Envelope of a Family of Curves	40
4-4	Edge of Regression	41
4-5	A Surface with Folds and a Developable Surface	44
5-1	A Developable Surface	48
5-2	Design of Developable B-Spline Strip Surface	50
5-3	Effect of Simple Bounds on Developable Surfaces	57
5-4	Design of Developable B-Spline Surfaces	61
5-5	Planar Constraint on Developable B-Spline Surface Design	64
5-6	Triangular Degenerate Cubic Bézier Patch	66
5-7	Development of B-Spline Developable Surface	69
5-8	Automobile Windshield, a Developable Degree (4-1) B-spline Strip Surface	70
5-9	Ship Stack, A Developable Degree (3,1) B-Spline Surface with $ K < 2.19 \times 10^{-7}$	71
6-1	Geodesics on a Closed Surface	74
6-2	Geodesic on a Degree (3,1) Developable Surface	75
6-3	Geodesic on a Degree (4,1) Developable Surface	78
6-4	Geodesic on a Degree (4,1) Handkerchief-like Developable Surface	79
7-1	Developable surface and its control polyhedron with inflection line.	86
7-2	(a) Lines of curvature of developable surface with inflection. (b) Magnification near inflection line.	86

7-3	(a) Lines of curvature on perturbed surface $\zeta = 0.02$. (b) Magnification near $u=0.57$	87
7-4	(a) Lines of curvature on perturbed surface $\zeta = 0.08$ (b) Magnification near $u=0.57$	87
8-1	Planing Boat Terminology	89
8-2	Boat Composed of Developable Degree (3-1) B-Spline Surfaces	91
8-3	Boat Bottom View	91
8-4	Boat Surfaces Developed onto a Plane	92
8-5	Geodesics on the Forward Side Section	93
8-6	Lines of Curvature on Boat Surfaces (Solid Lines are Maximum Curvature Lines, Dashed Lines are Minimum Curvature Lines)	94

List of Tables

6.1	Control Points for a Degree (3,1) Developable Surface	77
6.2	Control Points for a Degree (4,1) Developable Surface	78
6.3	Control Points for a Degree (4,1) Handkerchief-like Developable Surface . .	79
7.1	Control Points for a Degree (3,1) Developable Surface	85
8.1	Target Curve Data	90
8.2	Developable Surface Data, Starboard Side	90

Chapter 1

Introduction

1.1 Background and Motivation

A ruled surface is a curved surface which can be generated by the continuous motion of a straight line in space along a space curve called a directrix. This straight line is called a generator, or ruling, of the surface. Developable surfaces are a subset of ruled surfaces which have the same tangent plane at all points along the generator. A developable surface can be formed by bending or rolling a planar surface without stretching or tearing; in other words, it can be developed or unrolled isometrically onto a plane. Developable surfaces are also known as singly curved surfaces, since one of their principal curvatures is zero.

Developable surfaces are widely used in manufacturing with materials that are not amenable to stretching. Applications include the formation of ship hulls, ducts, shoes, clothing and automobile parts such as upholstery and body panels [14].

In shipbuilding, developable surfaces are shaped using only rollers or presses. Heat treatment is then used only to remove distortion induced by welding or other means. Doubly curved surfaces, on the other hand, must be heat treated after rolling to induce the additional curvature. The heat treatment is normally done by hand, by a skilled artisan with years of training to achieve the correct amount of bending. This is an extremely time consuming, labor intensive and thus expensive process.

According to Avondale/IHI Shipbuilding Technology Transfer data for a tanker, only 15.1% of the curved plates in a ship hull are singly curved, while 65.8% of the plates are doubly curved, requiring roller and heat treatment processes [28]. An intensive effort to increase the amount of developable surfaces in the hulls of merchant ships at Burmeister & Wain Shipyard [34] has resulted in a reported 20% reduction in manhours required to produce a hull. Designing a ship entirely of singly curved, or developable, surfaces would reduce construction costs even more.

Recently researchers in Computer Aided Geometric Design have been quite active in investigating the representation of developable surfaces in terms of Non-Uniform Rational B-Spline (NURBS) surfaces or a special case of NURBS called Bézier surfaces [1, 3, 14, 29]. NURBS curves and surface patches are the most popular representation method in CAD/CAM due to their generality, excellent properties and incorporation in international standards such as IGES (Initial Graphics Exchange Specification) and STEP (Standard for the Exchange of Product Model Data). Thus, it would be beneficial to design developable surfaces using a B-spline representation.

1.2 Research Objective

Recently, efforts have been underway to revitalize commercial shipbuilding in the United States. Several professors at MIT are involved with developing cost saving methods in ship fabrication to ensure that shipbuilding in the US will be competitive in the world market. This research is in support of one of those efforts.

The main goal of this research is to develop a user-friendly method of designing developable surfaces with a B-spline representation. The effort is then extended to address some common differential geometry properties that will be useful in the design and manufacturing process.

The ultimate goal is to provide a method to design a complete ship hull from developable surfaces and to generate cutting and bending information in a format that is user friendly for both the engineer and the worker. Although this thesis does not go that far, it takes a major step toward this goal.

1.3 Thesis Organization

In this thesis, Chapters 2 through 4 review basic differential geometry properties and introduce the concepts of developable surfaces. They also briefly review the Bézier and B-spline representations of curves and surfaces. The information introduced in these chapters will be used throughout the thesis.

Chapter 5 describes a new user friendly method for design of developable surfaces in B-spline representation. Section 5.1 reviews the current literature on developable surfaces. Section 5.2 describes the design of strip surfaces that are constrained between two parallel planes. Section 5.3 describes the design of surfaces with directrices that are space curves and treats special cases such as triangular degenerate patches and surfaces with a planar resultant curve. Section 5.4 describes the unrolling, or development, of the surfaces into a plane. Section 5.5 gives some engineering examples.

In Chapter 6, a geodesic on a developable surface is found as the solution to an initial value problem rather than a two point boundary value problem. The geodesics can be used in ship design for laying out butts and strakes, among other uses. In Chapter 7, the lines of curvature on a developable surface are analyzed and the line of inflection is defined. These concepts are required for the bending of steel plates into developable surfaces; the steel must enter the rolls in a direction parallel to the lines of zero curvature, and cannot be rolled past a line of inflection [33].

A small boat was designed using the methods described in this thesis. The boat is presented in Chapter 8 as a practical engineering example.

The thesis concludes with Chapter 9 which includes recommendations for further research.

Chapter 2

Review of Curves and Surfaces

2.1 Introduction

This chapter reviews the basic theory of curves and surfaces including such topics as the Serret-Frenet formulae, the first and second fundamental forms, curvatures and geodesic curves which will be used in derivations of many formulae in the later chapters. The information in this section follows the derivations in classical texts on differential geometry and geometric modeling such as those by Kreyszig [26], Struik [41] and Faux and Pratt [11].

2.2 Basic Theory of Curves

Throughout this thesis, curves are represented in a parametric manner, $\mathbf{r}(u)$, as a function of one parameter, u , that lies within a closed interval $u_1 \leq u \leq u_2$. The curve is a mapping from a one parameter interval to three-dimensional space

$$\mathbf{r}(u) = [x(u) \ y(u) \ z(u)]^T.$$

The points on a curve are regular as long as at least one of the first derivatives is not equal to zero. In other words, a point is singular if $dx/du = dy/du = dz/du = 0$. The curve can be reparameterized if u can be expressed as $u = f(u_1)$ as long as $du/du_1 \neq 0$.

Arc length is defined as the distance along a curve between parameter values u_0 and u , and can be represented as

$$s(u) = \int_{u_0}^u \sqrt{\dot{x}^2 + \dot{y}^2 + \dot{z}^2} \, du = \int_{u_0}^u \sqrt{\dot{\mathbf{r}} \cdot \dot{\mathbf{r}}} \, du. \quad (2.1)$$

In this thesis, derivatives with respect to the arc length s will be represented by a prime and derivatives with respect to u will be represented by a dot. Derivatives of arc length s with respect to parameter u and vice versa are

$$\begin{aligned} \dot{s} &= \frac{ds}{du} = \sqrt{\dot{\mathbf{r}} \cdot \dot{\mathbf{r}}} = |\dot{\mathbf{r}}| \\ \ddot{s} &= \frac{d\dot{s}}{du} = \frac{\dot{\mathbf{r}} \cdot \ddot{\mathbf{r}}}{\sqrt{\dot{\mathbf{r}} \cdot \dot{\mathbf{r}}}} \\ u' &= \frac{du}{ds} = \frac{1}{|\dot{\mathbf{r}}|} \end{aligned}$$

$$u'' = \frac{du'}{ds} = -\frac{\dot{\mathbf{r}} \cdot \ddot{\mathbf{r}}}{(\dot{\mathbf{r}} \cdot \dot{\mathbf{r}})^2}.$$

The unit *tangent vector* \mathbf{t} to a curve is defined by the unit vector that passes through two points in the curve, $\mathbf{r}(s)$ and $\mathbf{r}(s+h)$ (see Figure 2-1), as h approaches zero; i.e.

$$\begin{aligned} \mathbf{t} &= \lim_{h \rightarrow 0} \frac{\mathbf{r}(s+h) - \mathbf{r}(s)}{h} = \frac{d\mathbf{r}}{ds} = \mathbf{r}'(s) \\ &= \frac{d\mathbf{r}(u)}{du} \frac{du}{ds} = \frac{\dot{\mathbf{r}}(u)}{|\dot{\mathbf{r}}(u)|}. \end{aligned}$$

This final representation clearly shows that \mathbf{t} is a unit vector. The line passing through the point $\mathbf{r}(u_n)$ in the direction of $\mathbf{t}(u_n)$ is the tangent to the curve at u_n .

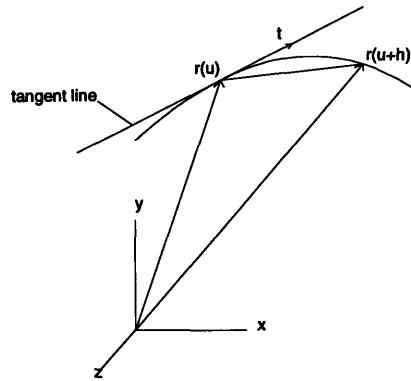


Figure 2-1: Tangent Vector

All vectors normal to $\mathbf{t}(u_n)$ at u_n lie in a plane called the *normal plane*. Much as the tangent is defined by two points that approach one another on a curve, the *osculating plane* is defined by three points that approach one another. In other words, the osculating plane is the plane in which the curve lies at a point on the curve. If the curve is planar, the entire curve lies in a single osculating plane, and the osculating plane is constant for the entire curve. To mathematically define the osculating plane following the derivation in Kreyszig [26, p.31], take three points at parameter values u , $u+h_1$ and $u+h_2$. The plane can be defined by the two linearly independent vectors $\mathbf{a}_i = \mathbf{r}(u+h_i) - \mathbf{r}(u)$, $i = 1, 2$ or linear combinations thereof. Let

$$\mathbf{v}^{(i)} = \frac{\mathbf{r}(u+h_i) - \mathbf{r}(u)}{h_i}$$

and

$$\mathbf{w} = \frac{2(\mathbf{v}^{(2)} - \mathbf{v}^{(1)})}{h_2 - h_1}.$$

The Taylor series expansion of $\mathbf{r}(u + h_i)$ is

$$\mathbf{r}(u + h_i) = \mathbf{r}(u) + h_i \dot{\mathbf{r}}(u) + \frac{h_i^2}{2} \ddot{\mathbf{r}}(u) + \mathbf{o}(h_i^2) \quad (2.2)$$

where $\mathbf{o}(h^n)$ is a vector of Landau symbols $\mathbf{o}(h^n)$ with the property that [41, p.3]

$$\lim_{h \rightarrow 0} \frac{\mathbf{o}(h^n)}{h^n} = \mathbf{0}.$$

Using (2.2), we obtain

$$\begin{aligned} \mathbf{v}^{(1)} &= \frac{\mathbf{r}(u + h_1) - \mathbf{r}(u)}{h_1} \\ &= \frac{\mathbf{r}(u) + h_1 \dot{\mathbf{r}}(u) + \frac{1}{2} h_1^2 \ddot{\mathbf{r}}(u) + \mathbf{o}(h_1^2) - \mathbf{r}(u)}{h_1} \\ &= \dot{\mathbf{r}}(u) + \frac{1}{2} h_1 \ddot{\mathbf{r}}(u) + \frac{\mathbf{o}(h_1^2)}{h_1} \end{aligned}$$

and

$$\begin{aligned} \mathbf{w} &= \frac{2(\mathbf{v}^{(2)} - \mathbf{v}^{(1)})}{h_2 - h_1} \\ &= \frac{2}{h_2 - h_1} \left[\left(\dot{\mathbf{r}}(u) + \frac{1}{2} h_2 \ddot{\mathbf{r}}(u) + \frac{\mathbf{o}(h_2^2)}{h_2} \right) - \left(\dot{\mathbf{r}}(u) + \frac{1}{2} h_1 \ddot{\mathbf{r}}(u) + \frac{\mathbf{o}(h_1^2)}{h_1} \right) \right] \\ &= \ddot{\mathbf{r}}(u) - \frac{2(h_1 \mathbf{o}(h_2^2) - h_2 \mathbf{o}(h_1^2))}{h_1 h_2 (h_2 - h_1)}. \end{aligned}$$

As $h_i \rightarrow 0$, $\mathbf{v}^{(1)} \rightarrow \dot{\mathbf{r}}(u)$ and $\mathbf{w} \rightarrow \ddot{\mathbf{r}}(u)$. Therefore, the osculating plane is defined by $\dot{\mathbf{r}}(u)$ and $\ddot{\mathbf{r}}(u)$. Note that $\mathbf{r}(u)$ must be at least twice continuously differentiable.

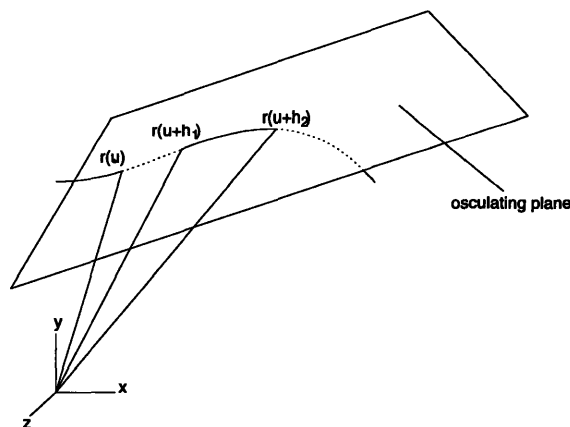


Figure 2-2: Osculating Plane

The *principal normal* is defined as the intersection of the osculating and normal planes. Using an arc length parameterization, we find that differentiating $\mathbf{t} \cdot \mathbf{t} = 1$ with respect to

s yields

$$\mathbf{t} \cdot \mathbf{t}' = 0,$$

so \mathbf{t}' is perpendicular to \mathbf{t} and lies in the normal plane. Since $\mathbf{t} = \mathbf{r}' = \dot{\mathbf{r}}u'$,

$$\mathbf{t}' = \dot{\mathbf{r}}u'' + \ddot{\mathbf{r}}(u')^2.$$

Thus \mathbf{t}' lies in the plane of $\dot{\mathbf{r}}$ and $\ddot{\mathbf{r}}$, and therefore in the osculating plane. Since \mathbf{t}' lies in both the osculating and normal planes, a unit vector in the direction of \mathbf{t}' is the *unit normal vector*

$$\mathbf{n} = \frac{\mathbf{t}'}{|\mathbf{t}'|}.$$

The magnitude of \mathbf{t}' is called the *curvature* and is represented as κ . The curvature vector \mathbf{k} is represented as

$$\mathbf{k} = \mathbf{t}' = \kappa \mathbf{n}. \quad (2.3)$$

A physical sense of the curvature can be found from the simple example of a line, which has a constant tangent vector, so \mathbf{t}' is zero. Therefore, $\kappa = |\mathbf{t}'| = 0$, and a line has zero curvature. Parameterized by u , \mathbf{k} and κ can be represented as [41, p.16]

$$\begin{aligned} \mathbf{k} &= \mathbf{t}' = \dot{\mathbf{r}}u'' + \ddot{\mathbf{r}}(u')^2 = \frac{(\dot{\mathbf{r}} \cdot \dot{\mathbf{r}})\ddot{\mathbf{r}} - (\dot{\mathbf{r}} \cdot \ddot{\mathbf{r}})\dot{\mathbf{r}}}{(\dot{\mathbf{r}} \cdot \dot{\mathbf{r}})^2} \\ \kappa^2 &= (\kappa \mathbf{n}) \cdot (\kappa \mathbf{n}) = \left[\frac{(\dot{\mathbf{r}} \cdot \dot{\mathbf{r}})\ddot{\mathbf{r}} - (\dot{\mathbf{r}} \cdot \ddot{\mathbf{r}})\dot{\mathbf{r}}}{(\dot{\mathbf{r}} \cdot \dot{\mathbf{r}})^2} \right] \cdot \left[\frac{(\dot{\mathbf{r}} \cdot \dot{\mathbf{r}})\ddot{\mathbf{r}} - (\dot{\mathbf{r}} \cdot \ddot{\mathbf{r}})\dot{\mathbf{r}}}{(\dot{\mathbf{r}} \cdot \dot{\mathbf{r}})^2} \right] = \frac{(\dot{\mathbf{r}} \times \ddot{\mathbf{r}}) \cdot (\dot{\mathbf{r}} \times \ddot{\mathbf{r}})}{(\dot{\mathbf{r}} \cdot \dot{\mathbf{r}})^3} \end{aligned}$$

where the Lagrange identity $(\mathbf{a} \times \mathbf{b}) \cdot (\mathbf{a} \times \mathbf{b}) = (\mathbf{a} \cdot \mathbf{a})(\mathbf{b} \cdot \mathbf{b}) - (\mathbf{a} \cdot \mathbf{b})^2$ is used.

The normal to the osculating plane is the binormal, which is defined as

$$\mathbf{b} = \mathbf{t} \times \mathbf{n}.$$

Since these three vectors are unit vectors that are mutually orthogonal, they satisfy the relations

$$\begin{array}{lll} \mathbf{b} \cdot \mathbf{b} = 1 & \mathbf{n} \cdot \mathbf{n} = 1 & \mathbf{t} \cdot \mathbf{t} = 1 \\ \mathbf{b} \cdot \mathbf{n} = 0 & \mathbf{n} \cdot \mathbf{t} = 0 & \mathbf{t} \cdot \mathbf{b} = 0. \end{array}$$

Differentiating $\mathbf{b} \cdot \mathbf{b} = 1$ and $\mathbf{b} \cdot \mathbf{t} = 0$ yields

$$\mathbf{b}' \cdot \mathbf{b} = 0$$

and

$$\mathbf{b}' \cdot \mathbf{t} = -\mathbf{b} \cdot \mathbf{t}' = -\mathbf{b} \cdot \kappa \mathbf{n} = -\kappa(\mathbf{b} \cdot \mathbf{n}) = 0.$$

Therefore, \mathbf{b}' is orthogonal to both \mathbf{b} and \mathbf{t} and must then be parallel to \mathbf{n} . Let

$$\mathbf{b}' = -\tau \mathbf{n}$$

where τ is the torsion of the curve. A physical sense of torsion can be found from the fact that a curve with zero torsion and nonzero curvature is a planar curve.

Finally, an equation for the derivative of the normal vector corresponding to the rate of change of the tangent plane [26, p.41] can be determined. Differentiating $\mathbf{n} \cdot \mathbf{n} = 1$ yields $\mathbf{n} \cdot \mathbf{n}' = 0$. Therefore, \mathbf{n}' is orthogonal to \mathbf{n} and must satisfy the relationship

$$\mathbf{n}' = \alpha \mathbf{t} + \beta \mathbf{b}. \quad (2.4)$$

Multiplying equation (2.4) by \mathbf{t} and \mathbf{b} respectively yields

$$\alpha = \mathbf{n}' \cdot \mathbf{t} \quad \text{and} \quad \beta = \mathbf{n}' \cdot \mathbf{b}.$$

Differentiating $\mathbf{n} \cdot \mathbf{t} = 0$ yields

$$\alpha = \mathbf{n}' \cdot \mathbf{t} = -\mathbf{n} \cdot \mathbf{t}' = -\mathbf{n} \cdot \kappa \mathbf{n} = -\kappa.$$

Similarly, differentiating $\mathbf{n} \cdot \mathbf{b} = 0$ yields

$$\beta = \mathbf{n}' \cdot \mathbf{b} = -\mathbf{n} \cdot \mathbf{b}' = -\mathbf{n} \cdot (-\tau \mathbf{n}) = \tau.$$

Thus,

$$\mathbf{n}' = -\kappa \mathbf{t} + \tau \mathbf{b}.$$

The representations of the derivatives of the three defining vectors for a curve are termed the Serret-Frenet formulae [41, p.18]

$$\begin{aligned} \mathbf{t}' &= \kappa \mathbf{n} \\ \mathbf{b}' &= -\tau \mathbf{n} \\ \mathbf{n}' &= -\kappa \mathbf{t} + \tau \mathbf{b}, \end{aligned}$$

which describe all aspects of a space curve, as shown in Figure 2-3.

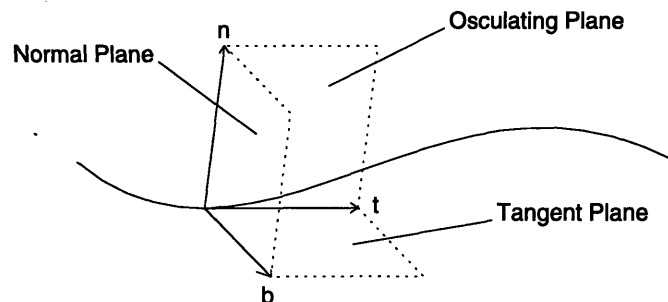


Figure 2-3: Space Curve

2.3 Basic Theory of Surfaces

A general parametric surface can be defined as a vector-valued mapping from a two-dimensional parametric uv -space to three-dimensional space

$$\mathbf{R}(u, v) = [x(u, v) \ y(u, v) \ z(u, v)]^T,$$

where the two parameters u and v lie in the closed intervals $u_1 \leq u \leq u_2$ and $v_1 \leq v \leq v_2$. The surface is regular at all points where the matrix

$$M = \begin{vmatrix} \frac{\partial x}{\partial u} & \frac{\partial y}{\partial u} & \frac{\partial z}{\partial u} \\ \frac{\partial x}{\partial v} & \frac{\partial y}{\partial v} & \frac{\partial z}{\partial v} \end{vmatrix} \quad (2.5)$$

has rank 2, or equivalently $\mathbf{R}_u \times \mathbf{R}_v \neq \mathbf{0}$ [41, p.56]. Partial derivatives of a surface will be represented as

$$\mathbf{R}_u = \frac{\partial \mathbf{R}}{\partial u} \quad \text{and} \quad \mathbf{R}_v = \frac{\partial \mathbf{R}}{\partial v}.$$

A curve on the surface is represented as $\mathbf{r}(u, v)$ with $u = u(t)$ and $v = v(t)$ or equivalently $\mathbf{R}(u(t), v(t)) = \mathbf{r}(t)$. This occurs when the rank of the matrix (2.5) is 1 at every point. When we keep u constant in $\mathbf{R}(u, v)$ by setting $u = u_n$, we have an equation for a curve that depends only on v , and is thus called an *isoparameter curve*. Similarly, $v = v_n$ is also an isoparameter curve.

The vector

$$\frac{d\mathbf{R}}{dt} = \mathbf{R}_u \frac{du}{dt} + \mathbf{R}_v \frac{dv}{dt} \quad (2.6)$$

is tangent to the curve when u and v are functions of t . This is of course also a tangent to the surface. The tangent plane to the surface at any point is determined by the two vectors \mathbf{R}_u and \mathbf{R}_v . The normal to the surface is orthogonal to this plane. A unit vector in the direction of the surface normal is given by

$$\mathbf{N} = \frac{\mathbf{R}_u \times \mathbf{R}_v}{|\mathbf{R}_u \times \mathbf{R}_v|}. \quad (2.7)$$

Note that this definition of the normal vector is undefined when $\mathbf{R}_u \times \mathbf{R}_v = \mathbf{0}$, supporting the assertion that a point on the surface is singular if $\mathbf{R}_u \times \mathbf{R}_v = \mathbf{0}$. This may be due to the shape of the surface or the choice of parameterization. In Section 5.3.5, an alternative definition of \mathbf{N} is explored for degenerate points.

Using the definition of arc length (2.1), the distance between two points on a curve on the surface is found by integrating

$$ds = \sqrt{dx dx + dy dy + dz dz} = \sqrt{d\mathbf{R} \cdot d\mathbf{R}}. \quad (2.8)$$

Combining (2.6) and (2.8) yields the *first fundamental form* of the surface

$$I = ds^2 = (\mathbf{R}_u du + \mathbf{R}_v dv) \cdot (\mathbf{R}_u du + \mathbf{R}_v dv) = Edu^2 + 2Fdudv + Gdv^2$$

where

$$E = \mathbf{R}_u \cdot \mathbf{R}_u, \quad F = \mathbf{R}_u \cdot \mathbf{R}_v, \quad G = \mathbf{R}_v \cdot \mathbf{R}_v.$$

Note that

$$\begin{aligned} EG - F^2 &= (\mathbf{R}_u \cdot \mathbf{R}_u)(\mathbf{R}_v \cdot \mathbf{R}_v) - (\mathbf{R}_u \cdot \mathbf{R}_v)^2 \\ &= (\mathbf{R}_u \times \mathbf{R}_v) \cdot (\mathbf{R}_u \times \mathbf{R}_v) \\ &= |(\mathbf{R}_u \times \mathbf{R}_v)|^2. \end{aligned} \quad (2.9)$$

Thus, $EG - F^2$ is always positive if the surface is regular.

The first fundamental form enables us to determine arc lengths, angles and areas on the surface. In order to determine curvatures, the *second fundamental form* is required. First, the curvature vector of the curve on the surface, found from equation (2.3), is split into its normal and tangential components

$$\mathbf{k} = \frac{d\mathbf{t}}{ds} = \mathbf{k}_n + \mathbf{k}_g = \kappa_n \mathbf{N} + \mathbf{k}_g$$

where \mathbf{k}_n is the normal curvature vector and κ_n is the *normal curvature* of the curve on the surface at that point. The tangential portion of the curvature vector, \mathbf{k}_g , is called the geodesic curvature vector. It will be discussed in more detail later.

If the angle between the surface normal and the normal to the curve is designated γ as shown in Figure 2-4, then [26, p.118]

$$\mathbf{n} \cdot \mathbf{N} = \cos(\gamma) |\mathbf{n}| |\mathbf{N}| = \cos(\gamma)$$

from the definition of a dot product. Since $\mathbf{t}' = \mathbf{R}'' = \kappa \cdot \mathbf{n}$,

$$\begin{aligned} \kappa \cos(\gamma) &= \kappa \cdot \mathbf{n} \cdot \mathbf{N} \\ &= \mathbf{R}'' \cdot \mathbf{N} \\ &= (\mathbf{R}_u du + \mathbf{R}_v dv)' \cdot \mathbf{N} \\ &= (\mathbf{R}_{uu} du du + 2\mathbf{R}_{uv} du dv + \mathbf{R}_{vv} dv dv + \mathbf{R}_u d^2 u + \mathbf{R}_v d^2 v) \cdot \mathbf{N}. \end{aligned} \quad (2.10)$$

Since $\mathbf{R}_u \cdot \mathbf{N} = \mathbf{R}_v \cdot \mathbf{N} = 0$, equation (2.10) reduces to the second fundamental form, represented by

$$\begin{aligned} II &= (\mathbf{R}_{uu} du du + 2\mathbf{R}_{uv} du dv + \mathbf{R}_{vv} dv dv) \cdot \mathbf{N} \\ &= L du du + 2M du dv + N dv dv \end{aligned}$$

where

$$L = \mathbf{R}_{uu} \cdot \mathbf{N} \quad (2.11)$$

$$M = \mathbf{R}_{uv} \cdot \mathbf{N} \quad \text{and} \quad (2.12)$$

$$N = \mathbf{R}_{vv} \cdot \mathbf{N}. \quad (2.13)$$

Also note that since $\mathbf{R}_u \cdot \mathbf{N} = 0$,

$$\frac{d(\mathbf{R}_u \cdot \mathbf{N})}{du} = \mathbf{R}_{uu} \cdot \mathbf{N} + \mathbf{R}_u \cdot \mathbf{N}_u = 0,$$

and therefore

$$\mathbf{R}_{uu} \cdot \mathbf{N} = -\mathbf{R}_u \cdot \mathbf{N}_u.$$

Similarly, $\mathbf{R}_{uv} \cdot \mathbf{N} = -\mathbf{R}_u \cdot \mathbf{N}_v = -\mathbf{R}_v \cdot \mathbf{N}_u$ and $\mathbf{R}_{vv} \cdot \mathbf{N} = -\mathbf{R}_v \cdot \mathbf{N}_v$. Therefore,

$$L = -\mathbf{R}_u \cdot \mathbf{N}_u \quad (2.14)$$

$$M = -\mathbf{R}_u \cdot \mathbf{N}_v = -\mathbf{R}_v \cdot \mathbf{N}_u \quad (2.15)$$

$$= -\frac{1}{2}(\mathbf{R}_u \cdot \mathbf{N}_v + \mathbf{R}_v \cdot \mathbf{N}_u) \quad \text{and}$$

$$N = -\mathbf{R}_v \cdot \mathbf{N}_v. \quad (2.16)$$

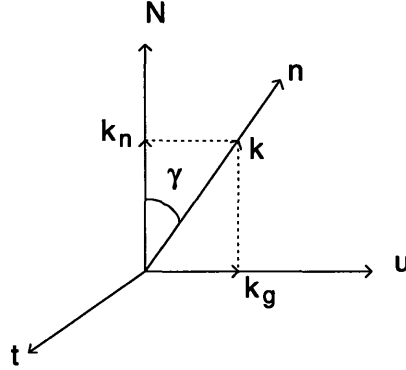


Figure 2-4: Curvature Vectors

To find the normal curvature, we begin with the fact that the surface normal is orthogonal to the tangent to the curve. Differentiating $\mathbf{t} \cdot \mathbf{N} = 0$ with respect to s yields

$$\frac{d\mathbf{t}}{ds} \cdot \mathbf{N} + \mathbf{t} \cdot \frac{d\mathbf{N}}{ds} = 0.$$

Thus we have

$$\mathbf{k} \cdot \mathbf{N} = \frac{d\mathbf{t}}{ds} \cdot \mathbf{N} = -\mathbf{t} \cdot \frac{d\mathbf{N}}{ds} = -\frac{d\mathbf{R}}{ds} \cdot \frac{d\mathbf{N}}{ds}.$$

Therefore,

$$\begin{aligned} \kappa_n &= -\mathbf{k} \cdot \mathbf{N} = \frac{d\mathbf{R}}{ds} \cdot \frac{d\mathbf{N}}{ds} = \frac{(\mathbf{R}_u du + \mathbf{R}_v dv) \cdot (\mathbf{N}_u du + \mathbf{N}_v dv)}{ds^2} = -\frac{II}{I} \\ &= -\frac{Ldu^2 + 2Mdudv + Ndv^2}{Edu^2 + 2Fdudv + Gdv^2} \end{aligned}$$

$$= -\frac{L + 2M\lambda + N\lambda^2}{E + 2F\lambda + G\lambda^2} \quad (2.17)$$

where $\lambda = dv/du$. The negative sign in equation (2.17) ensures that if κ_n is positive, the center of curvature lies opposite to the direction of the surface normal.

Any point on the surface has many curves passing through it, each of which has an associated κ_n . The maximum and minimum values of κ_n at a point are called the *principal curvatures* of the surface at that point and are designated κ_1 and κ_2 . The maximum and minimum values of κ_n occur when $\frac{d\kappa_n}{d\lambda} = 0$, [11, p. 112]

$$\frac{d\kappa_n}{d\lambda} = (E + 2F\lambda + G\lambda^2)(2M + 2N\lambda) - (L + 2M\lambda + N\lambda^2)(2F + 2G\lambda) = 0. \quad (2.18)$$

Using (2.18) in (2.17) yields

$$\kappa_n = -\frac{L + M\lambda}{E + F\lambda} = -\frac{M + N\lambda}{F + G\lambda}$$

given

$$\begin{aligned} (E + 2F\lambda + G\lambda^2) &= (E + F\lambda) + \lambda(F + G\lambda) \quad \text{and} \\ (L + 2M\lambda + N\lambda^2) &= (L + M\lambda) + \lambda(M + N\lambda). \end{aligned}$$

Therefore the extreme values of κ_n satisfy the two simultaneous equations

$$(L + \kappa_n E)du + (M + \kappa_n F)dv = 0 \quad \text{and} \quad (2.19)$$

$$(M + \kappa_n F)du + (N + \kappa_n G)dv = 0. \quad (2.20)$$

These equations can be simultaneously satisfied if and only if

$$\begin{vmatrix} L + \kappa_n E & M + \kappa_n F \\ M + \kappa_n F & N + \kappa_n G \end{vmatrix} = 0.$$

The discriminant of this quadratic equation in κ_n is greater than or equal to zero. Therefore the equation has either two distinct roots κ_{max} and κ_{min} , the maximum and minimum principal curvatures, or double roots κ_n , the normal curvature at an umbilical point. The corresponding directions λ define directions in the uv -plane. The corresponding directions in the tangent plane are called *principal directions of curvature* and are always orthogonal except at *umbilical points*, where κ_{max} and κ_{min} are identical. In the special case where the identical principal curvatures vanish, the surface becomes locally *flat*. The two roots are given by

$$\kappa_{max} = H + \sqrt{H^2 - K} \quad \text{and} \quad (2.21)$$

$$\kappa_{min} = H - \sqrt{H^2 - K} \quad (2.22)$$

where K is the *Gaussian curvature* and H is the *mean curvature* defined by

$$K = \frac{LN - M^2}{EG - F^2} \quad (2.23)$$

$$H = \frac{2FM - EN - GL}{2(EG - F^2)}. \quad (2.24)$$

Using (2.21) and (2.22) in (2.23) and (2.24), it can easily be shown that

$$\begin{aligned} K &= \kappa_{max}\kappa_{min} \\ H &= \frac{1}{2}(\kappa_{max} + \kappa_{min}). \end{aligned}$$

Note that at an umbilical point, $H^2 = K$ and at a *flat* point, $K = H = 0$.

The normal curvature can be represented in terms of the principal curvatures κ_1 and κ_2 as

$$\kappa_n = \kappa_1 \cos^2(\alpha) + \kappa_2 \sin^2(\alpha) \quad (2.25)$$

where α is the angle between the direction dv/du and the direction $dv = 0$. This is known as *Euler's theorem* [26].

Recall that the curvature vector of a curve on the surface can be split into its normal and tangential components

$$\mathbf{k} = \mathbf{k}_n + \mathbf{k}_g,$$

where the tangential component, \mathbf{k}_g , is known as the *geodesic curvature vector*. Let \mathbf{u} be a unit vector in the tangent plane perpendicular to \mathbf{t} such that \mathbf{t} , \mathbf{u} and \mathbf{N} form a right-handed coordinate system in that order as shown in Figure 2-4. The geodesic curvature κ_g can then be found from

$$\mathbf{k}_g = \kappa_g \mathbf{u}.$$

Additionally, since the magnitude of κ_n can be represented as $|\kappa \cos \gamma|$, the magnitude of κ_g can be represented as $|\kappa \sin \gamma|$.

Geodesic curvature can be represented using only the first fundamental form. Since $\mathbf{u} \cdot \mathbf{N} = 0$ and $\mathbf{u} \cdot \mathbf{u} = 1$,

$$\kappa_g = \mathbf{u} \cdot \mathbf{k} = \mathbf{u} \cdot \frac{d\mathbf{t}}{ds} = \mathbf{u} \cdot \mathbf{t}' = (\mathbf{N} \times \mathbf{t}) \cdot \mathbf{t}' = (\mathbf{t}\mathbf{t}'\mathbf{N}). \quad (2.26)$$

The unit tangent vector of the curve on the surface is given by

$$\mathbf{t} = \mathbf{R}_u u' + \mathbf{R}_v v';$$

thus

$$\mathbf{t}' = \mathbf{R}_{uu}(u')^2 + 2\mathbf{R}_{uv}u'v' + \mathbf{R}_{vv}(v')^2 + \mathbf{R}_u u'' + \mathbf{R}_v v''.$$

Therefore equation (2.26) can be rewritten as

$$\begin{aligned} \kappa_g &= (\mathbf{t} \times \mathbf{t}') \cdot \mathbf{N} \\ &= [(\mathbf{R}_u u' + \mathbf{R}_v v') \times (\mathbf{R}_{uu}(u')^2 + 2\mathbf{R}_{uv}u'v' + \mathbf{R}_{vv}(v')^2 + \mathbf{R}_u u'' + \mathbf{R}_v v'')] \cdot \mathbf{N} \\ &= [(\mathbf{R}_u \times \mathbf{R}_{uu})(u')^3 + (2\mathbf{R}_u \times \mathbf{R}_{uv} + \mathbf{R}_v \times \mathbf{R}_{uu})(u')^2 v' \\ &\quad + (\mathbf{R}_u \times \mathbf{R}_{vv} + 2\mathbf{R}_v \times \mathbf{R}_{uv})u'(v')^2 \\ &\quad + (\mathbf{R}_v \times \mathbf{R}_{vv})(v')^3 + (\mathbf{R}_u \times \mathbf{R}_v)(u'v'' - u''v')] \cdot \mathbf{N}. \end{aligned} \quad (2.27)$$

Each of the coefficients of the combinations of u and v derivatives in (2.27) can be written in terms of the coefficients of the first fundamental form and their derivatives. For example,

$$\begin{aligned}
(\mathbf{R}_u \times \mathbf{R}_{uu}) \cdot \mathbf{N} &= \frac{(\mathbf{R}_u \times \mathbf{R}_{uu}) \cdot (\mathbf{R}_u \times \mathbf{R}_v)}{\sqrt{EG - F^2}} \\
&= \frac{(\mathbf{R}_u \cdot \mathbf{R}_u)(\mathbf{R}_{uu} \cdot \mathbf{R}_v) - (\mathbf{R}_u \cdot \mathbf{R}_{uu})(\mathbf{R}_u \cdot \mathbf{R}_v)}{\sqrt{EG - F^2}} \\
&= \frac{2(E(\mathbf{R}_{uu} \cdot \mathbf{R}_v) - (\mathbf{R}_u \cdot \mathbf{R}_{uu})F)\sqrt{EG - F^2}}{2(EG - F^2)} \\
&= \frac{(2EF_u - EE_u - FE_u)\sqrt{EG - F^2}}{2(EG - F^2)} \\
&= \Gamma_{11}^2 \sqrt{EG - F^2}
\end{aligned}$$

where Γ_{11}^2 is one of the Christoffel symbols defined by the coefficients of the first fundamental form E , F and G and their derivatives, E_u , F_u , G_u , E_v , F_v and G_v

$$\begin{aligned}
\Gamma_{11}^1 &= \frac{GE_u - 2FF_u + FE_v}{2(EG - F^2)}, & \Gamma_{11}^2 &= \frac{2EF_u - EE_v + FE_u}{2(EG - F^2)} \\
\Gamma_{12}^1 &= \frac{GE_v - FG_u}{2(EG - F^2)}, & \Gamma_{12}^2 &= \frac{EG_u - FE_v}{2(EG - F^2)} \\
\Gamma_{22}^1 &= \frac{2GF_v - GG_u + FG_v}{2(EG - F^2)}, & \Gamma_{22}^2 &= \frac{EG_v - 2FF_v + FG_u}{2(EG - F^2)}.
\end{aligned}$$

Similarly reducing all the other coefficients in (2.27) yields

$$\begin{aligned}
\kappa_g &= [\Gamma_{11}^2 (u')^3 + (2\Gamma_{12}^2 - \Gamma_{11}^1)(u')^2 v' + (\Gamma_{22}^2 - 2\Gamma_{12}^1)u'(v')^2 - \Gamma_{22}^1 (v')^3 \\
&\quad + u'v'' - u''v']\sqrt{EG - F^2}.
\end{aligned} \tag{2.28}$$

A *geodesic* is defined as a curve with zero geodesic curvature [41]. Straight lines on a surface are geodesics since the curvature vector \mathbf{k} vanishes. For geodesics that are curved, the curvature vector coincides with the surface normal vector and, since the curvature vector lies in the osculating plane, the osculating and tangent planes are normal. The equation for the geodesic can be obtained by setting κ_g equal to zero in equation (2.28), which yields

$$u''v' - u'v'' = \Gamma_{11}^2 (u')^3 + (2\Gamma_{12}^2 - \Gamma_{11}^1)(u')^2 v' + (\Gamma_{22}^2 - 2\Gamma_{12}^1)u'(v')^2 - \Gamma_{22}^1 (v')^3$$

assuming that the geodesic is everywhere regular so $EG - F^2$ is always positive. An alternative representation for a geodesic is given by the set of coupled second order ordinary differential equations [41]

$$\frac{d^2 u}{ds^2} + \Gamma_{11}^1 \left(\frac{du}{ds}\right)^2 + 2\Gamma_{12}^1 \frac{du}{ds} \frac{dv}{ds} + \Gamma_{22}^1 \left(\frac{dv}{ds}\right)^2 = 0 \tag{2.29}$$

$$\frac{d^2 v}{ds^2} + \Gamma_{11}^2 \left(\frac{du}{ds}\right)^2 + 2\Gamma_{12}^2 \frac{du}{ds} \frac{dv}{ds} + \Gamma_{22}^2 \left(\frac{dv}{ds}\right)^2 = 0 \tag{2.30}$$

where the two equations are related by the condition $ds^2 = Edu^2 + 2Fdu dv + Gdv^2$.

Chapter 3

Curve and Surface Representation

3.1 Introduction

This chapter reviews the representation of curves and surfaces in Bézier and B-spline forms and treats the special properties associated with each. In addition, algorithms for knot insertion and removal, curve evaluation and splitting are summarized. The descriptions are based on texts by Hoschek and Lasser [22], Piegl and Tiller [36] and Yamaguchi [44].

3.2 Bézier Curves and Surfaces

Bernstein Polynomials

The *Bernstein polynomials* are defined as

$$B_{i,n}(u) = \frac{n!}{i!(n-i)!} (1-u)^{n-i} u^i, \quad i = 0, \dots, n, \quad (3.1)$$

and have several properties of interest. The *property of positivity* states that each polynomial factor is non-negative such that

$$B_{i,n}(u) \geq 0, \quad 0 \leq u \leq 1$$

for all i and n . The *partition of unity* property states that the Bernstein polynomials sum to 1 for all $0 \leq u \leq 1$, or

$$\sum_{i=0}^n B_{i,n}(u) = 1.$$

The derivative of a Bernstein polynomial is

$$\frac{dB_{i,n}(u)}{du} = n[B_{i-1,n-1}(u) - B_{i,n-1}(u)]$$

where $B_{-1,n-1} = B_{n,n-1} = 0$. The *linear precision property* of a Bernstein polynomial

$$u = \sum_{i=0}^n \frac{i}{n} B_{i,n}(u)$$

allows the monomial u to be expressed as the weighted sum of Bernstein polynomials with coefficients evenly spaced in the interval $[0,1]$.

Bézier Curves

A *Bézier curve* is a spline curve that uses the Bernstein polynomials as a basis. A Bézier curve of degree n (order $n + 1$) is represented by

$$\mathbf{r}(u) = \sum_{i=0}^n \mathbf{b}_i B_{i,n}(u), \quad 0 \leq u \leq 1.$$

The coefficients, \mathbf{b}_i , are the *control points* that determine the shape of the curve. Lines drawn between consecutive control points of the curve form the *control polygon*. A cubic Bézier curve is shown in Figure 3-1. Bézier curves have the following properties:

- The first and last control points are the endpoints of the curve. In other words, $\mathbf{b}_0 = \mathbf{r}(0)$ and $\mathbf{b}_n = \mathbf{r}(1)$.
- The curve is tangent to the control polygon at the endpoints.
- The *convex hull property* states that the entire curve is contained within the convex hull of the control points.
- The first derivative of a Bézier curve is represented by

$$\dot{\mathbf{r}}(u) = \frac{d\mathbf{r}(u)}{du} = n \sum_{i=0}^{n-1} (\mathbf{b}_{i+1} - \mathbf{b}_i) B_{i,n-1}(u), \quad 0 \leq u \leq 1.$$

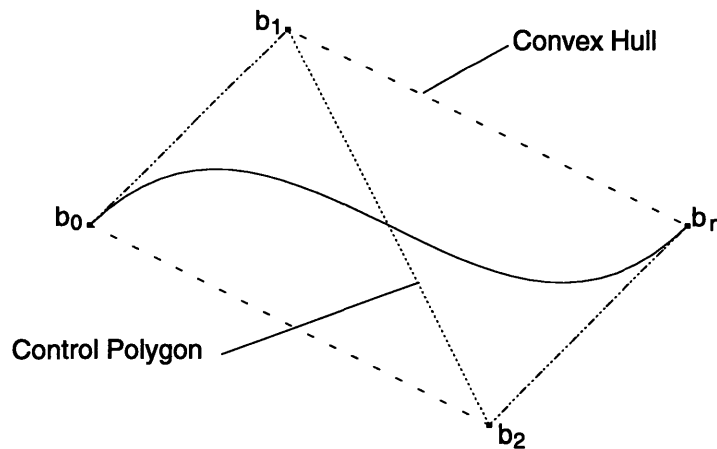


Figure 3-1: A Cubic Bézier Curve with Control Polygon

A Bézier curve can be evaluated at a specific parameter value u_0 and the curve can be split at that value using the *deCasteljau algorithm*, where [22, p.125]

$$\mathbf{b}_i^k(u_0) = (1 - u_0)\mathbf{b}_{i-1}^{k-1} + u_0\mathbf{b}_i^{k-1}, \quad k = 1, 2, \dots, n, \quad i = k, \dots, n$$

is applied recursively to obtain the new control points. The algorithm is illustrated in Figure 3-2, and has the following properties:

- The values \mathbf{b}_i^0 are the original control points of the curve.
- The value of the curve at parameter value u_0 is \mathbf{b}_n^n .
- The curve can be represented as two curves, with control points $(\mathbf{b}_0^n, \mathbf{b}_1^n, \dots, \mathbf{b}_n^n)$ and $(\mathbf{b}_n^n, \mathbf{b}_n^{n-1}, \dots, \mathbf{b}_n^0)$.
- Since this is merely a change in the basis representation, the curve itself remains parametrically and geometrically unchanged.

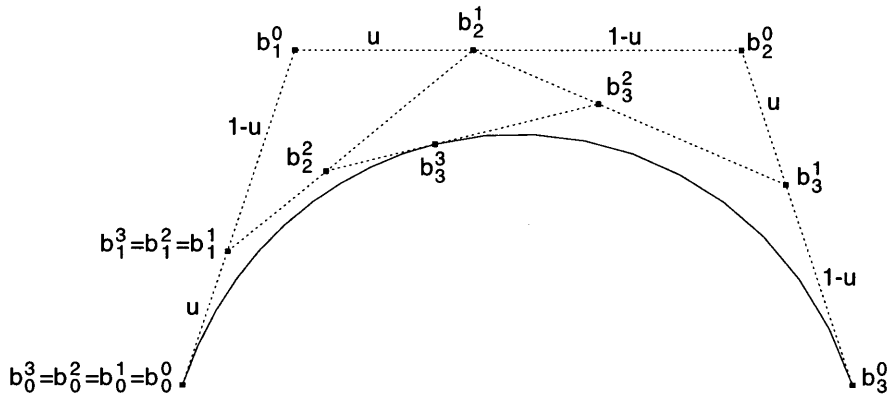


Figure 3-2: The deCasteljau Algorithm

Bézier Surfaces

A tensor product surface is formed by moving a curve through space while allowing deformations in that curve. This can be thought of as allowing each control point \mathbf{b}_i to sweep a curve in space. If this surface is represented using Bernstein polynomials, a Bézier surface is formed, with the following formula:

$$\mathbf{R}(u, v) = \sum_{i=0}^m \sum_{j=0}^n \mathbf{b}_{ij} B_{i,m}(u) B_{j,n}(v), \quad 0 \leq u, v \leq 1.$$

Here, the set of lines drawn between consecutive control points \mathbf{b}_{ij} is referred to as the *control net*. An example of a bi-quadratic Bézier surface with its control net can be seen in Figure 3-3. The following conditions apply:

- The boundary isoparametric curves ($u = 0$, $u = 1$, $v = 0$ and $v = 1$) have the same control points as the corresponding boundary points on the net.
- The corners of the surface coincide with the corner points of the net, and the derivatives in the u and v directions at the corners are tangent to the net.
- Bézier surfaces exhibit the convex hull property.

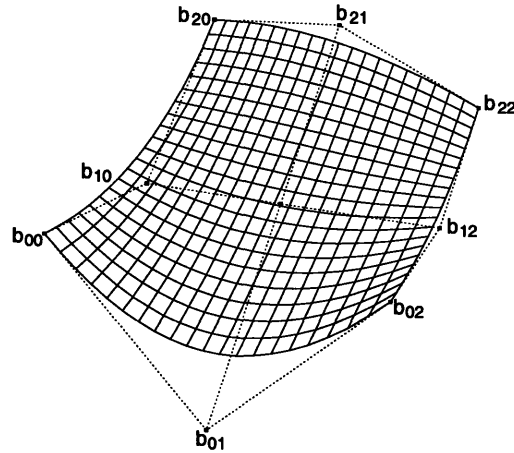


Figure 3-3: A Bézier Surface with Control Net

Continuity Conditions

Bézier curves can represent complex curves by increasing the degree and thus the number of control points. Alternatively, complex curves can be represented using composite curves, which can be formed by joining several Bézier curves end to end. If this method is adopted, the continuity between consecutive curves must be addressed.

One set of continuity conditions are the *geometric* continuity conditions, designated by the letter G with an integer exponent. *Position continuity*, or G^0 continuity, requires the endpoints of the two curves to coincide,

$$\mathbf{r}^{(1)}(1) = \mathbf{r}^{(2)}(0).$$

The superscripts denote the first and second curves. *Tangent continuity*, or G^1 continuity, requires the tangents of the curves to be in the same direction,

$$\begin{aligned}\dot{\mathbf{r}}^{(1)}(1) &= \alpha_1 \mathbf{t} \\ \dot{\mathbf{r}}^{(2)}(0) &= \alpha_2 \mathbf{t}\end{aligned}$$

where \mathbf{t} is the common unit tangent vector. G^1 continuity is important in minimizing stress concentrations and preventing flow separation.

Curvature continuity, or G^2 continuity, requires the center of curvature to move continuously past the connection point,

$$\ddot{\mathbf{r}}^{(2)}(0) = \left(\frac{\alpha_2}{\alpha_1}\right)^2 \ddot{\mathbf{r}}^{(1)}(1) + \mu \dot{\mathbf{r}}^{(1)}(1).$$

G^2 continuity is important for aesthetic reasons and for preventing fluid flow separation.

More stringent continuity conditions are the *parametric* continuity conditions, where C^k continuity requires the k th derivative of each curve to be equal at the joining point. In other words,

$$\frac{d^k \mathbf{r}^{(1)}(1)}{du^k} = \frac{d^k \mathbf{r}^{(2)}(0)}{du^k}.$$

The C^1 and C^2 continuity conditions for consecutive segments of a composite degree n Bézier curve can be stated as [44, p. 215]

$$h_{i+1} (\mathbf{b}_{ni} - \mathbf{b}_{ni-1}) = h_i (\mathbf{b}_{ni+1} - \mathbf{b}_{ni}), \quad \text{and} \quad (3.2)$$

$$\mathbf{b}_{ni-1} + \frac{h_{i+1}}{h_i} (\mathbf{b}_{ni-1} - \mathbf{b}_{ni-2}) = \mathbf{b}_{ni+1} + \frac{h_i}{h_{i+1}} (\mathbf{b}_{ni+1} - \mathbf{b}_{ni+2}) \quad (3.3)$$

where, for the i th Bézier curve segment with u values between knot values t_i and t_{i+1} inclusively, $h_i = t_{i+1} - t_i$. See Figure 3-4.

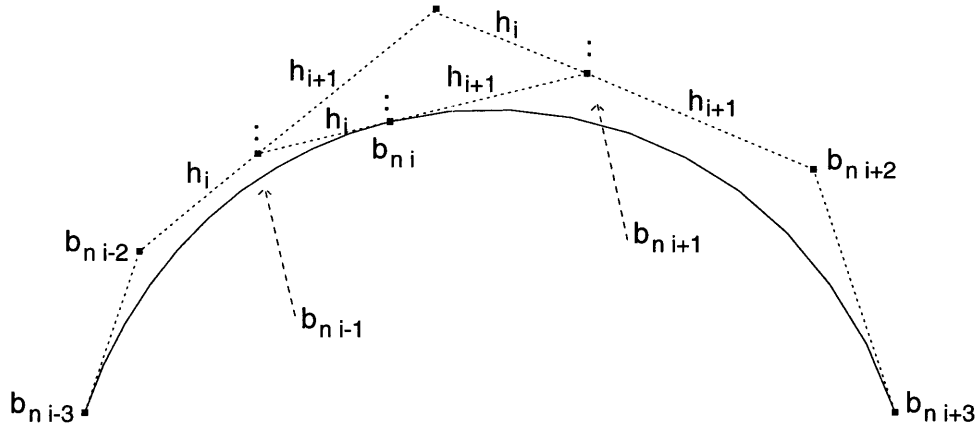


Figure 3-4: Continuity Conditions

3.3 B-Spline Curves and Surfaces

The Bézier representation has two main disadvantages. First, the number of control points is directly related to the degree. Therefore, to increase the complexity of the shape of the curve by adding control points requires increasing the degree of the curve or satisfying the continuity conditions between consecutive segments of a composite curve. Second, changing any one control point affects the entire curve or surface, making design of specific sections very difficult. These disadvantages are remedied with the introduction of the B-spline representation.

A B-spline (basis-spline) curve is a piecewise polynomial curve meaning it is made up of polynomial curve segments. It is a spline curve with a different basis than the Bézier curves, although a Bézier curve is a special case of a B-spline curve. The B-spline representation has the advantage that the control points affect the curve only locally, and a B-spline of order k may have as many control points as required to describe the curve.

A B-spline curve is a series of polynomial segments of degree $k - 1$ joined together at *knots* t_k . A B-spline of order k (degree $k - 1$) with $n + 1$ control points has the equation

$$\mathbf{r}(u) = \sum_{i=0}^n \mathbf{p}_i N_{i,k}(u), \quad n \geq k - 1, \quad u \in [t_{k-1}, t_{n+1}]$$

where t_k is a member of the knot vector with $n + k + 1$ elements

$$\mathbf{T} = (t_0, t_1, \dots, t_{k-1}, t_k, t_{k+1}, \dots, t_{n-1}, t_n, t_{n+1}, \dots, t_{n+k}), \quad t_0 \leq t_1 \leq \dots \leq t_{n+k}.$$

The basis functions, $N_{i,k}(u)$, are given by:

$$N_{i,1}(u) = \begin{cases} 1 & \text{for } t_i \leq u < t_{i+1} \\ 0 & \text{otherwise} \end{cases}$$

for $k = 1$, and

$$N_{i,k}(u) = \frac{u - t_i}{t_{i+k-1} - t_i} N_{i,k-1}(u) + \frac{t_{i+k} - u}{t_{i+k} - t_{i+1}} N_{i+1,k-1}(u)$$

for $k > 1$ and $i = 0, 1, \dots, n$. These equations have the following properties [22, p. 168]:

- $N_{i,k}(u) > 0$, for $t_i < u < t_{i+k}$
- $N_{i,k}(u) = 0$, for $t_0 \leq u \leq t_i$, and $t_{i+k} \leq u \leq t_{n+k}$
- $\sum_{i=0}^n N_{ik}(u) = 1$, for $u \in [t_{k-1}, t_{n+1}]$, and
- $N_{ik}(u)$ has continuity C^{k-2} at each simple knot t_l .

The first three properties show positivity and partition of unity for the B-Spline basis functions.

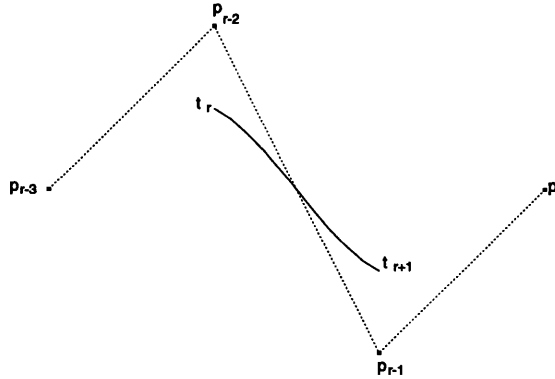


Figure 3-5: A Cubic B-spline Curve Segment with Control Polygon

Local control means that a single segment of the B-spline curve is controlled only by the nearest n points, and that any control point affects the nearest n spans. In other words, changing p_i affects the curve in the parameter range $t_i < u < t_{i+k}$ and the curve at a point u where $t_r < u < t_{r+1}$ is determined completely by the control points $p_{r-(k-1)}, \dots, p_r$.

The convex hull property for B-splines applies locally, so that a span lies within the convex hull of the control points that affect it. This provides a tighter convex hull property than that of a Bézier curve, as can be seen in Figure 3-6.

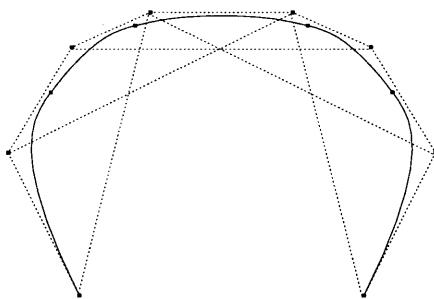


Figure 3-6: Convex Hull Property for a Cubic B-Spline Curve

Increasing the multiplicity of a knot reduces the continuity of the curve at that knot. Specifically, the curve is $(k-p-1)$ times continuously differentiable at a knot with multiplicity p ($\leq k$), and thus has $C^{(k-p-1)}$ continuity. Therefore, the control polygon will coincide with the curve at a knot of multiplicity $k-1$, and a knot with multiplicity k indicates C^{-1} continuity, or a discontinuous curve.

As you can see in Figure 3-5, the endpoints of the curve may not coincide with the control polygon. However, repeating the knots at the end k times will force the endpoints to coincide with the control polygon. Thus a knot vector described by

$$\mathbf{T} = (\underbrace{t_0, t_1, \dots, t_{k-1}}_{k \text{ equal knots}}, \underbrace{t_k, t_{k+1}, \dots, t_{n-1}, t_n}_{n-k+1 \text{ internal knots}}, \underbrace{t_{n+1}, \dots, t_{n+k}}_{k \text{ equal knots}})$$

will have $t_0 = t_1 = \dots = t_{k-1}$ and $t_{n+1} = t_{n+2} = \dots = t_{n+k}$ and hence the first and last control points of the curve coincide with the endpoints of the curve.

From this discussion, it can be seen that a Bézier curve of order k (degree $k-1$) is a B-spline curve with no internal knots and the end knots repeated k times. The knot vector is thus

$$\mathbf{T} = (\underbrace{t_0, t_1, \dots, t_{k-1}}_{k \text{ equal knots}}, \underbrace{t_{n+1}, \dots, t_{n+k}}_{k \text{ equal knots}})$$

where $n+k+1 = 2k$ or $n = k-1$.

A B-spline surface is a tensor product surface using a B-spline basis. This is represented mathematically as

$$\mathbf{R}(u, v) = \sum_{i=0}^m \sum_{j=0}^n \mathbf{p}_{ij} N_{i,k}(u) N_{j,l}(v).$$

Knot Insertion

A knot can be inserted into a B-spline curve without changing the geometry of the curve. The new curve is identical to the old one, with a new basis where

$$\sum_{i=0}^n \mathbf{p}_i N_{i,k}(u) \quad \text{becomes} \quad \sum_{i=0}^{n+1} \hat{\mathbf{p}}_i \hat{N}_{i,k}(u)$$

over $\mathbf{T} = [t_0, t_1, \dots, t_l, t_{l+1}, \dots]$ over $\mathbf{T} = [t_0, t_1, \dots, t_l, \hat{t}, t_{l+1}, \dots]$

when a new knot \hat{t} is inserted between knots t_l and t_{l+1} . The *deBoor algorithm* is used to insert the knot, and is represented as

$$\mathbf{p}_i^j = (1 - \alpha_i^j) \mathbf{p}_{i-1}^{j-1} + \alpha_i^j \mathbf{p}_i^{j-1} \quad i \geq l - k + 2 \quad (3.4)$$

where

$$\alpha_i = \begin{cases} 1 & i \leq l - k + 1 \\ 0 & l + 1 \leq i \\ \frac{u_0 - t_i}{t_{i+k-1} - t_i} & l - k + 2 \leq i \leq l \end{cases} .$$

To evaluate a B-spline curve at a specific parametric value or to split the curve at that value, the deBoor algorithm is used to repeatedly insert the same knot until the control polygon coincides with the curve at the parametric value u_0 , or in other words, until the multiplicity of the knot at $u_0 = k - 1$. Then,

$$\begin{aligned} \mathbf{p}_i^0 &= \mathbf{p}_i \\ \mathbf{p}_{k-1}^{k-1} &= \mathbf{r}(u_0). \end{aligned}$$

A B-spline curve is C^∞ continuous in the interior of a span. Inserting a knot does not change the curve, so it does not change the continuity. However, if any of the control points are moved after knot insertion, the continuity at the knot will become C^{k-p-1} , where p is the multiplicity of the knot. Figure 3-7 illustrates a single insertion of a knot at parameter value u_0 , resulting in a knot with multiplicity of one.

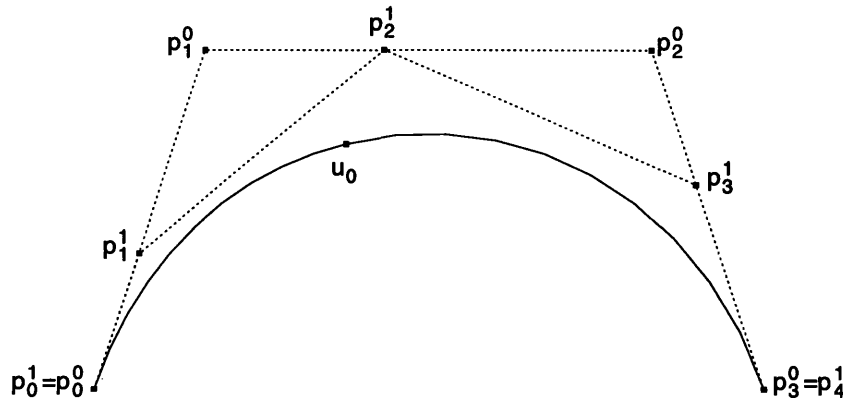


Figure 3-7: The deBoor Algorithm

The B-spline curve can be subdivided into Bézier segments by knot insertion at each internal knot until the multiplicity of each internal knot is the degree k . The above algorithm is also known as *Boehm's algorithm* [4, 5].

Knot Removal

Knot removal is the reverse process of knot insertion. This thesis uses the knot removal algorithm developed by Tiller [42], in which a knot is removed if and only if it leaves the curve or surface geometrically and parametrically unchanged.

To demonstrate the process, this example uses a cubic B-spline curve $\mathbf{r}(u)$ given by control points $(\mathbf{p}_0^0, \dots, \mathbf{p}_6^0)$ and knot vector (t_0, \dots, t_{10}) where $t_0 = \dots = t_3 = 0$, $t_4 = t_5 = t_6 = 1$ and $t_7 = \dots = t_{10} = 2$ as shown in Figure 3-8. As the basis functions only guarantee C^0 continuity at $u = 1$, the first derivative may or may not be continuous there. Using the C^1 continuity condition (3.2), the first derivative will be continuous if and only if

$$(t_7 - t_4)(\mathbf{p}_3^0 - \mathbf{p}_2^0) = (t_6 - t_3)(\mathbf{p}_4^0 - \mathbf{p}_3^0).$$

Since $t_4 = t_6 = u$,

$$\mathbf{p}_3^0 = \frac{u - t_3}{t_7 - t_3} \mathbf{p}_4^0 + \frac{t_7 - u}{t_7 - t_3} \mathbf{p}_2^0.$$

Since $\mathbf{p}_2^0 = \mathbf{p}_2^1$ and $\mathbf{p}_4^0 = \mathbf{p}_3^1$,

$$\mathbf{p}_3^0 = \alpha_3 \mathbf{p}_3^1 + (1 - \alpha_3) \mathbf{p}_2^1 \quad \alpha_3 = \frac{u - t_3}{t_7 - t_3}. \quad (3.5)$$

Note that (3.5) is the same as the deBoor algorithm equation (3.4) for inserting a new knot at $u = 1$, although the points and knots are numbered differently in this example.

A similar reasoning yields that fact that a knot $u = 1$ can be removed a second time if and only if the second derivative is continuous, yielding

$$\begin{aligned} \mathbf{p}_2^1 &= \alpha_2 \mathbf{p}_2^2 + (1 - \alpha_2) \mathbf{p}_1^2 \\ \mathbf{p}_3^1 &= \alpha_3 \mathbf{p}_3^2 + (1 - \alpha_3) \mathbf{p}_2^2 \\ \alpha_i &= \frac{u - t_i}{t_{i+p+2} - t_i} \quad i = 2, 3 \end{aligned} \quad (3.6)$$

and a knot $u = 1$ can be removed a third time if and only if the third derivative is continuous such that

$$\begin{aligned} \mathbf{p}_1^2 &= \alpha_1 \mathbf{p}_1^3 + (1 - \alpha_1) \mathbf{p}_0^3 \\ \mathbf{p}_2^2 &= \alpha_2 \mathbf{p}_2^3 + (1 - \alpha_2) \mathbf{p}_1^3 \\ \mathbf{p}_3^2 &= \alpha_3 \mathbf{p}_3^3 + (1 - \alpha_3) \mathbf{p}_2^3 \\ \alpha_i &= \frac{u - t_i}{t_{i+p+3} - t_i} \quad i = 1, 2, 3. \end{aligned} \quad (3.7)$$

Note that there are no unknowns in equation (3.5), one unknown, \mathbf{p}_2^2 , in equation (3.6) and two unknowns, \mathbf{p}_1^3 and \mathbf{p}_2^3 , in equation (3.7).

For the knot removal process, first the right hand side of equation (3.5) is computed and compared to \mathbf{p}_3^0 . If they are equal within a given tolerance, the knot and \mathbf{p}_3^0 are removed.

If the first knot removal is successful, equations (3.6) are solved for \mathbf{p}_2^2 and compared:

$$\mathbf{p}_2^2 = \frac{\mathbf{p}_2^1 - (1 - \alpha_2)\mathbf{p}_1^2}{\alpha_2}$$

$$\mathbf{p}_2^2 = \frac{\mathbf{p}_3^1 - \alpha_3\mathbf{p}_3^2}{1 - \alpha_3}.$$

If the two values for \mathbf{p}_2^2 are the same, then the knot and control points \mathbf{p}_2^1 and \mathbf{p}_3^1 are removed and control point \mathbf{p}_2^2 is inserted.

If the second knot removal is successful, the third step is to solve the first and third equations of (3.7) for

$$\mathbf{p}_1^3 = \frac{\mathbf{p}_1^2 - (1 - \alpha_1)\mathbf{p}_0^3}{\alpha_1}$$

$$\mathbf{p}_2^3 = \frac{\mathbf{p}_3^2 - \alpha_3\mathbf{p}_3^3}{1 - \alpha_3}.$$

The two values are then substituted into the second equation of (3.7). If the result is within tolerance of \mathbf{p}_2^2 , then the knot is removed and control points \mathbf{p}_1^2 , \mathbf{p}_2^2 and \mathbf{p}_3^2 are replaced by \mathbf{p}_1^3 and \mathbf{p}_2^3 .

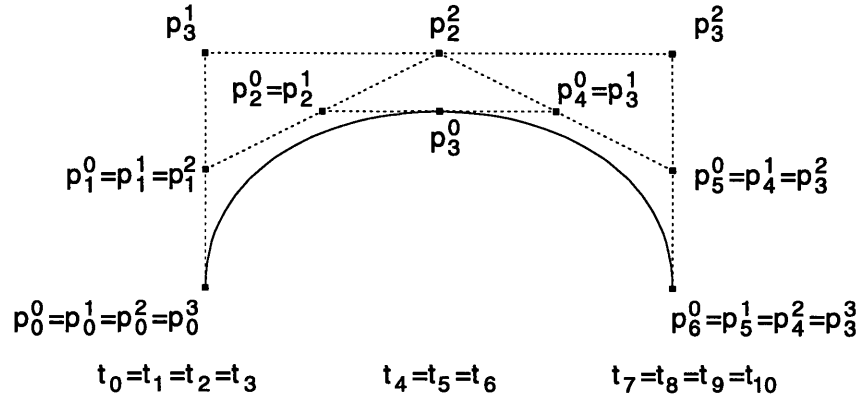


Figure 3-8: Knot Removal

This can be generalized to apply to any number of removals of any particular knot. For the n th removal, there will be a system of n equations with $n - 1$ unknowns. If n is even, two values of the final unknown control point will be calculated and compared. If they are within tolerance, the knot removal is successful. If n is odd, all new control points are computed and the final two are substituted into the middle equation. If the result is within the tolerance, the knot removal is successful. If the n th removal is successful, n control points will be replaced by $n - 1$ control points.

Knot removal from a surface is performed on the $m + 1$ rows or $n + 1$ columns of control points. However, the knot removal is successful only if the knot can be successfully removed from each row or column. Therefore, the result must be checked for each row or column before any control points are removed.

NURBS

The non-uniform rational B-spline (NURBS) curve is represented in a rational form

$$\mathbf{r}(u) = \frac{\sum_{i=0}^n w_i \mathbf{b}_i N_{i,k}(u)}{\sum_{i=0}^n w_i N_{i,k}(u)}$$

where $w_i > 0$ is a weighting factor and $N_{i,k}(u)$ are defined over a non-uniform knot vector. A NURBS surface patch can be represented as

$$\mathbf{R}(u, v) = \frac{\sum_{i=0}^m \sum_{j=0}^n w_{ij} \mathbf{b}_{ij} N_{i,k}(u) N_{j,l}(v)}{\sum_{i=0}^m \sum_{j=0}^n w_{ij} N_{i,k}(u) N_{j,l}(v)}$$

where $w_{ij} > 0$ is a weighting factor. A *uniform* knot vector is one where the knots are evenly spaced. If the knots are not evenly spaced, the knot vector is *non-uniform*. Thus, any knot vector with repeated knots is non-uniform. The NURBS representation of curves and surfaces allows the exact representation of figures such as circles, conics, quadratics, and surfaces of revolution with rational profiles such as torii. If $w_i = 1$ for all i or $w_{ij} = 1$ for all i, j , this representation is the same as the integral non-uniform B-spline described previously. In this thesis, all the B-splines used are integral, but the development could be extended to include NURBS.

Chapter 4

Review of Differential Geometry Properties of Developable Surfaces

4.1 Introduction

This chapter discusses the properties of ruled and developable surfaces. The representations and properties discussed herein are taken from classic texts by Struik [41], Kreyszig [26], Faux and Pratt [11] and Spivak [40].

4.2 Ruled and Developable Surfaces

Ruled Surfaces

A *ruled surface* is a surface generated by the motion of a straight line (a *generator* or *ruling*) through space [41]. A curve that passes through all the rulings of the surface is called a *directrix*. Any point on the surface can be expressed as

$$\mathbf{R}(u, v) = \boldsymbol{\alpha}(u) + v\boldsymbol{\beta}(u) \quad (4.1)$$

where $\boldsymbol{\alpha}(u)$ is a directrix or base curve of the ruled surface and $\boldsymbol{\beta}(u)$ is a unit vector which gives the direction of the ruling at each point on the directrix. Alternatively, the surface can be represented as a ruling joining corresponding points on two space curves. This is represented by

$$\mathbf{R}(u, v) = (1 - v)\mathbf{r}_A(u) + v\mathbf{r}_B(u) \quad 0 \leq u, v \leq 1 \quad (4.2)$$

where $\mathbf{r}_A(u)$ and $\mathbf{r}_B(u)$ are directrices, as shown in Figure 4-1. The two representations are identical if

$$\boldsymbol{\alpha}(u) = \mathbf{r}_A(u) \quad \text{and} \quad \boldsymbol{\beta}(u) = \mathbf{r}_B(u) - \mathbf{r}_A(u). \quad (4.3)$$

Throughout the thesis it is assumed that the constant u isoparametric lines correspond to the generators of the developable surface or, in other words, the straight line rulings are in the v direction.

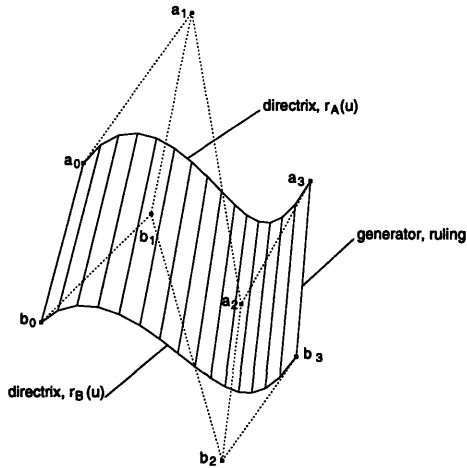


Figure 4-1: A Ruled Surface

Developable Surfaces - A Subset of Ruled Surfaces

Developable surfaces are a subset of ruled surfaces that have a constant tangent plane along each generator. Since surface normals are orthogonal to the tangent plane and the tangent plane along a generator is constant, all normal vectors along a generator are parallel. This is shown in Figure 4-2.

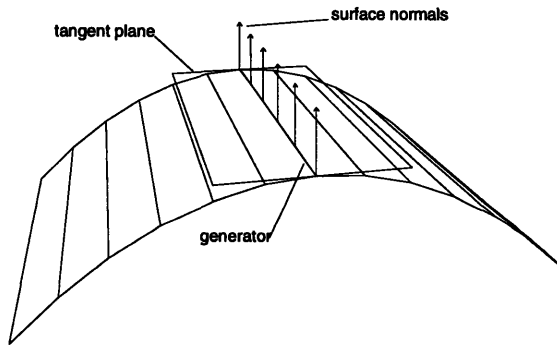


Figure 4-2: A Developable Surface with Tangent Plane along a Ruling

Given two points on a single generator that are selected at parameter values (u_0, v_1) and (u_0, v_2) , the surface is developable if the tangent planes at these points coincide. The tangent planes are defined by the vectors \mathbf{R}_u and \mathbf{R}_v . Using the representation of a ruled surface shown in (4.2), we obtain

$$\mathbf{R}_u(u_0, v_1) = (1 - v_1) \frac{d\mathbf{r}_A(u_0)}{du} + v_1 \frac{d\mathbf{r}_B(u_0)}{du} \quad (4.4)$$

$$\mathbf{R}_u(u_0, v_2) = (1 - v_2) \frac{d\mathbf{r}_A(u_0)}{du} + v_2 \frac{d\mathbf{r}_B(u_0)}{du} \quad (4.5)$$

$$\mathbf{R}_v(u_0, v_1) = \mathbf{R}_v(u_0, v_2) = \mathbf{r}_B(u_0) - \mathbf{r}_A(u_0). \quad (4.6)$$

If the tangent planes at the two points coincide, the vectors $\mathbf{R}_u(u_0, v_1)$, $\mathbf{R}_u(u_0, v_2)$ and $\mathbf{r}_B(u_0) - \mathbf{r}_A(u_0)$ must be coplanar. Therefore, the triple product must equal zero:

$$|\mathbf{R}_u(u_0, v_1) \ \mathbf{R}_u(u_0, v_2) \ (\mathbf{r}_B(u_0) - \mathbf{r}_A(u_0))| = 0. \quad (4.7)$$

Let $\mathbf{R}_u(u_0, v_1) = \mathbf{R}_{u1}$ and $\mathbf{R}_u(u_0, v_2) = \mathbf{R}_{u2}$. Then

$$\mathbf{R}_{u1} \times \mathbf{R}_{u2} = [\mathbf{R}_{u1}^y \mathbf{R}_{u2}^z - \mathbf{R}_{u1}^z \mathbf{R}_{u2}^y] \hat{\mathbf{i}} - [\mathbf{R}_{u1}^x \mathbf{R}_{u2}^z - \mathbf{R}_{u1}^z \mathbf{R}_{u2}^x] \hat{\mathbf{j}} + [\mathbf{R}_{u1}^x \mathbf{R}_{u2}^y - \mathbf{R}_{u1}^y \mathbf{R}_{u2}^x] \hat{\mathbf{k}} \quad (4.8)$$

Expanding the first term of (4.8) by employing (4.4) and (4.5) yields

$$\begin{aligned} \mathbf{R}_{u1}^y \mathbf{R}_{u2}^z - \mathbf{R}_{u1}^z \mathbf{R}_{u2}^y &= [(1 - v_1) \dot{\mathbf{r}}_A^y + v_1 \dot{\mathbf{r}}_B^y][(1 - v_2) \dot{\mathbf{r}}_A^z + v_2 \dot{\mathbf{r}}_B^z] \\ &\quad - [(1 - v_1) \dot{\mathbf{r}}_A^z + v_1 \dot{\mathbf{r}}_B^z][(1 - v_2) \dot{\mathbf{r}}_A^y + v_2 \dot{\mathbf{r}}_B^y] \\ &= (1 - v_1)(1 - v_2) \dot{\mathbf{r}}_A^y \dot{\mathbf{r}}_A^z + v_1(1 - v_2) \dot{\mathbf{r}}_A^z \dot{\mathbf{r}}_B^y + v_2(1 - v_1) \dot{\mathbf{r}}_A^y \dot{\mathbf{r}}_B^z + v_1 v_2 \dot{\mathbf{r}}_B^y \dot{\mathbf{r}}_B^z - \\ &\quad [(1 - v_1)(1 - v_2) \dot{\mathbf{r}}_A^z \dot{\mathbf{r}}_A^y + v_1(1 - v_2) \dot{\mathbf{r}}_A^y \dot{\mathbf{r}}_B^z + v_2(1 - v_1) \dot{\mathbf{r}}_A^z \dot{\mathbf{r}}_B^y + v_1 v_2 \dot{\mathbf{r}}_B^z \dot{\mathbf{r}}_B^y] \\ &= (v_1 - v_1 v_2 - v_2 + v_1 v_2) \dot{\mathbf{r}}_A^z \dot{\mathbf{r}}_B^y + (v_2 - v_1 v_2 - v_1 + v_1 v_2) \dot{\mathbf{r}}_A^y \dot{\mathbf{r}}_B^z \\ &= (v_2 - v_1)(\dot{\mathbf{r}}_A^y \dot{\mathbf{r}}_B^z - \dot{\mathbf{r}}_A^z \dot{\mathbf{r}}_B^y). \end{aligned}$$

Similarly,

$$\mathbf{R}_{u1}^x \mathbf{R}_{u2}^z - \mathbf{R}_{u1}^z \mathbf{R}_{u2}^x = (v_2 - v_1)(\dot{\mathbf{r}}_A^x \dot{\mathbf{r}}_B^z - \dot{\mathbf{r}}_A^z \dot{\mathbf{r}}_B^x)$$

and

$$\mathbf{R}_{u1}^x \mathbf{R}_{u2}^y - \mathbf{R}_{u1}^y \mathbf{R}_{u2}^x = (v_2 - v_1)(\dot{\mathbf{r}}_A^x \dot{\mathbf{r}}_B^y - \dot{\mathbf{r}}_A^y \dot{\mathbf{r}}_B^x).$$

Therefore,

$$\mathbf{R}_{u1} \times \mathbf{R}_{u2} = (v_2 - v_1)(\dot{\mathbf{r}}_A \times \mathbf{r}_B)$$

and thus (4.7) can be reduced to

$$(\mathbf{r}_B(u) - \mathbf{r}_A(u)) \times \dot{\mathbf{r}}_A(u) \cdot \dot{\mathbf{r}}_B(u) = 0 \quad (4.9)$$

for any u as long as $v_1 \neq v_2$. Conversely, any surface that satisfies (4.9) must satisfy (4.7) and, therefore, the tangent planes must be the same and the surface must be developable. Thus, a surface is developable if and only if (4.9) is satisfied. Substituting (4.3) into (4.9) and using the fact that $\dot{\mathbf{r}}_A \times \dot{\mathbf{r}}_A = \mathbf{0}$ yields the equivalent condition

$$\dot{\boldsymbol{\alpha}} \times \boldsymbol{\beta} \cdot \dot{\boldsymbol{\beta}} = 0. \quad (4.10)$$

Developable Surfaces - Envelopes of Families of Planes

An alternative representation of a developable surface is as an *envelope* of a family of planes. The concept of an envelope will be described here for a family of curves, then extended to planes. First, we represent a curve as $\mathbf{r}(u, \alpha)$ where u is the curve parameter and α is the family parameter. In other words, each curve in the family is $\mathbf{r}(u, \alpha_n)$. There may be a curve $\mathbf{r}_e(\alpha)$ that is tangent to each curve in the family, as shown in Figure 4-3. This curve

would be the envelope of that family of curves [11].

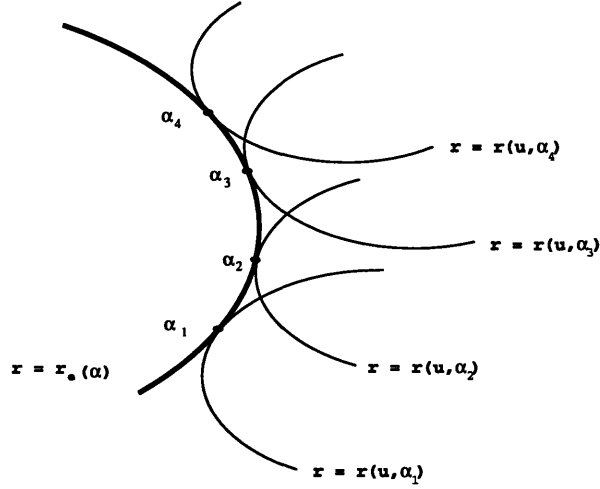


Figure 4-3: An Envelope of a Family of Curves

Similarly, a surface can be the envelope of a family of surfaces. Let a one-parameter family of surfaces be represented by $G(\mathbf{x}, \alpha)$, where α is the family parameter, and assume that the surfaces are twice continuously differentiable. Also assume that consecutive surfaces intersect one another. The intersection is

$$G(\mathbf{x}, \alpha) = 0 \quad G(\mathbf{x}, \alpha + h) = 0$$

where $|h|$ is sufficiently small. This may also be represented by

$$\frac{G(\mathbf{x}, \alpha + h) - G(\mathbf{x}, \alpha)}{h} = 0. \quad (4.11)$$

The limit of (4.11) as h tends to zero is $\partial G(\mathbf{x}, \alpha) / \partial \alpha = 0$. The set of points represented by

$$G(\mathbf{x}, \alpha) = 0 \quad \frac{\partial G(\mathbf{x}, \alpha)}{\partial \alpha} = 0$$

is the *characteristic* of the surface. If the characteristics of all the possible surfaces in the family form a surface, that surface is called the *envelope*. If the envelope exists, then at every point of the characteristic of a surface in the family, the tangent planes of the surface and of the envelope coincide.

A characteristic point is determined by the intersection of the characteristic with another surface in the family. These points of intersection are determined by

$$G(\mathbf{x}, \alpha) = 0 \quad \frac{\partial G(\mathbf{x}, \alpha)}{\partial \alpha} = 0 \quad G(\mathbf{x}, \alpha + k) = 0.$$

where $|k|$ is sufficiently small. Using the Taylor series expansion

$$G(\mathbf{x}, \alpha + k) = G(\mathbf{x}, \alpha) + k \frac{\partial G(\mathbf{x}, \alpha)}{\partial \alpha} + \frac{k^2}{2} \frac{\partial^2 G(\mathbf{x}, \alpha + \theta k)}{\partial \alpha^2}, \quad 0 < \theta < 1,$$

the third equation can be rewritten as

$$\frac{\partial^2 G(\mathbf{x}, \alpha + \theta k)}{\partial \alpha^2} = 0.$$

Then, taking the limit as k approaches zero, the characteristic points of the surface are

$$G(\mathbf{x}, \alpha) = 0 \quad \frac{\partial G(\mathbf{x}, \alpha)}{\partial \alpha} = 0 \quad \frac{\partial^2 G(\mathbf{x}, \alpha)}{\partial \alpha^2} = 0.$$

If the characteristic points exist and if they form a curve as α varies, the curve lies on the envelope of the family and is called the *edge of regression* of the envelope. If the envelope and the edge of regression exist, then, at every point of the edge of regression, the tangents of the edge of regression and the corresponding characteristics coincide. The characteristics then form two sheets corresponding to the tangents of the edge of regression in the positive and negative directions. These sheets form a cusp at the edge of regression, as shown in Figure 4-4.

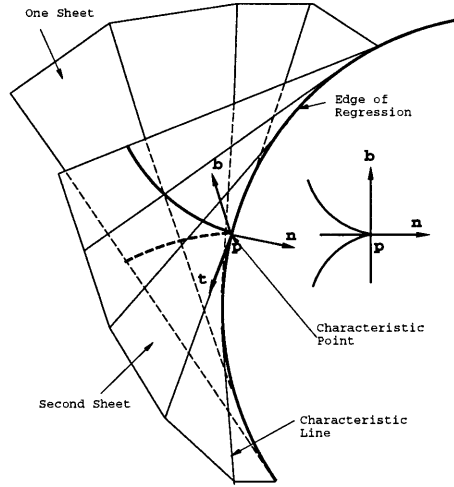


Figure 4-4: Edge of Regression

Let us now consider a family of planes and their derivatives which can be represented by

$$\begin{aligned} G(\mathbf{x}, \alpha) &= \mathbf{a}(\alpha) \cdot \mathbf{x} + c(\alpha) = 0 \\ \frac{\partial G}{\partial \alpha} &= \frac{\partial \mathbf{a}}{\partial \alpha} \cdot \mathbf{x} + \frac{\partial c}{\partial \alpha} = 0 \\ \frac{\partial^2 G}{\partial \alpha^2} &= \frac{\partial^2 \mathbf{a}}{\partial \alpha^2} \cdot \mathbf{x} + \frac{\partial^2 c}{\partial \alpha^2} = 0 \end{aligned}$$

where $\mathbf{a}(\alpha)$ is the unit normal vector to the corresponding plane. When all planes are parallel, no intersection exists and no characteristic curves are formed. When all planes intersect in a single line forming a pencil, the envelope is a line instead of a surface. Therefore, these two cases are excluded [26]. When the envelope exists, it is formed of the characteristics of the family of planes. Since planes intersect in straight lines, the envelope is a ruled surface. Furthermore, the tangent plane along a characteristic is constant since this is an envelope of planes, and hence the surface is developable.

When the vectors $\mathbf{a}(\alpha)$ are all parallel to a single plane P, then all the planes in the family are parallel to a vector normal to the plane P. Thus, the envelope of the family of planes forms a cylinder (except when they form a pencil which has been excluded). When all the characteristic points coincide, all the characteristics intersect in a single point and the surface is a cone. When the characteristic points form a curve, the curve is the edge of regression and the surface is the tangent surface to the curve. Therefore, all developable surfaces can be represented as planes, cylinders, cones and tangent surfaces, or combinations thereof [41].

This description of developable surfaces leads to the following duality between space curves and developable surfaces [41, p.72]:

<i>Curves</i>	<i>Developable Surfaces</i>
2 points determine a line.	2 planes determine a line.
3 points determine a plane.	3 planes determine a point.
2 consecutive points on a curve determine a tangent line.	2 consecutive planes of the family of planes determine a characteristic line.
The curve is the envelope of tangents.	The developable surface is generated by characteristic lines.

Gaussian Curvature

Using equation (4.1)

$$\mathbf{R}(u, v) = \alpha(u) + v\beta(u),$$

the first and second derivatives of a surface can be represented as

$$\mathbf{R}_u(u, v) = \dot{\alpha}(u) + v\dot{\beta}(u) \quad (4.12)$$

$$\mathbf{R}_v(u, v) = \beta(u) \quad (4.13)$$

$$\mathbf{R}_{uu}(u, v) = \ddot{\alpha}(u) + v\ddot{\beta}(u) \quad (4.14)$$

$$\mathbf{R}_{uv}(u, v) = \dot{\beta}(u) \quad \text{and} \quad (4.15)$$

$$\mathbf{R}_{vv}(u, v) = 0. \quad (4.16)$$

Also recall from (2.9) that

$$EG - F^2 = |\mathbf{R}_u \times \mathbf{R}_v|^2 > 0$$

for a regular surface. The surface normal is given by (2.7)

$$\begin{aligned} \mathbf{N} &= \frac{\mathbf{R}_u \times \mathbf{R}_v}{|\mathbf{R}_u \times \mathbf{R}_v|} \\ &= \frac{(\dot{\alpha}(u) + v\dot{\beta}(u)) \times \beta(u)}{\sqrt{EG - F^2}} \\ &= \frac{\dot{\alpha}(u) \times \beta(u) + v(\dot{\beta}(u) \times \beta(u))}{\sqrt{EG - F^2}} \\ &= \frac{\dot{\alpha}(u) \times \beta(u)}{\sqrt{EG - F^2}}. \end{aligned} \quad (4.17)$$

Recall from (2.23) that Gaussian curvature is represented as

$$K = \frac{LN - M^2}{EG - F^2}.$$

where, from equations (2.13) and (2.12)

$$\begin{aligned} N &= \mathbf{R}_{vv} \cdot \mathbf{N} \quad \text{and} \\ M &= \mathbf{R}_{uv} \cdot \mathbf{N}. \end{aligned}$$

Thus, from (4.16), $N = 0$ and the Gaussian curvature can be rewritten as

$$\begin{aligned} K &= -\frac{M^2}{EG - F^2} \\ &= -\frac{(\mathbf{R}_{uv} \cdot \mathbf{N})^2}{EG - F^2} \\ &= -\frac{(\dot{\boldsymbol{\beta}}(u) \cdot \dot{\boldsymbol{\alpha}}(u) \times \boldsymbol{\beta}(u))^2}{(EG - F^2)^2} \\ &= -\frac{(\dot{\boldsymbol{\alpha}} \times \boldsymbol{\beta} \cdot \dot{\boldsymbol{\beta}})^2}{(EG - F^2)^2}. \end{aligned} \tag{4.18}$$

Thus, from condition (4.10), zero Gaussian curvature is a sufficient and necessary condition for a surface to be developable.

Since the Gaussian curvature of a developable surface is zero everywhere, the maximum and minimum principal curvatures (2.21) and (2.22) of a developable surface can be written as

$$\kappa_{max} = H + |H|, \quad \kappa_{min} = H - |H|.$$

These principal curvatures reduce to

$$\kappa_{max} = 2H, \quad \kappa_{min} = 0 \quad \text{when } H > 0, \tag{4.19}$$

$$\kappa_{max} = 0, \quad \kappa_{min} = 0 \quad \text{when } H = 0 \quad \text{and} \tag{4.20}$$

$$\kappa_{max} = 0, \quad \kappa_{min} = 2H \quad \text{when } H < 0. \tag{4.21}$$

It is clear from equations (4.19) to (4.21) that at least one of the principal curvatures is always zero on a developable surface, which agrees with the fact that the Gaussian curvature is zero everywhere (see equation (4.18)). κ_{max} and κ_{min} from (4.19) and (4.21) respectively are each termed the *nonzero principal curvature*, κ^* , where

$$\kappa^* = 2H. \tag{4.22}$$

Mapping

Isometric mapping is defined as a mapping that preserves arc lengths between the mapped surfaces. Two surfaces that can be isometrically mapped to one another are called *isometrics*. Since arc lengths are preserved, the first fundamental forms of isometrics are the same. Since the Gaussian curvature of a surface and the geodesic curvature of a curve on a surface depend only upon the coefficients of the first fundamental form, corresponding points

on two isometric surfaces have the same Gaussian curvature and corresponding curves on isometric surfaces have the same geodesic curvature at corresponding points [26].

A *conformal* mapping is one in which the angle between every pair of intersecting arcs is the same on both surfaces. This occurs if the coefficients of the first fundamental form on the original surface are proportional to those on the inverse surface [26]. Therefore, every isometric surface is conformal.

Since a plane has zero Gaussian curvature, only a surface with zero Gaussian curvature can be mapped to it. Therefore, only a developable surface can be isometrically mapped to a plane [26, p.189].

Since the tangent planes along any ruling are constant, developable surfaces can be unrolled, or developed, isometrically into a plane without stretching or tearing by successively placing each ruling on the plane. One can think of a developable surface as a paper with folds. As the number of folds approaches infinity, the surface becomes smooth. The surface can then be unfolded again into a plane. This is shown in Figure 4-5.

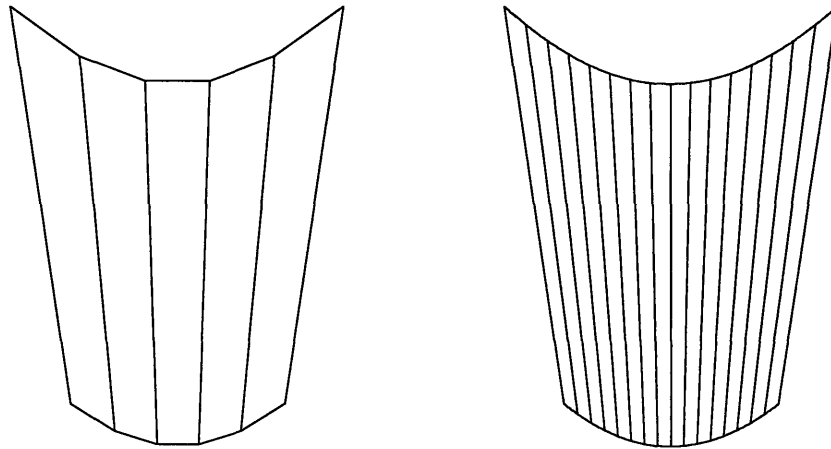


Figure 4-5: A Surface with Folds and a Developable Surface

A geodesic represents the curve with the shortest length between two points on a surface. Therefore, geodesics on a plane are straight lines. Since developable surfaces map isometrically to planes, geodesics on developable surfaces map to straight lines on a plane and straight lines on a plane map to geodesics on a developable surface.

Developable Surface Properties

The following statements are equivalent necessary and sufficient conditions for a surface to be developable. Each has been described above. Thorough proofs can be found in Struik [41] and Kreyszig [26].

1. Developable surfaces possess the same tangent plane at all points of the same generator.
2. The normal vectors on a developable surface along a ruling are parallel.
3. A developable surface is the envelope of a one-parameter family of planes.
4. Gaussian curvature is zero.

5. The mapping of a developable surface onto a plane is isometric.
6. Geodesics on a developable surface map to straight lines on a plane, and straight lines on a plane map into geodesics on a developable surface.

Chapter 5

Design With B-Spline Developable Surfaces

5.1 Introduction and Literature Review

In the current literature, there are three main approaches to representing developable surfaces in Bézier form. These approaches are described below. This chapter explores user-friendly methods for the design of developable surfaces. Section 5.2 describes the design of developable B-spline strip surfaces that lie between parallel planes. Section 5.3 describes the design of developable B-spline surfaces with general three-dimensional directrices. The development of a developable surface onto a plane is described in Section 5.4. This is an efficient implementation of the method in the current literature, also described below. Section 5.5 provides some engineering examples.

5.1.1 Developable Bézier Strips

Aumann [1] provides the basis for a user friendly and computationally inexpensive method of designing developable surfaces. He represents developable surfaces in terms of two Bézier curves (directrices) and rulings between pairs of points from each curve, as discussed in Section 4.2, but restricts the two directrices ($\mathbf{r}_A(u), \mathbf{r}_B(u)$) to lie on parallel planes so that the tangent vectors $\dot{\mathbf{r}}_A(u)$ and $\dot{\mathbf{r}}_B(u)$ are parallel, i.e. $\dot{\mathbf{r}}_B(u) = \rho(u)\dot{\mathbf{r}}_A(u)$, where $\rho(u)$ is a linear function of u . This condition automatically satisfies the condition (4.9).

His design philosophy is to consider $\mathbf{r}_A(u)$ as a design curve, which means its degree, knot vector and control points are specified. In addition, the two end points $\mathbf{r}_B(0)$ and $\mathbf{r}_B(1)$ of the resulting directrix are provided as boundary conditions. The knots and internal control points of the second directrix $\mathbf{r}_B(u)$ are then computed using a simple system of linear equations. He investigates the case when the design curve is a cubic Bézier curve and $\rho(u)$ is a linear function of u . Hence, the resulting directrix is quartic. Figure 5-1 illustrates the terminology.

Frey and Bindschadler [14] extend the work of Aumann [1] by generalizing the degree of the directrices and by considering the case where $\rho(u)$ is quadratic. Aumann [2] further extends his work so $\mathbf{r}_A(u)$ and $\mathbf{r}_B(u)$ have the same degree. All three papers discuss regularity conditions of the developable surfaces.

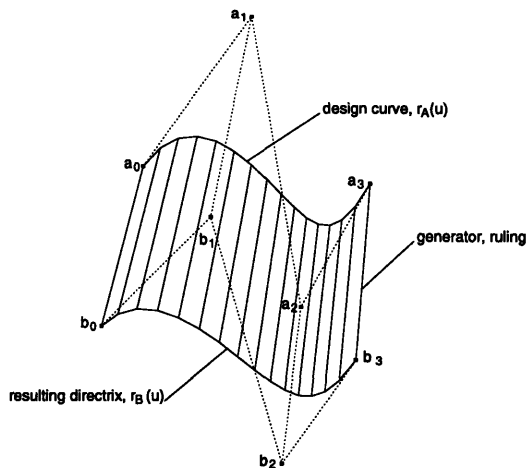


Figure 5-1: A Developable Surface

5.1.2 Duality Between Points and Planes

The second approach, introduced by Bodduluri and Ravani [3], is based on the representation of developable surfaces as an envelope of a one-parameter set of planes as described in Section 4.2. They express the surfaces in terms of plane geometry using the concept of duality between points and planes in 3D projective space. They interpret the developable surface as the set of its tangent planes represented in the dual form. Their method is mathematically elegant; however, it is somewhat less user friendly and requires a conversion to a standard tensor product form [37].

Pottmann and Farin [37] generalize the results of Bodduluri and Ravani [3] by providing algorithms for converting the dual representation of developables to standard tensor product form. Hoschek and Pottmann [23] derive algorithms for interpolation or approximation with developable B-spline surfaces. Given a developable surface patch Ω , they pick out an appropriate number of tangent planes Y_i of a developable surface patch Ω , and either interpolate or approximate this data with a developable B-spline surface.

5.1.3 Nonlinear Representation

The third approach is due to Lang and Röschel [29]. They obtain conditions for the control nets and weights of rational Bézier surfaces to be developable, which leads to a complicated nonlinear system of conditions. Although their work provides a useful criterion for checking the developability of a given ruled surface patch, it is difficult to design a developable surface with this method.

5.1.4 Development

Faux and Pratt [11] provided a method for the development of a curve on a developable surface onto a plane based on the fact that a developable surface maps isometrically onto a plane. This method is also described by Gurunathan and Dhande [16]. Another method is described by Clements and Leon [7], in which a geodesic on the surface is mapped to the plane and points on the plane are determined in reference to this geodesic. This method,

however, requires the mapping of the geodesic and then the calculation of the location of each edge, and is therefore slower than the other method [11].

5.2 B-Spline Developable Surfaces with Directrices in Parallel Planes

This section further extends Aumann's work [1] such that n Bézier developable surfaces, whose two directrices lie in parallel planes, are strung together by joining them along their end rulings. In this manner, they can be represented as a single B-spline surface with C^2 continuity.

From Section 4.2, a surface is developable if and only if the tangent plane is constant along a generator. If the two directrices $\mathbf{r}_A(u)$ and $\mathbf{r}_B(u)$ are restricted to lie in parallel planes, then the tangent vectors to $\mathbf{r}_A(u)$ and $\mathbf{r}_B(u)$ must be parallel at every u for the surface to be developable. Therefore, condition (4.9) is equivalent to

$$\dot{\mathbf{r}}_B(u) = \rho(u)\dot{\mathbf{r}}_A(u) \quad (5.1)$$

where $\rho(u)$ is a scalar function of u . In this thesis, $\rho(u)$ is selected to be linear, expressed as

$$\rho(u) = \rho_0(1 - u) + \rho_1 u.$$

The design philosophy is to consider $\mathbf{r}_A(u)$ as a design curve [1, 14], which means its degree, knot vector and control points are specified. Also, the two end points $\mathbf{r}_B(0)$ and $\mathbf{r}_B(1)$ are provided as boundary conditions. The knots and internal control points of the second directrix, $\mathbf{r}_B(u)$, are then computed. Since multiplication of B-spline functions is complex and computationally expensive, the Bézier segments are first extracted from the B-spline curve by knot insertion using Boehm's algorithm [22] described in Section 3.3.

Figure 5-2(a) shows the design curve $\mathbf{r}_A(u)$ which is a planar cubic B-spline curve with knot vector $T = (0 \ 0 \ 0 \ 0 \ \frac{1}{3} \ \frac{2}{3} \ 1 \ 1 \ 1 \ 1)$ and control points $(0, 2, 0)$, $(0.8, 0.5, 0)$, $(1.6, 1.5, 0)$, $(2.4, 1.5, 0)$, $(2.6, -0.5, 0)$ and $(4, 0, 0)$. Figure 5-2(b) shows three Bézier segments after knot insertion with the two endpoints of $\mathbf{r}_B(u)$, which are supplied by the user to be $\mathbf{r}_B(0) = (-1, 3, -3)$ and $\mathbf{r}_B(1) = (2, 1.3, -3)$. Note that $\mathbf{r}_A(u)$ is in the $z = 0$ plane and the \mathbf{r}_B endpoints are in the $z = 3$ plane, parallel to the plane of \mathbf{r}_A .

Let $\mathbf{r}_A(u)$ be a degree n curve with m Bézier segments. Since $\rho(u)$ is linear, the degree of $\mathbf{r}_B(u)$ is $n + 1$. We denote the j th Bézier segments as

$$\begin{aligned} \mathbf{r}_A^j(u) &= \sum_{i=0}^n \mathbf{a}_{jn+i} B_{i,n}(u) \quad j = 0, \dots, m-1 \quad \text{and} \\ \mathbf{r}_B^j(u) &= \sum_{i=0}^{n+1} \mathbf{b}_{j(n+1)+i} B_{i,n+1}(u) \quad j = 0, \dots, m-1. \end{aligned} \quad (5.2)$$

The control points \mathbf{a} and \mathbf{b} are two-dimensional vectors since they have been restricted to lie in parallel z planes. Substituting (5.2) into equation (5.1) yields

$$(n+1) \sum_{i=0}^n (\mathbf{b}_{j(n+1)+i+1} - \mathbf{b}_{j(n+1)+i}) B_{i,n}(u)$$

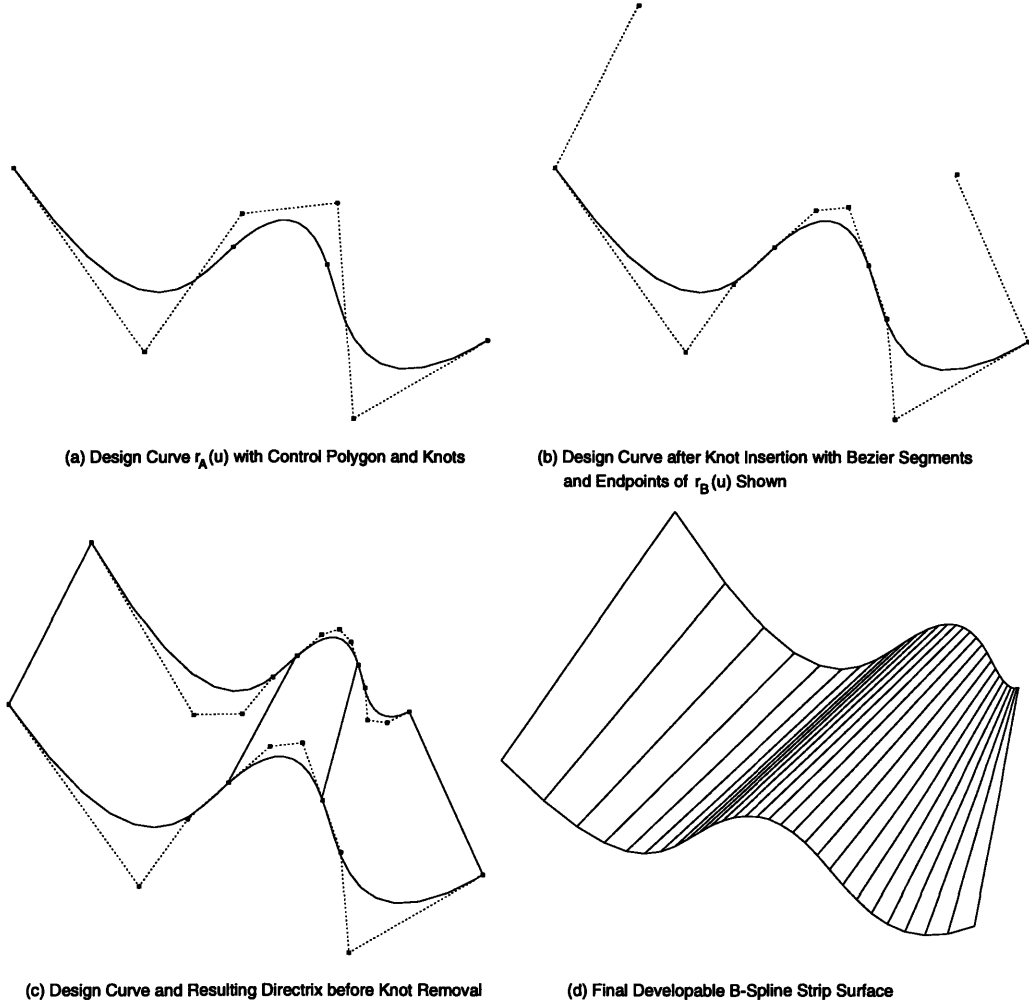


Figure 5-2: Design of Developable B-Spline Strip Surface

$$\begin{aligned}
 &= \rho(u)n \sum_{i=0}^{n-1} (\mathbf{a}_{jn+i+1} - \mathbf{a}_{jn+i}) B_{i,n-1}(u) \\
 &= n \sum_{i=0}^{n-1} (\rho_0(1-u) + \rho_1 u) (\mathbf{a}_{jn+i+1} - \mathbf{a}_{jn+i}) B_{i,n-1}(u) \quad (5.3)
 \end{aligned}$$

for $j = 0, \dots, m-1$. Using the definition of a Bernstein polynomial (3.1),

$$\begin{aligned}
 (1-u)B_{i,n-1}(u) &= (1-u) \frac{(n-1)!}{i!(n-1-i)!} (1-u)^{n-1-i} u^i \\
 &= \frac{n-1}{n} \frac{(n)!}{i!(n-i)!} (1-u)^{n-i} u^i \\
 &= \frac{n-1}{n} B_{i,n}(u) \quad (5.4)
 \end{aligned}$$

and

$$\begin{aligned}
uB_{i,n-1}(u) &= u \frac{(n-1)!}{i!(n-1-i)!} (1-u)^{n-1-i} u^i \\
&= \frac{i+1}{n} \frac{n!}{(i+1)!(n-(i+1))!} (1-u)^{n-(i+1)} u^{i+1} \\
&= \frac{i+1}{n} B_{i+1,n}(u).
\end{aligned} \tag{5.5}$$

Substituting (5.4) and (5.5) into (5.3) yields

$$\begin{aligned}
(n+1) \sum_{i=0}^n (\mathbf{b}_{j(n+1)+i+1} - \mathbf{b}_{j(n+1)+i}) B_{i,n}(u) \\
&= n \sum_{i=0}^{n-1} [\rho_0(1-u)B_{i,n-1}(u) + \rho_1 u B_{i,n-1}(u)] (\mathbf{a}_{jn+i+1} - \mathbf{a}_{jn+i}) \\
&= \sum_{i=0}^{n-1} [\rho_0(n-i)B_{i,n}(u) + \rho_1(i+1)B_{i+1,n}(u)] (\mathbf{a}_{jn+i+1} - \mathbf{a}_{jn+i}) \\
&= \rho_0 n (\mathbf{a}_{jn+1} - \mathbf{a}_{jn}) B_{0,n}(u) \\
&\quad + \sum_{i=1}^{n-1} [\rho_0(n-i)(\mathbf{a}_{jn+i+1} - \mathbf{a}_{jn+i}) + \rho_1 i (\mathbf{a}_{jn+i} - \mathbf{a}_{jn+i-1})] B_{i,n}(u) \\
&\quad + \rho_1 n (\mathbf{a}_{jn+n} - \mathbf{a}_{jn+n-1}) B_{n,n}(u).
\end{aligned}$$

Since Bernstein basis polynomials are linearly independent, each set of coefficients must be equal, yielding the following system of $n-1$ equations [14] for the j th Bézier segment

$$\begin{aligned}
n\rho_0^j (\mathbf{a}_{jn+1} - \mathbf{a}_{jn}) &= (n+1)(\mathbf{b}_{j(n+1)+1} - \mathbf{b}_{j(n+1)}) \tag{5.6} \\
(n-i)\rho_0^j (\mathbf{a}_{jn+i+1} - \mathbf{a}_{jn+i}) + i\rho_1^j (\mathbf{a}_{jn+i} - \mathbf{a}_{jn+i-1}) &= (n+1)(\mathbf{b}_{j(n+1)+i+1} - \mathbf{b}_{j(n+1)+i}) \\
n\rho_1^j (\mathbf{a}_{(j+1)n} - \mathbf{a}_{(j+1)n-1}) &= (n+1)(\mathbf{b}_{(j+1)(n+1)} - \mathbf{b}_{(j+1)(n+1)-1}),
\end{aligned}$$

where $i = 1, \dots, n-1$.

Now consider joining two consecutive Bézier patches with C^2 continuity. First, C^1 continuity requires that the first derivatives along the connecting edges of both patches must be equal. Since the connecting edge is a ruling and is therefore linear, this requirement reduces to

$$\dot{\mathbf{r}}_A^j(1) = \dot{\mathbf{r}}_A^{j+1}(0) \tag{5.7}$$

$$\dot{\mathbf{r}}_B^j(1) = \dot{\mathbf{r}}_B^{j+1}(0). \tag{5.8}$$

From equation (5.1) we have

$$\begin{aligned}
\dot{\mathbf{r}}_B^j(1) &= \rho^j(1) \dot{\mathbf{r}}_A^j(1) \\
\dot{\mathbf{r}}_B^{j+1}(0) &= \rho^{j+1}(0) \dot{\mathbf{r}}_A^{j+1}(0).
\end{aligned} \tag{5.9}$$

Substituting equations (5.9) into equation (5.8) and using equation (5.7) yields

$$\rho_1^j = \rho_0^{j+1}. \tag{5.10}$$

C^2 continuity requires that the second derivatives along the connecting edges must be equal. Again, the connecting edge is linear, which reduces this requirement to

$$\ddot{\mathbf{r}}_A^j(1) = \ddot{\mathbf{r}}_A^{j+1}(0) \quad (5.11)$$

$$\ddot{\mathbf{r}}_B^j(1) = \ddot{\mathbf{r}}_B^{j+1}(0). \quad (5.12)$$

Taking the derivative of equation (5.1) yields

$$\dot{\mathbf{r}}_B(u) = \rho(u)\dot{\mathbf{r}}_A(u) + \dot{\rho}(u)\dot{\mathbf{r}}_A(u) \quad (5.13)$$

where

$$\dot{\rho}(u) = \rho_1 - \rho_0.$$

Evaluating equation (5.13) at the connecting edge yields

$$\begin{aligned} \dot{\mathbf{r}}_B^j(1) &= \rho_1^j \dot{\mathbf{r}}_A^j(1) + (\rho_1^j - \rho_0^j) \dot{\mathbf{r}}_A^j(1) \\ \dot{\mathbf{r}}_B^{j+1}(0) &= \rho_0^{j+1} \dot{\mathbf{r}}_A^{j+1}(0) + (\rho_1^{j+1} - \rho_0^{j+1}) \dot{\mathbf{r}}_A^{j+1}(0). \end{aligned} \quad (5.14)$$

Substituting equations (5.14) into equation (5.12) and using equation (5.11) yields

$$2\rho_0^{j+1} = \rho_0^j + \rho_1^{j+1}. \quad (5.15)$$

Each Bézier patch has $n + 1$ control points along $\mathbf{r}_A(u)$ and $n + 2$ control points along $\mathbf{r}_B(u)$, where n is the degree of the original B-spline design curve. The system of equations for a single patch derived in equation (5.6) can be solved for the coefficients of the second directrix

$$\begin{aligned} \mathbf{b}_{j(n+1)+1} &= \mathbf{b}_{j(n+1)} + \frac{n}{n+1} \rho_0^j (\mathbf{a}_{jn+1} - \mathbf{a}_{jn}) \\ \mathbf{b}_{j(n+1)+i+1} &= \mathbf{b}_{j(n+1)+i} + \frac{n-i}{n+1} \rho_0^j (\mathbf{a}_{jn+i+1} - \mathbf{a}_{jn+i}) \\ &\quad + \frac{i}{n+1} \rho_1^j (\mathbf{a}_{jn+i} - \mathbf{a}_{jn+i-1}), \quad i = 1, \dots, n-1 \\ \mathbf{b}_{(j+1)(n+1)} &= \mathbf{b}_{(j+1)(n+1)-1} + \frac{n}{n+1} \rho_1^j (\mathbf{a}_{(j+1)n} - \mathbf{a}_{(j+1)(n-1)}) \end{aligned} \quad (5.16)$$

where $j = 0, \dots, m-1$ for a system of m patches. Adding equations (5.16) for m patches yields a vector equation that can be solved for ρ_0^0 and ρ_1^{m-1} in terms of the first and last points of the second directrix:

$$\mathbf{b}_{m(n+1)} - \mathbf{b}_0 = \rho_0^0 \mathbf{v}_0 + \rho_1^{m-1} \mathbf{v}_1 \quad (5.17)$$

where

$$\begin{aligned} \mathbf{v}_0 &= \left[\frac{1}{m(n+1)} \left(\sum_{i=0}^{mn} \mathbf{a}_i + \sum_{i=1}^{m-1} \mathbf{a}_{in} \right) - \mathbf{a}_0 \right] \quad \text{and} \\ \mathbf{v}_1 &= \left[\mathbf{a}_{mn} - \frac{1}{m(n+1)} \left(\sum_{i=0}^{mn} \mathbf{a}_i + \sum_{i=1}^{m-1} \mathbf{a}_{in} \right) \right]. \end{aligned}$$

Combining equations (5.10) and (5.15), we can express ρ_0^j and ρ_1^{j+1} in terms of the two end coefficients ρ_0^0 and ρ_1^{m-1} as follows:

$$\rho_1^{j-1} = \rho_0^j = \frac{m-j}{m}\rho_0^0 + \frac{j}{m}\rho_1^{m-1} \quad j = 0, \dots, m-1. \quad (5.18)$$

Therefore, given a design directrix, $\mathbf{r}_A(u)$, and the endpoints of the second directrix, $\mathbf{r}_B(0)$ and $\mathbf{r}_B(1)$, all the interior control points of the second directrix can be obtained successively using equations (5.16). After the second directrix is calculated, the first directrix is degree elevated so the two curves may be combined into a B-spline strip. Any knots that may be removed from the surface while leaving the curve geometrically and parametrically unchanged are removed using the knot removal technique [42] described in Section 3.2.

Figure 5-2(c) shows the computed $\mathbf{r}_B(u)$ together with $\mathbf{r}_A(u)$ in Bézier form and the two end rulings. Figure 5-2(d) shows the final B-spline developable surface after knot removal.

Developable surfaces become irregular when $|\mathbf{R}_u \times \mathbf{R}_v|$ vanishes, which leads to the regularity condition for a strip surface [14]

$$\rho(u) > 0, \quad 0 \leq u \leq 1.$$

From a user's point of view, once he/she determines one of the endpoints, it is convenient to know the range that the other end point can take. From (5.18) it can be seen that if both ρ_0^0 and ρ_1^{m-1} are positive, then all ρ coefficients are positive and the surface is regular. The coefficients ρ can be determined by solving the vector equation (5.17). The resulting equations for ρ_0^0 and ρ_1^{m-1} must be positive for the surface to be regular, yielding the following restrictions:

$$\rho_0^0 = \frac{(b_{m(n+1)}^x - b_0^x)v_1^y - (b_{m(n+1)}^y - b_0^y)v_1^x}{v_0^x v_1^y - v_1^x v_0^y} > 0 \quad (5.19)$$

and

$$\rho_1^{m-1} = \frac{(b_{m(n+1)}^y - b_0^y)v_0^x - (b_{m(n+1)}^x - b_0^x)v_0^y}{v_0^x v_1^y - v_1^x v_0^y} > 0 \quad (5.20)$$

where the superscripts denote the x and y components of the vectors. Given one endpoint, a regular surface may be formed by selecting the second endpoint to lie within the range of values determined by equations (5.19) and (5.20).

It is also interesting to observe [14] that when the two vectors joining two end points of each directrix are parallel and their magnitudes are multiples of a constant, the resulting developable surface is a generalized cone. When the constant is equal to one, the surface is a cylindrical surface. In other words, if $\rho(u)$ is a constant not equal to one, the surface is a generalized cone, and if $\rho(u) = 1$, the surface is a cylinder.

Algorithm

The following steps describe the algorithm for the solution method.

1. The user provides the design curve $\mathbf{r}_A(u)$ and the endpoint $\mathbf{r}_B(0)$. The program provides a range of values for $\mathbf{r}_B(1)$ that ensure a regular surface, and the user supplies a specific value for $\mathbf{r}_B(1)$.

2. Bézier segments are extracted from $\mathbf{r}_A(u)$ by knot insertion.
3. The system of equations (5.16) is solved for the internal control points of $\mathbf{r}_B(u)$.
4. Once the resultant directrix $\mathbf{r}_B(u)$ is computed, the developable Bézier surface is obtained by degree raising $\mathbf{r}_A(u)$ and substituting in equation (4.2).
5. Knots that can be removed while leaving the surface unchanged are removed using the method described in Section 3.2.

5.3 Developable Surfaces with 3D Directrices

5.3.1 Developable $(n, 1)$ Bézier Surfaces

In Section 5.2, we restricted the two directrices to lie on parallel planes. In such case, $\dot{\mathbf{r}}_A(u)$ and $\dot{\mathbf{r}}_B(u)$ must be parallel to satisfy condition (4.9). In this section, the directrices are not constrained to lie on parallel planes, so equation (5.1), $\dot{\mathbf{r}}_B = \rho(u)\dot{\mathbf{r}}_A$, no longer applies.

The design philosophy here is the same as that of the previous section. Namely, $\mathbf{r}_A(u)$ is designated the design curve with its degree, knot vector and control points specified. The two end points $\mathbf{r}_B(0)$ and $\mathbf{r}_B(1)$ are provided as boundary conditions and the knots and internal control points of the second directrix, $\mathbf{r}_B(u)$ are computed.

We begin this development by assuming the design curve $\mathbf{r}_A(u)$ is a Bézier curve of degree n ,

$$\mathbf{r}_A(u) = \sum_{i=0}^n \mathbf{a}_i B_{i,n}(u), \quad 0 \leq u \leq 1,$$

where $\mathbf{a}_i = (a_i^x, a_i^y, a_i^z)^T$ are control points. The resultant curve $\mathbf{r}_B(u)$ is also a Bézier curve of degree n . In Section 5.3.2 we investigate the case when the curves $\mathbf{r}_A(u)$ and $\mathbf{r}_B(u)$ are B-spline curves. If $\mathbf{b}_i = (b_i^x, b_i^y, b_i^z)^T$, $i = 0, \dots, n$, are the control points of the degree n Bézier curve $\mathbf{r}_B(u)$, and $\bar{\mathbf{a}}_i$, $\bar{\mathbf{b}}_i$ and \mathbf{c}_i are

$$\begin{aligned} \bar{\mathbf{a}}_i &= (\bar{a}_i^x, \bar{a}_i^y, \bar{a}_i^z)^T = \mathbf{a}_{i+1} - \mathbf{a}_i & i = 0, \dots, n-1 \\ \bar{\mathbf{b}}_i &= (\bar{b}_i^x, \bar{b}_i^y, \bar{b}_i^z)^T = \mathbf{b}_{i+1} - \mathbf{b}_i & i = 0, \dots, n-1 \\ \mathbf{c}_i &= (c_i^x, c_i^y, c_i^z)^T = \mathbf{b}_i - \mathbf{a}_i & i = 0, \dots, n, \end{aligned}$$

then equation (4.9) can be expressed as

$$\left(\sum_{i=0}^n \mathbf{c}_i B_{i,n}(u) \right) \times \left(n \sum_{i=0}^{n-1} \bar{\mathbf{a}}_i B_{i,n-1}(u) \right) \cdot \left(n \sum_{i=0}^{n-1} \bar{\mathbf{b}}_i B_{i,n-1}(u) \right) = 0. \quad (5.21)$$

Since equation (5.21) is a scalar polynomial equation of degree $3n - 2$, we can rewrite it (upon division by n^2) in the form

$$\sum_{k=0}^{3n-2} E_k B_{k,3n-2}(u) = 0 \quad (5.22)$$

where

$$E_k = \sum_{i=\max(0,k-n+1)}^{\min(2n-1,k)} (P_i^x \bar{\mathbf{b}}_{k-i}^x - P_i^y \bar{\mathbf{b}}_{k-i}^y + P_i^z \bar{\mathbf{b}}_{k-i}^z) \frac{\binom{2n-1}{i} \binom{n-1}{k-i}}{\binom{3n-2}{k}} \quad (5.23)$$

and

$$\begin{aligned} P_i^x &= \sum_{j=\max(0,i-n+1)}^{\min(n,i)} (c_j^y \bar{a}_{i-j}^z - c_j^z \bar{a}_{i-j}^y) \frac{\binom{n}{j} \binom{n-1}{i-j}}{\binom{2n-1}{i}} \\ P_i^y &= \sum_{j=\max(0,i-n+1)}^{\min(n,i)} (c_j^x \bar{a}_{i-j}^z - c_j^z \bar{a}_{i-j}^x) \frac{\binom{n}{j} \binom{n-1}{i-j}}{\binom{2n-1}{i}} \\ P_i^z &= \sum_{j=\max(0,i-n+1)}^{\min(n,i)} (c_j^x \bar{a}_{i-j}^y - c_j^y \bar{a}_{i-j}^x) \frac{\binom{n}{j} \binom{n-1}{i-j}}{\binom{2n-1}{i}} \end{aligned}$$

using the algorithms for multiplication of polynomials in Bernstein form described by Farouki and Rajan [10]. Since equation (5.22) is valid for all u and the Bernstein basis functions are linearly independent, E_k must be zero for all k , $0 \leq k \leq 3n-2$. This leads us to a system of $3n-1$ polynomial equations with $3(n-1)$ unknowns, i.e. \mathbf{b}_i ($i = 1, \dots, n-1$) where the two boundary points, \mathbf{b}_0 and \mathbf{b}_n , are given. Therefore, there are two more equations than unknowns and the system is overdetermined. The system of equations was solved using a Numerical Algorithms Group program [35] for minimization.

Solution Method Using Unconstrained Optimization

One way to solve the overdetermined system is to seek a least squares solution to $\mathbf{E}(\mathbf{x}) = \mathbf{0}$ where

$$\mathbf{x} = (b_1^x, b_1^y, b_1^z, \dots, b_{n-1}^x, b_{n-1}^y, b_{n-1}^z)^T$$

and

$$\mathbf{E}(\mathbf{x}) = (E_0(\mathbf{x}), E_1(\mathbf{x}), \dots, E_{3n-2}(\mathbf{x}))^T.$$

This can be obtained by minimizing the function

$$F(\mathbf{x}) = \frac{1}{2} (E_0^2(\mathbf{x}) + E_1^2(\mathbf{x}) + \dots + E_{3n-2}^2(\mathbf{x})) = \frac{1}{2} \mathbf{E}^T(\mathbf{x}) \mathbf{E}(\mathbf{x}) = \frac{1}{2} \sum_{i=0}^{3n-2} E_i^2(\mathbf{x}). \quad (5.24)$$

The problem can then be reduced to searching for zeros of the gradient vector field $\nabla F(\mathbf{x})$, i.e.

$$\nabla F(\mathbf{x}) = \mathbf{0}. \quad (5.25)$$

The Newton-Raphson method can be used to iteratively solve the nonlinear system (5.25). The Taylor series expansion about the current point is

$$\nabla F(\mathbf{x} + \delta \mathbf{x}) \approx \mathbf{g}(\mathbf{x}) + [\mathbf{H}(\mathbf{x})] \delta \mathbf{x} \quad (5.26)$$

where $\mathbf{g}(\mathbf{x})$ and $[\mathbf{H}(\mathbf{x})]$ are the gradient vector and the Hessian matrix of the objective function $F(\mathbf{x})$. Using (5.26), the step direction $\delta\mathbf{x}$ is found from

$$[\mathbf{H}(\mathbf{x})]\delta\mathbf{x} = -\mathbf{g}(\mathbf{x}). \quad (5.27)$$

The value for the subsequent iteration, $\bar{\mathbf{x}}$ is

$$\bar{\mathbf{x}} = \mathbf{x} + \delta\mathbf{x}.$$

Using the special properties of a least squares function such as equation (5.24), the derivatives of $F(\mathbf{x})$ are represented as

$$\mathbf{g}(\mathbf{x}) = \nabla F(\mathbf{x}) = [\mathbf{\Lambda}(\mathbf{x})]\mathbf{E}(\mathbf{x})$$

and

$$[\mathbf{H}(\mathbf{x})] = \nabla^2 F(\mathbf{x}) = [\mathbf{\Lambda}(\mathbf{x})][\mathbf{\Lambda}(\mathbf{x})]^T + \sum_{i=0}^{3n-2} E_i(\mathbf{x}) \nabla^2 E_i(\mathbf{x})$$

where

$$[\mathbf{\Lambda}(\mathbf{x})] = [\nabla E_0, \nabla E_1, \dots, \nabla E_{3n-2}]$$

is the $(3n - 3) \times (3n - 1)$ Jacobian matrix, the columns of which are the first derivative vectors ∇E_i of the components of \mathbf{E} ($[\mathbf{\Lambda}_{ij}] = \frac{\partial E_i}{\partial x_j}$).

In any minimization process, the initial approximation for \mathbf{x} greatly affects the resulting solution. Here we use a linear interpolation to obtain the initial values for \mathbf{b}_i , where

$$\mathbf{b}_i = \mathbf{a}_i + \frac{i}{n}(\mathbf{b}_0 - \mathbf{a}_0) + \frac{n-i}{n}(\mathbf{b}_n - \mathbf{a}_n), \quad i = 1, \dots, n-1.$$

Simple Bounds

In many applications, it is helpful to introduce simple bounds on the variables [15] such that $l_i \leq x_i \leq u_i$, where l_i and u_i are lower and upper bounds, respectively. This is a constrained optimization problem; however, it has a particularly simple form. A solution \mathbf{x}^* is termed *feasible* if it satisfies all constraints. A step $\delta\mathbf{x}$ is in a feasible direction if it does not cause \mathbf{x} to exceed any of the bounds.

The following discussion treats a generic iteration, so the iteration number has been left out for simplicity. At any iteration, some of the variables will be equal to their upper or lower bounds. These variables \mathbf{x}_{FX} , are fixed on their bounds and are consequently termed *fixed* variables. The associated bounds are placed in the *active set*. The remaining *free* variables \mathbf{x}_{FR} are allowed to vary within the bounds. The search direction $\delta\mathbf{x}$ is chosen to change only the free variables. Therefore, $\delta\mathbf{x}_{\text{FX}} = 0$ and equation (5.27) reduces to

$$[\mathbf{H}_{\text{FR}}(\mathbf{x})]\delta\mathbf{x}_{\text{FR}} = -\mathbf{g}_{\text{FR}}(\mathbf{x}). \quad (5.28)$$

With $\delta\mathbf{x}_{\text{FR}}$ we update \mathbf{x} for the subsequent iteration as

$$\bar{\mathbf{x}} = \begin{bmatrix} \mathbf{x}_{\text{FR}} + \delta\mathbf{x}_{\text{FR}} \\ \mathbf{x}_{\text{FX}} \end{bmatrix}.$$

If δx_{FR} forces x_{FR} to violate one of the bounds, that bound is added to the active set for the subsequent iteration.

At each iteration, the active set must be analyzed to determine if the constraints in the active set should remain active. A solution \mathbf{x}^* is a local minimum only if there is no feasible step $\delta \mathbf{x}$ that results in a lower value. Thus, if

$$(\delta \mathbf{x})^T \mathbf{g}(\mathbf{x}) \tag{5.29}$$

is non-zero for any $\delta \mathbf{x}$, then \mathbf{x}^* is not a local minimum. Then (5.29) can be represented as

$$\mathbf{g}(\mathbf{x}) = [\mathbf{A}]^T \lambda$$

where $[\mathbf{A}]$ is the set of constraint coefficients and λ are Lagrange multipliers. For simple bounds, $[\mathbf{A}]$ is composed of 1 for l_i and -1 for u_i , so the Lagrange multipliers can be estimated as

$$\lambda_i = \begin{cases} \mathbf{g}_i(\mathbf{x}) & \text{for } x_i = l_i \\ -\mathbf{g}_i(\mathbf{x}) & \text{for } x_i = u_i \end{cases} \tag{5.30}$$

Thus, if a Lagrange multiplier for an active simple bound is negative, the corresponding bound should be removed from the active set for the subsequent iteration.

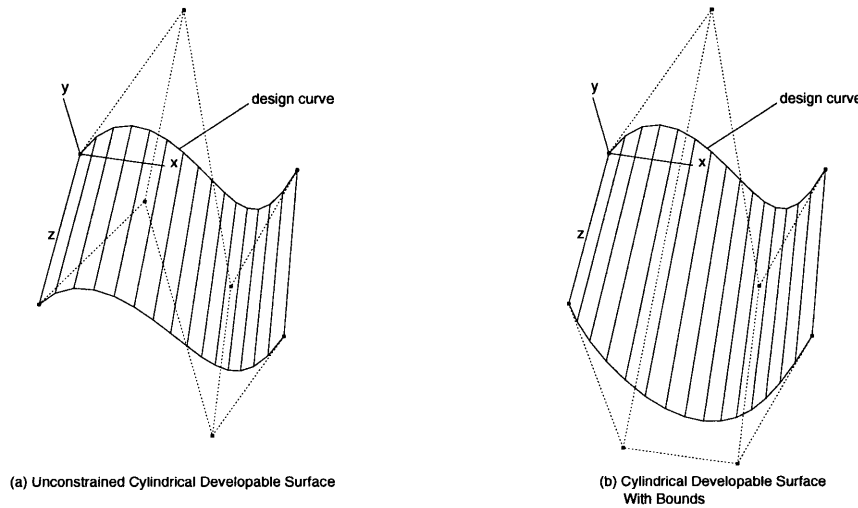


Figure 5-3: Effect of Simple Bounds on Developable Surfaces

Many solutions are possible for a single set of equations. For example, Figure 5-3 shows two equally viable solutions to the same set of equations. Both examples have design curves with control points $(0, 0, 0)$, $(1.8, 3, -0.7)$, $(3.3, -2, 1.5)$ and $(4, 0.5, 0)$ and endpoints $(0, 0, 3)$ and $(4, 0.5, 3)$ for the second directrix. Figure 5-3(a) is unconstrained, yielding interior control points for \mathbf{r}_B of $(1.8, 3, 3)$ and $(3.3, -2, 3)$. Figure 5-3(b) is unconstrained in the x and y directions, but has a lower bound equal to 5 set in the z direction. This produces a resultant curve with interior control points $(1.8, 3, 5)$ and $(3.3, -2, 5)$. Since both cylinders are developable surfaces with C^2 continuity that include the endpoints specified by the user, they are equally valid solutions to the equations. Both surfaces are exactly developable with zero Gaussian curvature. Although this example is rather trivial, it demonstrates the control available to the user to affect the shape of the resulting surface by specifying bounds on the

solution. Another example is given in Section 5.3.2.

Generalized Elimination Method

From equation (5.23) it can be seen that $E_0(\mathbf{x}) = 0$ reduces to a linear equation,

$$(\mathbf{b}_0 - \mathbf{a}_0) \times (\mathbf{a}_1 - \mathbf{a}_0) \cdot (\mathbf{b}_1 - \mathbf{b}_0) = 0, \quad (5.31)$$

where \mathbf{b}_1 is the only unknown. This condition forces the first four control points, namely \mathbf{a}_0 , \mathbf{a}_1 , \mathbf{b}_0 and \mathbf{b}_1 , to lie on a plane, and has the following geometric interpretation. The two Bézier curves $\mathbf{r}_A(u)$ and $\mathbf{r}_B(u)$ pass through the points \mathbf{a}_0 and \mathbf{b}_0 and their tangents are in the directions of the vectors $\mathbf{a}_0\mathbf{a}_1$ and $\mathbf{b}_0\mathbf{b}_1$. Since a developable surface has the same tangent plane at all points along a ruling and these tangents are on the same ruling, $u = 0$, they must be coplanar. Therefore, \mathbf{a}_0 , \mathbf{a}_1 , \mathbf{b}_0 and \mathbf{b}_1 must lie on the same plane.

Similarly, the last equation, $E_{3n-2}(\mathbf{x}) = 0$, is linear in \mathbf{b}_{n-1} :

$$(\mathbf{b}_n - \mathbf{a}_n) \times (\mathbf{a}_n - \mathbf{a}_{n-1}) \cdot (\mathbf{b}_n - \mathbf{b}_{n-1}) = 0. \quad (5.32)$$

The linear equations (5.31) and (5.32) can be used to reduce the dimensionality of the optimization by two. The new objective function can be introduced without terms $E_0^2(\mathbf{x})$ and $E_{3n-2}^2(\mathbf{x})$, i.e.

$$F(\mathbf{x}) = E_1^2(\mathbf{x}) + E_2^2(\mathbf{x}) + \dots + E_{3n-3}^2(\mathbf{x}).$$

The following discusses the *generalized elimination method* [13, 15], in which the number of variables in the optimization is reduced by the number of independent linear constraints. In general, if we denote the number of variables in the optimization as N (i.e. $\mathbf{x} \in \mathbf{R}^N$) and the number of linear equations as M , the set of linear equations can be written as

$$[\mathbf{A}]\mathbf{x} = \mathbf{b}$$

in which $[\mathbf{A}]$ is $M \times N$ and $\mathbf{b} \in \mathbf{R}^M$. In other words, the i th row of $[\mathbf{A}]$ contains the coefficients corresponding to the i th linear equation, and is therefore the gradient of that equation.

This reduction in dimensionality can be described formally in terms of two subspaces, which can be described as

- the M -dimensional subspace defined by the rows of $[\mathbf{A}]$.
- the $N - M$ complementary subspace of vectors orthogonal to the rows of $[\mathbf{A}]$.

Let $[\mathbf{Y}]$ denote any $N \times M$ matrix whose columns form a basis for the range space of $[\mathbf{A}]^T$. In fact, $[\mathbf{Y}]$ may be taken as $[\mathbf{A}]^T$. Let $[\mathbf{Z}]$ denote an $N \times (N - M)$ matrix whose columns form a basis for the set of vectors orthogonal to the rows of $[\mathbf{A}]$, so that $[\mathbf{A}][\mathbf{Z}] = [\mathbf{0}]$. The matrix $[\mathbf{Z}]$ has linearly independent columns $\mathbf{z}_1, \mathbf{z}_2, \dots, \mathbf{z}_{N-M}$ which are in the null space and act as basis vectors for the null space. Since $[\mathbf{Y}]$ and $[\mathbf{Z}]$ define complementary subspaces, every N -vector \mathbf{x} has a unique expansion as a linear combination of the columns of $[\mathbf{Y}]$ and $[\mathbf{Z}]$

$$\mathbf{x} = [\mathbf{Y}]\mathbf{x}_y + [\mathbf{Z}]\mathbf{x}_z, \quad (5.33)$$

where M -vector \mathbf{x}_y is the range-space portion of \mathbf{x} and $(N - M)$ -vector \mathbf{x}_z is the null-space portion of \mathbf{x} . By using the chain rule on the derivative of equation (5.33), it follows that

$$\nabla_{x_z} = [\mathbf{Z}]^T \nabla_x.$$

Thus,

$$\nabla_{x_z} F(\mathbf{x} + [\mathbf{Z}]\mathbf{x}) = [\mathbf{Z}]^T \nabla_x F(\mathbf{x}) = [\mathbf{Z}]^T \mathbf{g}(\mathbf{x})$$

is the reduced gradient vector and

$$\nabla_{x_z}^2 F(\mathbf{x} + [\mathbf{Z}]\mathbf{x}) = [\mathbf{Z}]^T \nabla_x^2 F(\mathbf{x}) [\mathbf{Z}] = [\mathbf{Z}]^T [\mathbf{H}(\mathbf{x})] [\mathbf{Z}]$$

is the reduced Hessian matrix. Given a feasible initial point \mathbf{x}_0 we solve a reduced size $(N - M) \times (N - M)$ linear system

$$[\mathbf{Z}]^T [\mathbf{H}(\mathbf{x})] [\mathbf{Z}] \mathbf{x}_z = -[\mathbf{Z}]^T \mathbf{g}(\mathbf{x})$$

for \mathbf{x}_z , where the subsequent iteration is

$$\bar{\mathbf{x}} = \mathbf{x} + [\mathbf{Z}]\mathbf{x}_z.$$

5.3.2 B-Spline Developable Surfaces

In this section we merge m Bézier patches together by joining them along their end rulings with C^2 continuity such that the resulting developable surface can be represented by a single B-spline surface. The design procedure is the same as that of the Bézier case, except that the design curve is a B-spline curve. Since multiplication of B-spline functions is complex and computationally expensive, we first extract the Bézier segments from the B-spline curve by knot insertion [5] as described in Section 3.3. We then evaluate equation (5.23) for each Bézier segment and add the resulting equations to the objective function after squaring them. If equations E_0 and $E_{m(3n-2)}$ are used in the general elimination method, they are not included in the objective function.

Recall from Section 3.2 that, for a degree $(n, 1)$ B-spline surface with m Bézier segments, the C^1 and C^2 continuity conditions at the joints are given by

$$h_i(\mathbf{b}_{ni+1} - \mathbf{b}_{ni}) = h_{i+1}(\mathbf{b}_{ni} - \mathbf{b}_{ni-1}), \quad 1 \leq i \leq m \quad (5.34)$$

and

$$\mathbf{b}_{ni-1} + \frac{h_{i+1}}{h_i}(\mathbf{b}_{ni-1} - \mathbf{b}_{ni-2}) = \mathbf{b}_{ni+1} + \frac{h_i}{h_{i+1}}(\mathbf{b}_{ni+1} - \mathbf{b}_{ni+2}). \quad (5.35)$$

Equations (5.34) and (5.35) reduce to six scalar linear equations for each junction. Using these linear equations in the generalized elimination method described in Section 5.3.1 ensures that the surfaces will be exactly C^2 continuous; otherwise they may have some residual value after optimization that would cause discontinuity. For a degree $(n, 1)$ B-spline patch with m Bézier segments, the number of unknowns and linear equations is $3(mn - 1)$ and $6(m - 1) + 2$ respectively, so the reduced number of unknowns is $3m(n - 2) + 1$.

For a B-spline surface, the initial approximation for \mathbf{x} is calculated in the same manner

as for the Bézier case, expressed as

$$\mathbf{b}_i = \mathbf{a}_i + \frac{i}{mn}(\mathbf{b}_0 - \mathbf{a}_0) + \frac{mn-i}{mn}(\mathbf{b}_{mn} - \mathbf{a}_{mn}), \quad i = 1, \dots, mn - 1. \quad (5.36)$$

Once the control points of the second directrix are computed, any knots that may be removed from the curve while leaving the curve geometrically and parametrically unchanged are removed using the knot removal technique described in Section 3.3.

Figure 5-4(a) shows the design curve $\mathbf{r}_A(u)$ which is a cubic B-spline curve with control points $(0, 4, 0)$, $(1, 2, 1)$, $(2, 4, 1)$, $(3, 1, 0)$ and $(4, 2, 0)$ and knot vector $(0, 0, 0, 0, .5, 1, 1, 1, 1)$. Figure 5-4(b) shows the design curve after knot insertion with the resulting two Bézier segments and the selected endpoints $\mathbf{r}_B(0)$ and $\mathbf{r}_B(1)$, which are $(0, 4, 3)$ and $(8, 0, 3)$. When this problem is treated as an unconstrained optimization, the answer converges to the trivial solution where the internal control points of the new curve are equal to the internal control points of the design curve as shown in Figure 5-4(c). To avoid this situation, lower bounds are set on the z variables where $l_i = 3.0$, $i = 2, 5, 8, 11$ and 14 , and the resulting internal control points are $(2, 0, 5)$, $(4, 4, 5)$ and $(6, -2, 3)$. The resulting surface is shown in Figure 5-4(d) with two Bézier patches and the control mesh delineated. Figure 5-4(e) shows the final developable B-spline surface after knot removal.

Aumann [2] proves that a degree (3-1) Bézier surface whose directrices lie in parallel planes is developable if and only if one of the following conditions holds:

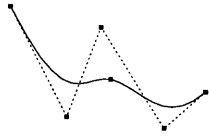
1. The rulings $\mathbf{R}(0, v)$ and $\mathbf{R}(1, v)$ are intersecting or parallel.
2. The coefficient of the cubic term of the design curve is zero.
3. The design curve contains exactly one singular point.

In constructing examples for this thesis, it was found that skew end rulings induce non-zero Gaussian curvature into (3-1) Bézier surfaces whose directrices are 3D space curves as well.

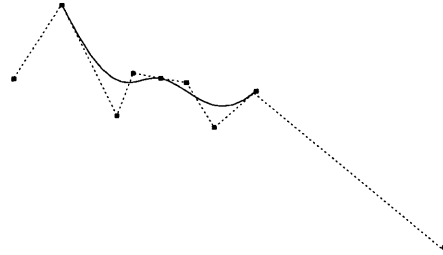
Algorithm

The following steps describe the algorithm for the solution method.

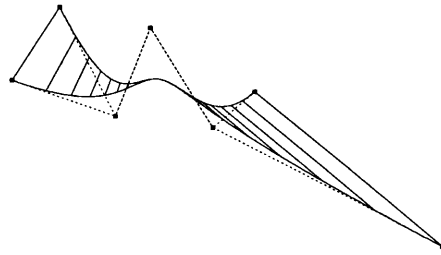
1. The design curve $\mathbf{r}_A(u)$ and the endpoints $\mathbf{r}_B(0)$ and $\mathbf{r}_B(1)$ are provided by the user along with any constraints such as simple bounds or constraining planes on the interior control points of $\mathbf{r}_B(u)$.
2. Bézier segments are subdivided out of the B-spline curve by knot insertion as described in Section 3.3.
3. Initial values for $\mathbf{x} = (b_0^x, b_0^y, b_0^z, \dots, b_{mn}^x, b_{mn}^y, b_{mn}^z)$ are calculated using a linear interpolation method (5.36).
4. The objective function is optimized in two steps. First, beginning with the initial values, an initial feasible point is calculated that meets all constraints and bounds. Then, an optimal solution is found following the method described in Section 5.3.1, using the following steps:
 - If \mathbf{x} satisfies the objective function $F(\mathbf{x}) = \mathbf{0}$ and the Lagrangian multiplier estimates are non-negative for all active bounds, the iteration process is complete.



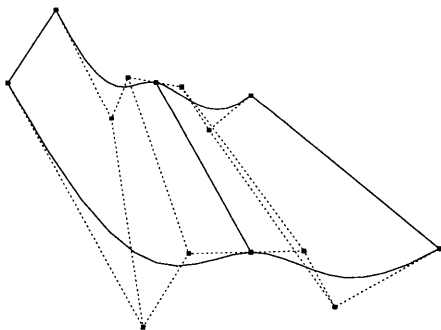
(a) Design Curve $r_A(u)$ with Control Polygon and Knots



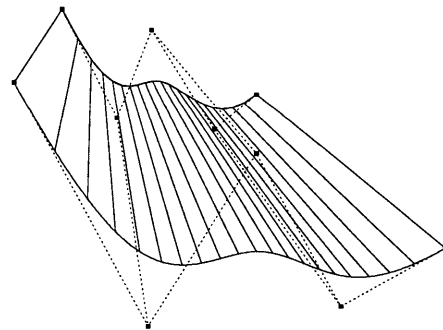
(b) Design Curve after Knot Insertion with Bezier Segments and Endpoints of $r_B(u)$ Shown



(c) Resulting Surface Without Simple Bounds



(d) Design Curve and Resulting Directrix before Knot Removal



(e) Final Developable (3,1) B-Spline Surface

Figure 5-4: Design of Developable B-Spline Surfaces

(Note that the objective function is a sum of squares, so the minimum possible sum is zero.)

- A feasible step direction $\delta \mathbf{x}$ is found using (5.28).
 - If $\delta \mathbf{x}$ causes \mathbf{x} to exceed any of the bounds, those bounds are added to the active set.
 - The Lagrangian multiplier estimates are calculated for all bounds in the active set using (5.30). If any are negative, the associated bound is removed from the active set.
 - $\bar{\mathbf{x}}$ is set to $\mathbf{x} + \delta \mathbf{x}$ and the next iteration is begun.
5. Once the resultant directrix $\mathbf{r}_B(u)$ is computed, the developable B-spline surface is found using equation (4.2).
 6. Knots that can be removed while leaving the surface unchanged are removed using the method described in Section 3.2.
 7. The Gaussian curvature bound is calculated using the method described in Section 5.3.3 to gauge the quality of the resulting surface.
 8. The surface is developed onto a plane using the technique described in Section 5.4.

5.3.3 Accuracy of Resulting Developable Surfaces

Since the optimization results do not always precisely satisfy $F(\mathbf{x}) = \mathbf{0}$, we need a measure to determine how close the resulting surface is to an exactly developable surface. Recall from Section 4.2 that a necessary and sufficient condition for a surface to be developable is for the Gaussian curvature to be zero. This property can be used as a measure. For each resulting Bézier patch $\mathbf{R}(u, v) = \sum_{i=0}^n \sum_{j=0}^1 \mathbf{R}_{ij} B_{i,n}(u) B_{j,1}(v)$, the Gaussian curvature, K , can be expressed in terms of ratios of bivariate Bernstein polynomials as [31]

$$\begin{aligned}
 K(u, v) &= \frac{(\mathbf{S} \cdot \mathbf{R}_{uu})(\mathbf{S} \cdot \mathbf{R}_{vv}) - (\mathbf{S} \cdot \mathbf{R}_{uv})^2}{S^4} \\
 &= \frac{K_{num}(u, v)}{K_{denom}(u, v)} \\
 &= \frac{\sum_{i=0}^{6n-4} \sum_{j=0}^2 K_{ij} B_{i,6n-4}(u) B_{j,2}(v)}{\sum_{i=0}^{8n-4} \sum_{j=0}^4 S_{ij} B_{i,8n-4}(u) B_{j,4}(v)} \tag{5.37}
 \end{aligned}$$

where $\mathbf{S} = \mathbf{R}_u \times \mathbf{R}_v$ and $S = |\mathbf{R}_u \times \mathbf{R}_v|$. If $\mathbf{R}(u, v)$ is a developable surface, then K_{ij} must be zero for $i = 0, \dots, 6n - 4$ and $j = 0, \dots, 2$. However, for surfaces where $F(\mathbf{x}) \neq \mathbf{0}$, the K_{ij} coefficients are not necessarily always precisely zero.

From equation (5.37), we have

$$|K(u, v)| = \left| \frac{K_{num}(u, v)}{K_{denom}(u, v)} \right| = \frac{|K_{num}(u, v)|}{|K_{denom}(u, v)|}. \tag{5.38}$$

We can easily find the upper bound of $|K_{num}(u, v)|$ as

$$|K_{num}(u, v)| = \left| \sum_{i=0}^{6n-4} \sum_{j=0}^2 K_{ij} B_{i,6n-4}(u) B_{j,2}(v) \right|$$

$$\begin{aligned}
&\leq \sum_{i=0}^{6n-4} \sum_{j=0}^2 |K_{ij}| B_{i,6n-4}(u) B_{j,2}(v) \\
&\leq \max_{ij} |K_{ij}| \sum_{i=0}^{6n-4} \sum_{j=0}^2 B_{i,6n-4}(u) B_{j,2}(v) \\
&= \max_{ij} |K_{ij}|.
\end{aligned}$$

The denominator $K_{denom}(u, v)$ is always positive if the surface is regular, since $|\mathbf{R}_u \times \mathbf{R}_v|$ is always positive for a regular surface. However, some of the coefficients S_{ij} can be zero or negative. If there are non-positive S_{ij} we can subdivide the surface into smaller patches until all S_{ij} become positive. This is always possible by virtue of the convergence of the control polyhedron to the surface with repeated subdivision [22]. Then if all $S_{ij} > 0$ we have the inequality

$$\begin{aligned}
|K_{denom}(u, v)| &= \left| \sum_{i=0}^{8n-4} \sum_{j=0}^4 S_{ij} B_{i,8n-4}(u) B_{j,4}(v) \right| \\
&\geq \min_{ij} |S_{ij}| \sum_{i=0}^{8n-4} \sum_{j=0}^4 B_{i,8n-4}(u) B_{j,4}(v) \\
&= \min_{ij} S_{ij}.
\end{aligned}$$

Therefore we can rewrite equation (5.38) as

$$|K(u, v)| \leq \frac{\max_{ij} |K_{ij}|}{\min_{ij} S_{ij}}. \quad (5.39)$$

If $\min_{ij} S_{ij}$ is very small, the bound of the Gaussian curvature can be extremely large. In such case we further subdivide the patch and re-evaluate the bound until such bound converges to a stable value.

Alternatively, the curvature may be analyzed at discrete locations on the surface, which provides a rough estimate but may not find the actual bound of the maximum curvature.

We use the Gaussian curvature bound to give a physical measure of the developability of the surface. Throughout this thesis we say the surface is exactly developable if $|K| < 10^{-10}$. For example, the curvature of the surface shown in Figure 5-4, as determined using ten sub-patches per Bézier patch in equation (5.39), is zero, so the surface is exactly developable.

5.3.4 Developable Surfaces Constrained by Planes

In many engineering applications, one or both of the directrices are restricted to planar curves which are not necessarily parallel. In this situation, we can force the control points \mathbf{b}_i and thus the directrix $\mathbf{r}_B(u)$ to lie in a plane. This plane is determined by the two end points, \mathbf{b}_0 and \mathbf{b}_{mn} for a degree $(n, 1)$ B-spline patch with m Bézier segments, and a point \mathbf{g} chosen by the user. The equation of the plane is given by

$$ax + by + cz + d = 0 \quad (5.40)$$

where, for a degree $(n, 1)$ B-spline patch with m Bézier segments,

$$\begin{aligned} a &= (b_0^y - g^y)(b_{mn}^z - g^z) - (b_0^z - g^z)(b_{mn}^y - g^y) \\ b &= (b_0^z - g^z)(b_{mn}^x - g^x) - (b_0^x - g^x)(b_{mn}^z - g^z) \\ c &= (b_0^x - g^x)(b_{mn}^y - g^y) - (b_0^y - g^y)(b_{mn}^x - g^x) \\ d &= -ag^x - bg^y - cg^z. \end{aligned}$$

For each control point \mathbf{b}_i to lie on the plane, its x , y and z components must satisfy equation (5.40). These linear constraints can be used to reduce the number of unknowns in the equation using the generalized elimination method described in Section 5.3.1.

However, if the $(mn-1)$ planar constraints, the $(6m-6)$ C^1 and C^2 continuity conditions and the two linear developability conditions E_0 and $E_{m(3n-2)}$ are all used to reduce the number of variables, the problem may become so overconstrained that it is difficult or impossible to find a feasible solution. For example, a cubic B-spline design curve with two Bézier segments has 15 unknowns ($\mathbf{b}_1, \mathbf{b}_2, \mathbf{b}_3, \mathbf{b}_4, \mathbf{b}_5$) and 13 linear equations, leaving just 2 variables for the entire problem. In this case, we use a subset of the total available linear equations as linear constraints and add the remaining equations to the objective function after squaring them. In selecting the linear equations to be used as constraints, it is important to remember that the linear constraints may be satisfied exactly while the objective function equations may not be. For example, if C^2 continuity is a must, equations (5.34) and (5.35) are used as linear equality constraints and the equations for planar constraints are included in the objective function.

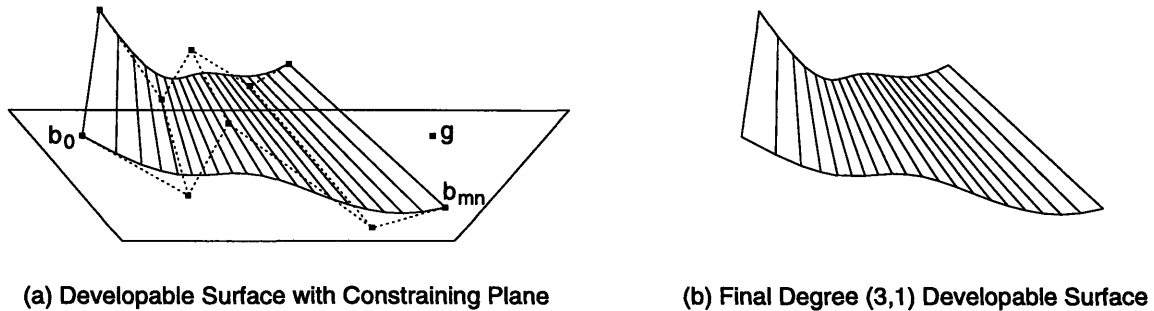


Figure 5-5: Planar Constraint on Developable B-Spline Surface Design

Figure 5-5 shows a developable B-spline surface that was designed with the second directrix constrained to a plane. The same design curve and endpoints were used as those used for Figure 5-4, except the second directrix was constrained to lie in the $z = 3$ plane. Note that since the second directrix was constrained to a plane, the trivial solution was not an option, and simple bounds were not required. The continuity conditions were used as linear constraints.

5.3.5 Degenerate Developable Surfaces

Sometimes topologically triangular patches are required to produce a desired surface design. A three sided patch parameterized over a rectangular domain can be constructed by allowing one of the boundary generators to be zero length, say $\mathbf{R}(0, v)$. Faux and Pratt [11] showed

that the surface normal at this point may be evaluated using a limiting process based on a Taylor series expansion

$$\lim_{u \rightarrow 0} \mathbf{N}(u, v) = \frac{\mathbf{R}_u(0, v) \times \mathbf{R}_{uv}(0, v)}{|\mathbf{R}_u(0, v) \times \mathbf{R}_{uv}(0, v)|}. \quad (5.41)$$

For a degree $(n-1)$ developable Bézier patch, equation (5.41) reduces to

$$\mathbf{N}(0, v) = \frac{(\mathbf{P}_{1,0} - \mathbf{P}_{0,0}) \times (\mathbf{P}_{1,1} - \mathbf{P}_{1,0})}{|(\mathbf{P}_{1,0} - \mathbf{P}_{0,0}) \times (\mathbf{P}_{1,1} - \mathbf{P}_{1,0})|}.$$

Therefore, the unit normal vector at the degenerate point always exists as long as the three control points, $\mathbf{P}_{0,0}$, $\mathbf{P}_{1,0}$ and $\mathbf{P}_{1,1}$, do not coincide with each other, and it is orthogonal to the plane formed by the three control points as shown in Figure 5-6.

The Gaussian curvature at the degenerate point cannot be calculated using the method described in Section 5.3.3 because the denominator, $|\mathbf{R}_u \times \mathbf{R}_v|^4$, vanishes. Wolter and Tuohy [43] devised a method for determining Gaussian curvature at a degenerate point using the second order partial derivatives of a local height function representation of the surface assuming the surface has a tangent plane and well defined curvatures at the degenerate point. For this description, assume that the degenerate point occurs at $\mathbf{R}(0, v)$. The coordinate system is shifted such that the origin coincides with the degenerate point, the z axis is aligned with the normal to the surface and the x axis is aligned with the tangent to the surface in the non-degenerate parameter direction; in this case, $\mathbf{R}_u(0, 0)$. The y axis is orthogonal to the others to form a right-handed system. Three linearly independent isoparameter curves in u are selected on the surface such that $\alpha_n(u) = \mathbf{R}(u, v_n)$, $n = 1, \dots, 3$. The normal curvature in the direction

$$w_n = \frac{\partial \mathbf{R}(0, v_n)}{\partial u} = \frac{\partial \alpha_n(0)}{\partial u} = (x_n, y_n)$$

at the point $\mathbf{R}(0, 0)$ is given as

$$\begin{aligned} \mathbf{n} \cdot \mathbf{k}_n &= \mathbf{n} \cdot \alpha_n''(0) \\ &= g_{xx}(0, 0)x_n^2 + 2g_{xy}(0, 0)x_n y_n + g_{yy}y_n^2 \end{aligned}$$

which can be represented in matrix form as

$$[\mathbf{L}]\mathbf{a} = \mathbf{b} \quad (5.42)$$

where

$$\begin{aligned} \mathbf{a} &= (g_{xx}, g_{xy}, g_{yy})^T \\ \mathbf{b} &= (\mathbf{n} \cdot \alpha_1''(0), \mathbf{n} \cdot \alpha_2''(0), \mathbf{n} \cdot \alpha_3''(0))^T \end{aligned}$$

and

$$[\mathbf{L}] = \begin{bmatrix} x_1^2 & 2x_1y_1 & y_1^2 \\ x_2^2 & 2x_2y_2 & y_2^2 \\ x_3^2 & 2x_3y_3 & y_3^2 \end{bmatrix}.$$

If the fundamental forms are converted to the new coordinate system, the Gaussian curva-

ture can be represented as

$$K = g_{xx}g_{yy} - g_{xy}^2. \quad (5.43)$$

The Gaussian curvature at a degenerate point can thus be determined by solving (5.42) for a and substituting the resulting values for g_{xx} , g_{xy} and g_{yy} into (5.43).

To estimate the maximum absolute value of the Gaussian curvature bound of a degenerate surface with the degenerate point at $\mathbf{R}(0,0)$, the surface is first subdivided at $u = \epsilon$, where ϵ is a small positive number so that the resulting patch with $\epsilon \leq u \leq 1$ is a nondegenerate patch. The Gaussian curvature is calculated at $u = 0$ using equation (5.43), and the bound for the Gaussian curvature for the nondegenerate patch is evaluated using the technique described in Section 5.3.3.

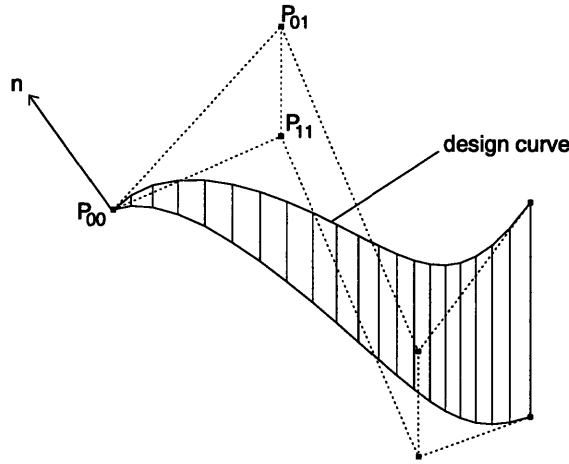


Figure 5-6: Triangular Degenerate Cubic Bézier Patch

Figure 5-6 shows a degenerate cubic-linear Bézier patch with non-planar directrices. The design curve is made up of the control points $(0, 0, 0)$, $(1.8, 3, -0.7)$, $(3.3, -2, 1.5)$ and $(4, 0.5, 0)$. The selected end points are $(0, 0, 0)$ and $(4, 0.5, 2)$. The Gaussian curvature at the degenerate point was found to be 8.91×10^{-14} . The surface was split at the parameter value $u = 0.0001$ resulting in a maximum bound for the Gaussian curvature of zero. Therefore, the surface is exactly developable. Note that there are only three points which define the end rulings and they always lie on the same plane. Therefore, there is no skew between the two end rulings and the surface often results in an exact developable surface.

5.4 Development of a Developable Surface onto a Plane

In the manufacture of developable surfaces, it is necessary to calculate the plane development of these surfaces. This determines cut information for the flat piece of metal so it can be cut to the proper dimensions before it is rolled.

This formulation follows the method of Faux and Pratt [11, p.274], using the fact that a developable surface may be mapped isometrically onto a plane. The Frenet-Serret formulae state that

$$\mathbf{t}' = \kappa \mathbf{n} \quad (5.44)$$

where \mathbf{t} is the unit tangent vector to a curve, \mathbf{n} is the unit normal vector to a curve and κ is the curvature. For a planar curve in the (X, Y) plane, we can define the unit normal vector as

$$\mathbf{n} = e_z \times \mathbf{t} \quad (5.45)$$

where $e_z = (0, 0, 1)$. Substituting (5.45) into (5.44) yields

$$\frac{d^2 X}{ds^2} - \kappa \frac{dY}{ds} = 0 \quad (5.46)$$

$$\frac{d^2 Y}{ds^2} + \kappa \frac{dX}{ds} = 0 \quad (5.47)$$

where (X, Y) denote the 2D coordinates on the developed plane (X, Y) . If we rewrite equation (5.46) in terms of the parameter u , we obtain

$$\begin{aligned} \frac{d^2 X}{ds^2} - \kappa \frac{dY}{ds} &= \frac{d}{ds} \left(\frac{dX}{ds} \right) - \kappa \frac{dY}{ds} \\ &= \frac{d}{ds} \left(\frac{dX}{du} \frac{du}{ds} \right) - \kappa \frac{dY}{du} \frac{du}{ds} \\ &= \frac{d^2 X}{du^2} \left(\frac{du}{ds} \right)^2 + \frac{dX}{du} \left(\frac{d^2 u}{ds^2} \right) - \kappa \frac{dY}{du} \frac{du}{ds} = 0. \end{aligned}$$

If $(du/ds)^2 \neq 0$, this reduces to

$$\frac{d^2 X}{du^2} + \frac{\left(\frac{d^2 u}{ds^2} \right) dX}{\left(\frac{du}{ds} \right)^2 du} - \frac{\kappa}{\left(\frac{du}{ds} \right)} \frac{dY}{du} = 0. \quad (5.48)$$

Similarly, equation (5.47) can be represented as

$$\frac{d^2 Y}{du^2} + \frac{\left(\frac{d^2 u}{ds^2} \right) dY}{\left(\frac{du}{ds} \right)^2 du} - \frac{\kappa}{\left(\frac{du}{ds} \right)} \frac{dX}{du} = 0. \quad (5.49)$$

The development is based on the fact that curves on isometric surfaces have the same geodesic curvatures. It can be seen from Figure 2-4 that for a planar curve, since the angle between the surface normal and the normal to a curve is 90 degrees, the curvature vector equals the geodesic curvature vector. Therefore, κ in equations (5.48) and (5.49) can be replaced by κ_g , the geodesic curvature of the curve on the developable surface. If we choose the curve on the developable surface to be an isoparametric curve in terms of u , $\mathbf{R}(u, v_n)$, we can replace du/ds and $d^2 u/ds^2$ in equations (5.48) and (5.49) by

$$\begin{aligned} \frac{du}{ds} &= \frac{1}{|\mathbf{R}_u(u, v_n)|} \quad \text{and} \\ \frac{d^2 u}{ds^2} &= -\frac{\mathbf{R}_u(u, v_n) \cdot \mathbf{R}_{uu}(u, v_n)}{\mathbf{R}_u(u, v_n) \cdot \mathbf{R}_u(u, v_n)}. \end{aligned}$$

Thus we have

$$\begin{aligned}
\frac{dX}{du} &= p \\
\frac{dY}{du} &= q \\
\frac{dp}{du} &= p \frac{(\mathbf{R}_u \cdot \mathbf{R}_{uu})}{(\mathbf{R}_u \cdot \mathbf{R}_u)} - q \kappa_g |\mathbf{R}_u| \\
\frac{dq}{du} &= q \frac{(\mathbf{R}_u \cdot \mathbf{R}_{uu})}{(\mathbf{R}_u \cdot \mathbf{r}_u)} + p \kappa_g |\mathbf{R}_u|.
\end{aligned} \tag{5.50}$$

The surface will be developed onto the plane oriented such that the point $\mathbf{R}(0,0)$ is located at the origin of the (X,Y) coordinate system in the plane and the vector $\mathbf{R}_u(0,0)$ coincides with the X axis, as shown in Figure 5-7. We integrate the system (5.50) along the directrix that corresponds to $v = 0$ from $u = 0$ to $u = 1$, using, for example, a Runge Kutta scheme. Since isometric maps are conformal, the angle between the directrix and the generator at $(0,0)$ is the same in both representations and can be found by

$$\cos \theta = \frac{\mathbf{R}_u(0,0) \cdot \mathbf{R}_v(0,0)}{|\mathbf{R}_u(0,0)| |\mathbf{R}_v(0,0)|}.$$

Straight lines on the surface map to straight lines on the plane, so the generator length on the surface is measured and transferred to the plane, giving the initial point for the development of the second directrix. Then the system of ordinary differential equations (5.50) is integrated using a fourth order Runge-Kutta method [38] along the directrix that corresponds to $v = 1$ from $u = 0$ to $u = 1$. Finally, the endpoints of the two directrices are connected.

To verify that the development of the surface is accurate, one can check the results by computing the angle between the directrix corresponding to $v = 0$ and the generator corresponding to $u = 1$, computing the length of that generator, and determining the location of the point $\mathbf{R}(1,1)$ in the plane. Comparing this point to the point calculated above determines the accuracy of the development. The development will be more accurate with increased steps in the Runge-Kutta scheme.

The surface that was designed in Section 5.3.2 is developed onto a plane here. This surface is shown in Figure 5-7(a). It was developed onto a plane using 31 steps in a fourth order Runge-Kutta routine as shown in Figure 5-7(b). The accuracy for the check at $\mathbf{R}(1,1)$ was 10^{-6} .

5.5 Examples

5.5.1 Example of a Developable B-Spline Strip Surface

This example is a windshield of an automobile as depicted in Figure 5-8. Since automobile windshields are generally sandwiched between two parallel planes, we can use the technique introduced in Section 5.2. The design curve, $\mathbf{r}_A(u)$, is given in the xy -plane by a cubic B-spline curve with control points $(0, 2.1, 0)$, $(0.5, 0.9, 0)$, $(1.5, 0.3, 0)$, $(4.5, 0, 0)$, $(7.5, 0.3, 0)$, $(8.5, 0.9, 0)$, $(9, 2.1, 0)$ and a knot vector $(0, 0, 0, 0, 0.3, 0.5, 0.7, 1, 1, 1, 1)$. The two end boundary conditions are chosen to be $\mathbf{b}_0 = (0.2, 3.5, 1.5)$ and $\mathbf{b}_6 = (8.8, 3.5, 1.5)$. The design curve is first split into four cubic Bézier curves and the control points of $\mathbf{r}_B(u)$ are

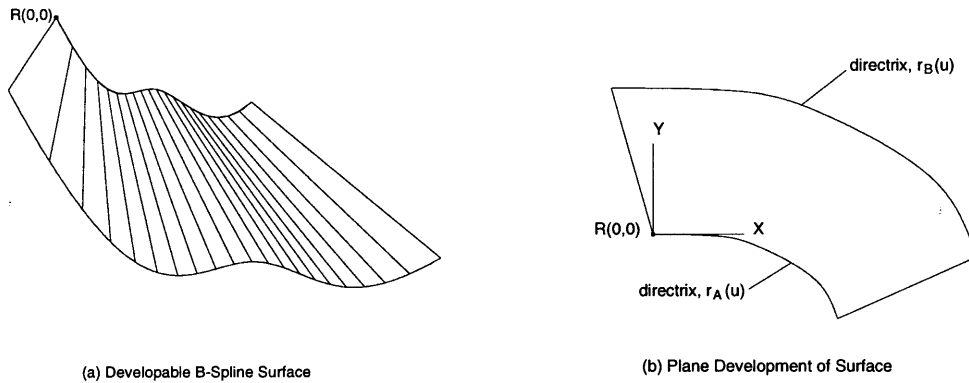
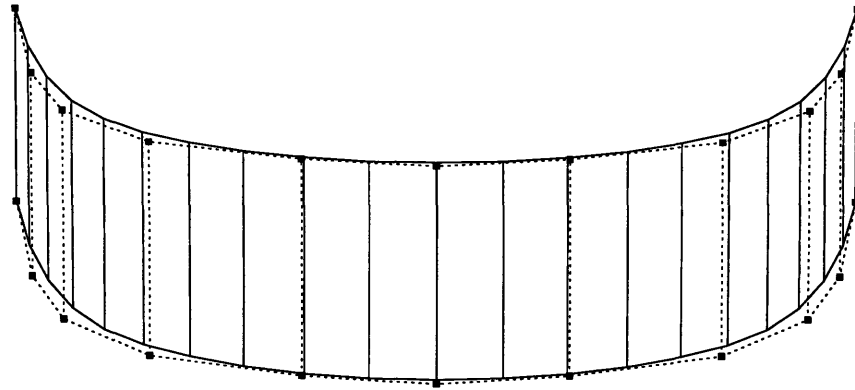


Figure 5-7: Development of B-Spline Developable Surface

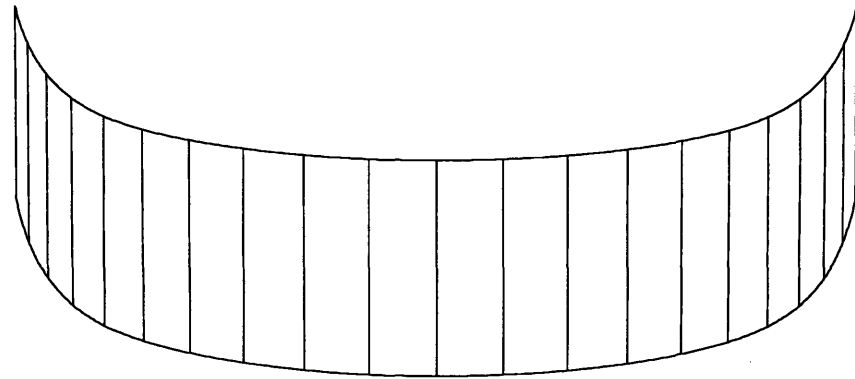
evaluated. The resulting B-spline curve, $\mathbf{r}_B(u)$, has internal control points (0.56, 2.64, 1.5), (0.96, 2.18, 1.5), (1.84, 1.81, 1.5), (3.27, 1.62, 1.5), (4.5, 1.53, 1.5), (5.73, 1.62, 1.5), (7.16, 1.81, 1.5), (8.04, 2.18, 1.5) and (8.44, 2.64, 1.5), with knot vector (0 0 0 0 0 .3 .3 .5 .5 .7 .7 1 1 1 1). Note that the resulting surface is not cylindrical. After degree elevating the design curve by one and removing the knots from $\mathbf{r}_B(u)$, we obtain the degree (4-1) B-spline developable surface shown in Figure 5-8. The windshield surface is then developed onto the plane as shown in Figure 5-8(c).

5.5.2 Example of a Developable B-Spline Surface with 3D Directrices

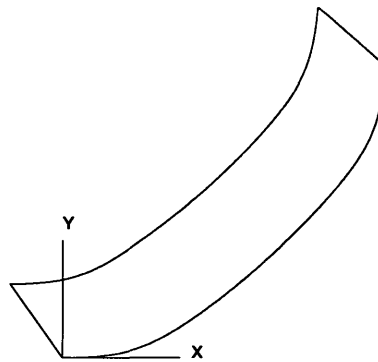
The stack of a ship, depicted in Figure 5-9, was constructed using a B-spline design curve with the resulting curve constrained to a plane not parallel to the plane of the design curve. Therefore, the method described in Section 5.3 was required. The stack was split along the plane of symmetry (the xz plane) from forward to aft. The simple shape allowed definition of the design curve with a single B-spline curve of two Bézier segments for each half stack. A cubic design curve was selected that defined the base of the stack, with control points (0, 0, 0), (0, 10, 0), (15, 10, 0), (35, 3, 0) and (35, 0, 0) and knot vector (0, 0, 0, 0, .5, 1, 1, 1, 1). The two endpoints were selected to be $\mathbf{b}_0 = (6, 0, 31)$ and $\mathbf{b}_6 = (24, 0, 29)$. The second directrix was constrained to lie on a plane, with the third point to define the plane being (24, 10, 29). The optimization process was conducted using equations (5.34) and (5.35) to reduce the number of variables, and no simple bounds were employed. The resulting surface was degree (3,1). The maximum Gaussian curvature determined using equation (5.39) with 10 Bézier subpatches was 2.19×10^{-7} . The surface was then reflected with respect to the xz plane, resulting in a symmetric body. One of the surfaces surfaces was developed onto a plane, as shown in Figure 5-9(c).



(a) Developable Surface with Control Points



(b) Final Developable Surface



(c) Surface Developed onto Plane

Figure 5-8: Automobile Windshield, a Developable Degree (4-1) B-spline Strip Surface

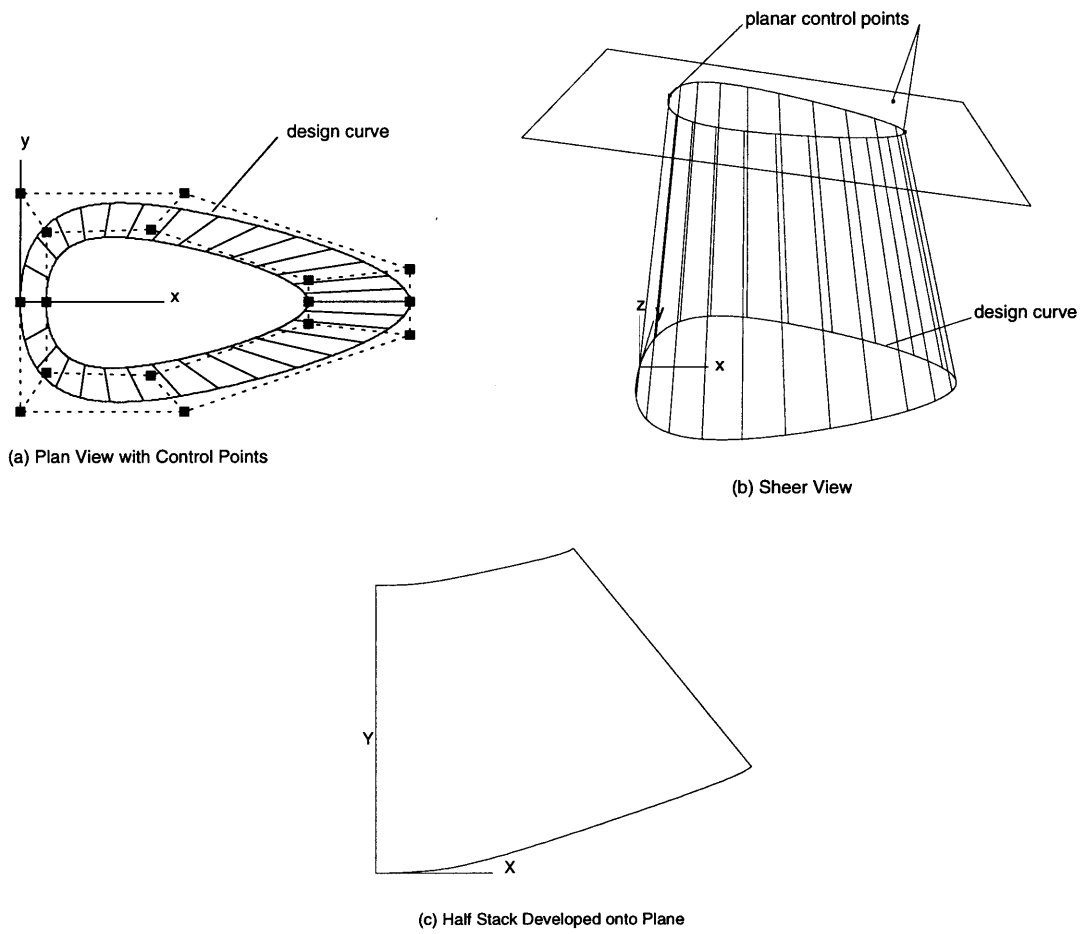


Figure 5-9: Ship Stack, A Developable Degree (3,1) B-Spline Surface with $|K| < 2.19 \times 10^{-7}$

Chapter 6

Geodesics on Developable Surfaces

6.1 Introduction

Geodesics are useful in ship design and shipbuilding for determining the layout of seams and butts in a ship hull, as described by Munchmeyer and Haw [33]. This chapter shows that a two point boundary value problem (BVP) for computing geodesics on a developable surface can always be reduced to an initial value problem (IVP), with a corresponding savings in time for the solution process. Most problems that arise in applications of geodesics are BVPs, which are much more difficult to solve than IVPs.

6.2 Formulation

Recall from Section 2.3 that the governing equations of a geodesic are given by a set of coupled second order ordinary differential equations (2.29) and (2.30)

$$\begin{aligned}\frac{d^2u}{ds^2} + \Gamma_{11}^1 \left(\frac{du}{ds}\right)^2 + 2\Gamma_{12}^1 \frac{du}{ds} \frac{dv}{ds} + \Gamma_{22}^1 \left(\frac{dv}{ds}\right)^2 &= 0 \\ \frac{d^2v}{ds^2} + \Gamma_{11}^2 \left(\frac{du}{ds}\right)^2 + 2\Gamma_{12}^2 \frac{du}{ds} \frac{dv}{ds} + \Gamma_{22}^2 \left(\frac{dv}{ds}\right)^2 &= 0\end{aligned}$$

where u and v are related by the first fundamental form $ds^2 = Edu^2 + 2Fdudv + Gdv^2$. These two second order differential equations can be rewritten as a system of four first order differential equations

$$\frac{du}{ds} = p \tag{6.1}$$

$$\frac{dv}{ds} = q \tag{6.2}$$

$$\frac{dp}{ds} = -\Gamma_{11}^1 p^2 - 2\Gamma_{12}^1 pq - \Gamma_{22}^1 q^2 \tag{6.3}$$

$$\frac{dq}{ds} = -\Gamma_{11}^2 p^2 - 2\Gamma_{12}^2 pq - \Gamma_{22}^2 q^2. \tag{6.4}$$

We can solve the system as an initial-value problem (IVP), where all four boundary conditions are given at one point, or as a boundary-value problem (BVP), where the four boundary conditions are specified at two distinct points. Most of the problems that arise

in applications of geodesics are BVPs, which are much more difficult to solve than IVPs.

The solution of an IVP is unique; however for a BVP it is possible that the differential equations will have many solutions or even no solution [25]. General methods for the solutions of two-point BVPs can be found in [12, 25]. There are two commonly used approaches to the numerical solution of a BVP, namely the shooting method and the finite difference method (relaxation method). The shooting method was originally used to adjust the settings of artillery equipment to hit a target. To implement the method, the unknown boundary conditions are guessed at the initial point and an IVP method is implemented. Based on the resulting values at the end point, the initial guess is adjusted until the “target” is “hit”. The second approach is based on a finite difference approximation to $\frac{dy}{ds}$ where $y = (u, v, p, q)$ on a mesh of points in the interval $[A, B]$. This method starts with an initial guess and improves the solution iteratively. Maekawa [30] solves the geodesic BVP on free-form parametric surfaces by the finite difference method. In general, the shooting method is very sensitive to the initial guess at point A, and is much less stable than the finite difference method [30].

For a B-spline developable surface patch there is a single unique solution to the system. Since a geodesic on a developable maps to a straight line on a developed plane, there is only one solution to the system on a developable surface. Here we exclude periodic surfaces such as cylinders where there can be more than one solution, as shown in Figure 6-1.

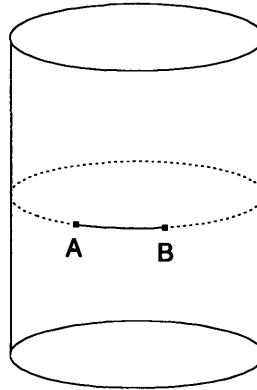


Figure 6-1: Geodesics on a Closed Surface

In this section it is shown that all two point BVPs for solving geodesics on developables can be reduced to IVPs using the following properties described in Section 4.2:

- A developable surface can be mapped isometrically onto a plane.
- Isometric surfaces have the same Gaussian curvature at corresponding points.
- Corresponding curves on these surfaces have the same geodesic curvature at corresponding points.
- Every isometric mapping is conformal; i.e. the angle of intersection of every arbitrary pair of intersecting arcs on a developable surface is the same as that of the corresponding inverse image in the plane at the corresponding points.

- A geodesic on a developable surface maps to a straight line in the plane.

The basic procedure is to map the two desired points on the developable surface to a plane, draw the straight line between them and determine the angle between the generator and the geodesic line at one of the end points. The angle can be used to determine du/ds and dv/ds . Thus, all the information required for an IVP is available.

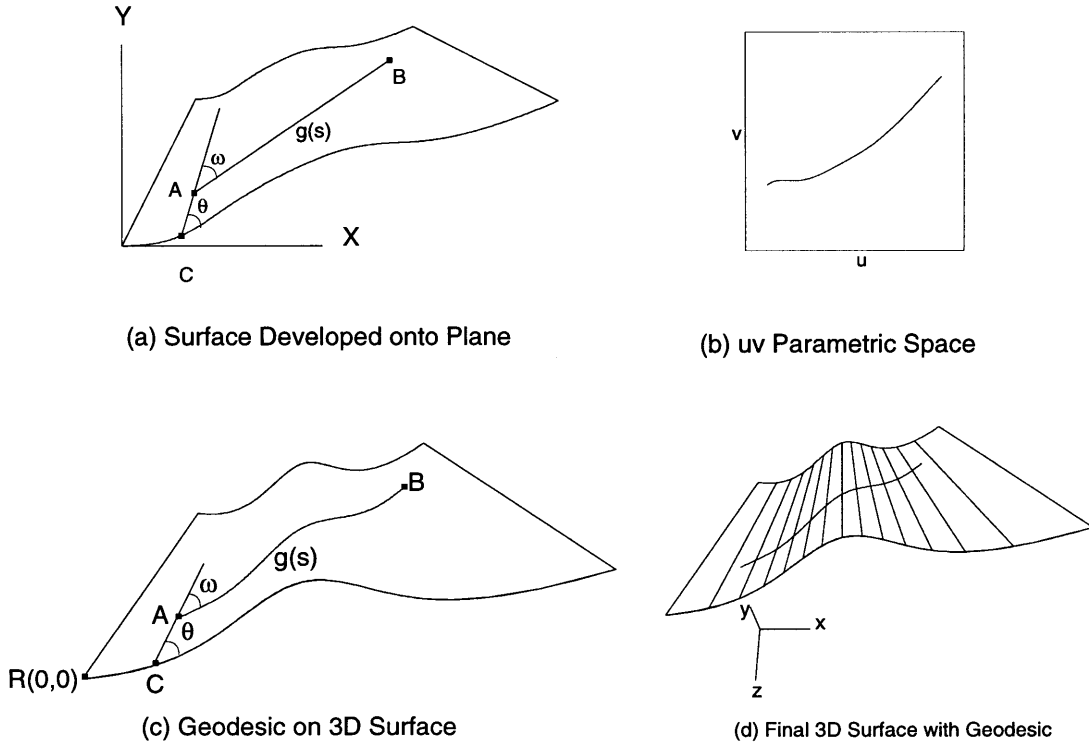


Figure 6-2: Geodesic on a Degree (3,1) Developable Surface

Given two points A and B on the developable surface $\mathbf{R}(u, v)$ as shown in Figure 6-2(c), the corresponding points (X_A, Y_A) and (X_B, Y_B) in the developed plane are required. To find the points in the plane, (X_0, Y_0) is set as the $(0, 0)$ point in the plane corresponding to $\mathbf{R}(0, 0)$ on the surface. Using the method presented in Section 5.4, the directrix corresponding to $v = 0$ is developed into the plane to determine the point $C = (u_A, 0)$, shown in Figure 6-2(a). The angle between the directrix and the generator at $(u_A, 0)$ is the same in both representations and can be found by

$$\cos \theta = \frac{\mathbf{R}_u(u_A, 0) \cdot \overrightarrow{CA}}{|\mathbf{R}_u(u_A, 0)| \cdot |\overrightarrow{CA}|}$$

where \overrightarrow{CA} is an isoparametric line $\mathbf{R}(u_A, v)$ which is a straight line on the surface. Therefore it is a geodesic and will be developed into the plane as a straight line. The distance $|\overrightarrow{CA}|$

is given by

$$|\vec{CA}| = \sqrt{(x_A - x_C)^2 + (y_A - y_C)^2 + (z_A - z_C)^2}.$$

The point A on the plane is found using C , $|\vec{CA}|$ and θ . The point B on the plane is found by following the same procedure, and the points are connected as shown in Figure 6-2(a). The angle ω between \vec{CA} and \vec{AB} is given by

$$\cos \omega = \frac{\vec{AB} \cdot \vec{CA}}{|\vec{AB}| |\vec{CA}|}.$$

This angle ω is preserved between the isoparametric line $\mathbf{r}(u_A, v)$ and the geodesic curve $\mathbf{g}(s)$ on the developable surface at point A . Thus we have

$$\cos \omega = \frac{\mathbf{R}_v \cdot \mathbf{g}'(s)}{|\mathbf{R}_v| |\mathbf{g}'(s)|}$$

where the tangent vector to the geodesic is given by

$$\mathbf{g}'(s) = \mathbf{R}_u \frac{du}{ds} + \mathbf{R}_v \frac{dv}{ds}. \quad (6.5)$$

The angles ω and θ are shown in Figures 6-2(a) and (c). Multiplying (6.5) by \mathbf{R}_v yields

$$\mathbf{R}_v \cdot \mathbf{g}'(s) = \mathbf{R}_u \cdot \mathbf{R}_v \frac{du}{ds} + \mathbf{R}_v \cdot \mathbf{R}_v \frac{dv}{ds} = \cos(\omega) |\mathbf{R}_v| |\mathbf{g}'(s)|$$

which (since $|\mathbf{g}'(s)| = 1$) can be reduced to

$$F \frac{du}{ds} + G \frac{dv}{ds} = \cos(\omega) \sqrt{G}$$

where $F = \mathbf{R}_u \cdot \mathbf{R}_v$ and $G = \mathbf{R}_v \cdot \mathbf{R}_v$ (coefficients of the first fundamental form). Thus,

$$\frac{dv}{ds} = \frac{\cos(\omega)}{\sqrt{G}} - \frac{F}{G} \left(\frac{du}{ds} \right). \quad (6.6)$$

From the first fundamental form,

$$\mathbf{g}'(s) \cdot \mathbf{g}'(s) = E \left(\frac{du}{ds} \right)^2 + 2F \frac{du}{ds} \frac{dv}{ds} + G \left(\frac{dv}{ds} \right)^2 = 1. \quad (6.7)$$

Plugging (6.6) into (6.7) and solving for du/ds yields

$$\frac{du}{ds} = \pm \sqrt{\frac{\sin^2(\omega) G}{EG - F^2}}$$

and thus (6.6) reduces to

$$\frac{dv}{ds} = \frac{\cos(\omega)}{\sqrt{G}} \pm \frac{1}{\sqrt{G}} \frac{F}{\sqrt{EG - F^2}} \sin(\omega).$$

Hence, we have all the initial conditions required to solve the IVP (equations (6.1) to (6.4)) for a geodesic. The solution to the IVP yields the uv parametric values for the geodesic that are graphed in Figure 6-2(b). The corresponding three-dimensional coordinate values are shown in Figures 6-2(c) and (d). The developable degree (3,1) surface shown in Figure 6-2 has the control points and knot vectors shown in Table 6.1. The geodesic runs from

$$(u_A, v_A) = (0.1, 0.3) \quad \text{to} \quad (u_B, v_B) = (0.9, 0.8).$$

$\mathbf{P}_{0,0}$	(-2, 1, 0)	$\mathbf{P}_{0,1}$	(0, 2, -3)
$\mathbf{P}_{1,0}$	(0, -1, -1)	$\mathbf{P}_{1,1}$	(1, 1, -3.5)
$\mathbf{P}_{2,0}$	(2, 5, -1.4)	$\mathbf{P}_{2,1}$	(2, 4, -3.7)
$\mathbf{P}_{3,0}$	(4, 1, -1)	$\mathbf{P}_{3,1}$	(3, 2, -3.5)
$\mathbf{P}_{4,0}$	(6, 5, 0)	$\mathbf{P}_{4,1}$	(4, 4, -3)
T_u	0, 0, 0, 0, .5, 1, 1, 1, 1	T_v	0, 0, 1, 1

Table 6.1: Control Points for a Degree (3,1) Developable Surface

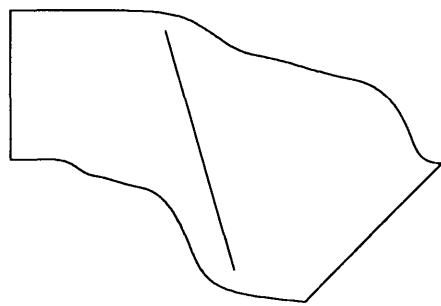
6.3 Examples

In this section we conduct numerical experiments to compare the performance of the IVP to the finite difference based BVP on developable surfaces. For a fair comparison, we determine the minimum number of steps in the BVP to reliably meet the given tolerance $\epsilon = 10^{-5}$ for Newton's method, see [31]. We then find the minimum number of steps for the IVP to achieve the same order of accuracy at the endpoint B. The examples were run on a 180 MHz Silicon Graphics workstation.

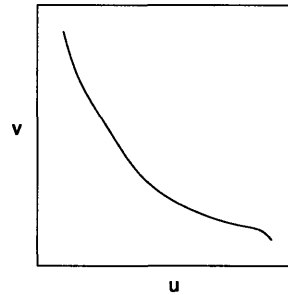
The example shown in Figure 6-2 runs using an IVP solution with 66 steps in 0.25 seconds, as compared to 0.60 seconds for a BVP solution with 135 steps and 7 iterations. This is over twice as fast, with a very simple surface and a geodesic that is very close to a straight line in uv space.

A more complex degree (4,1) developable surface with five Bézier patches also runs over twice as fast: 0.88 seconds for the IVP solution with 194 steps instead of 2.28 seconds for the BVP solution with 294 steps and 11 iterations. The control points and knot vectors for this example are displayed in Table 6.2. The geodesic runs from $(u_A, v_A) = (0.1, 0.9)$ to $(u_B, v_B) = (0.9, 0.1)$. The surface and its geodesic are displayed in Figure 6-3.

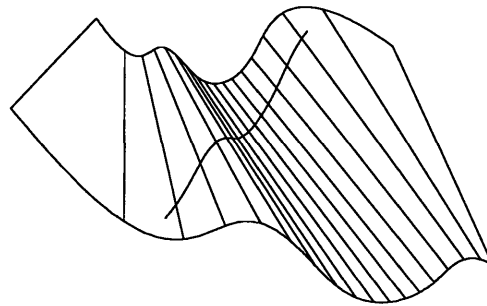
The final example is a handkerchief-like surface. This degree (4,1) developable surface with four Bézier patches runs in 0.50 seconds for the IVP and 2.66 seconds for the BVP, which is over 5 times faster. The IVP required 176 steps, while the BVP required 320 steps and 12 iterations. The control points and knot vectors for this example are shown in Table 6.3. The geodesic runs from $(u_A, v_A) = (0,0)$ to $(u_B, v_B) = (1,1)$. The surface and its geodesic are displayed in Figure 6-4.



(a) Surface Developed onto Plane



(b) uv Parametric Space



(c) Geodesic on 3D Surface

Figure 6-3: Geodesic on a Degree (4,1) Developable Surface

$P_{0,0}$	(0.00, 3.00, 0.00)	$P_{0,1}$	(0.00, 3.00, -5.00)
$P_{1,0}$	(0.75, 1.50, 0.00)	$P_{1,1}$	(2.42,-1.84, -5.00)
$P_{2,0}$	(1.25, 1.50, 0.00)	$P_{2,1}$	(3.88,-1.53, -5.00)
$P_{3,0}$	(1.96, 2.58, 0.00)	$P_{3,1}$	(5.85, 1.34, -5.00)
$P_{4,0}$	(2.50, 2.00, 0.00)	$P_{4,1}$	(7.12,-2.28, -5.00)
$P_{5,0}$	(3.00, 1.17, 0.00)	$P_{5,1}$	(8.21,-1.97, -5.00)
$P_{6,0}$	(3.50, 1.00, 0.00)	$P_{6,1}$	(9.09,-2.20, -5.00)
$P_{7,0}$	(4.00, 1.08, 0.00)	$P_{7,1}$	(9.86,-2.03, -5.00)
$P_{8,0}$	(4.50, 1.50, 0.00)	$P_{8,1}$	(1.04,-1.53, -5.00)
$P_{9,0}$	(5.04, 2.29, 0.00)	$P_{9,1}$	(1.09,-6.81, -5.00)
$P_{10,0}$	(5.75, 4.25, 0.00)	$P_{10,1}$	(1.13, 4.04, -5.00)
$P_{11,0}$	(6.75, 4.50, 0.00)	$P_{11,1}$	(1.18, 1.05, -5.00)
$P_{12,0}$	(9.00, 3.00, 0.00)	$P_{12,1}$	(1.20,-1.11, -5.00)
T_u	0, 0, 0, 0, 0, .2, .2, .4, .4, .6, .6, .8, .8, 1, 1, 1, 1, 1	T_v	0, 0, 1, 1

Table 6.2: Control Points for a Degree (4,1) Developable Surface

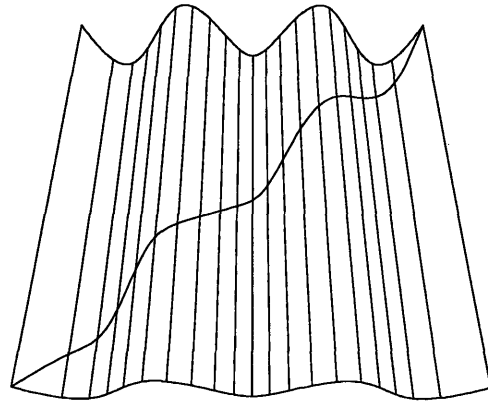
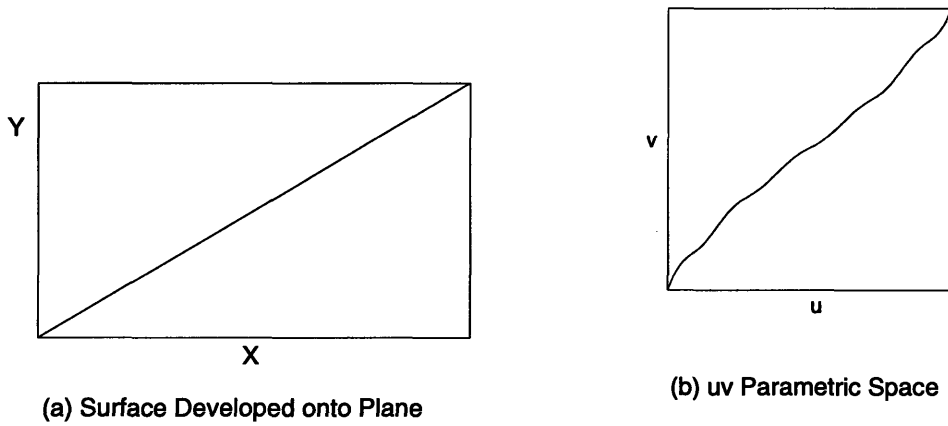


Figure 6-4: Geodesic on a Degree (4,1) Handkerchief-like Developable Surface

$P_{0,0}$	(0.50, 3.00, 0.00)	$P_{0,1}$	(0.50, 3.00, -5.00)
$P_{1,0}$	(0.88, 1.50, 0.00)	$P_{1,1}$	(0.88, 1.50, -5.00)
$P_{2,0}$	(1.25, 2.00, 0.00)	$P_{2,1}$	(1.25, 2.00, -5.00)
$P_{3,0}$	(1.96, 4.17, 0.00)	$P_{3,1}$	(1.96, 4.17, -5.00)
$P_{4,0}$	(2.50, 3.00, 0.00)	$P_{4,1}$	(2.50, 3.00, -5.00)
$P_{5,0}$	(3.00, 1.67, 0.00)	$P_{5,1}$	(3.00, 1.67, -5.00)
$P_{6,0}$	(3.50, 3.00, 0.00)	$P_{6,1}$	(3.50, 3.00, -5.00)
$P_{7,0}$	(4.04, 4.17, 0.00)	$P_{7,1}$	(4.04, 4.17, -5.00)
$P_{8,0}$	(4.75, 2.00, 0.00)	$P_{8,1}$	(4.75, 2.00, -5.00)
$P_{9,0}$	(5.13, 1.50, 0.00)	$P_{9,1}$	(5.13, 1.50, -5.00)
$P_{10,0}$	(5.50, 3.00, 0.00)	$P_{10,1}$	(5.50, 3.00, -5.00)
T_u	0, 0, 0, 0, 0, .25, .25, .5, .5, .75, .75, 1, 1, 1, 1, 1	T_v	0, 0, 1, 1

Table 6.3: Control Points for a Degree (4,1) Handkerchief-like Developable Surface

Chapter 7

Lines of Curvature on Developable Surfaces

7.1 Introduction

This chapter discusses the behavior of the lines of curvature on a developable surface near the inflection line. A developable surface does not possess isolated generic flat points but rather may contain a line of non-generic flat points along the generator. This property can be used to detect an *inflection line* where the (only) non-zero principal curvature whose principal direction is perpendicular to the generator changes its sign. Munchmeyer [33] indicates that a developable surface can be shaped purely by rolling and should be fed into the roller so that the direction of the generator is parallel to the rolls. However, when the non-zero principal curvature changes sign, the plate can no longer be fed into the roller in the same direction, since the bending direction changes at the inflection line. Locating the inflection line prior to fabrication allows the manufacturer to either cut the plate along the inflection line or reverse the direction the plate is fed through the rollers at that line. Surface inflection was studied by Hoitsma [21], who showed that a surface has an inflection at a point P if and only if its mean curvature changes sign in the neighborhood of P. This chapter further extends this result.

7.2 Inflection Line

This section establishes the definition of an inflection line on a developable surface. First, some additional differential geometry properties are required.

Recall that throughout this thesis, it is assumed that the $u = \text{const}$ isoparametric line corresponds to the generator of the developable surface or, in other words, the straight line ruling is in the v direction. With this assumption, $\mathbf{R}_{vv} = \mathbf{0}$; consequently, from (2.13), $N = \mathbf{R}_{vv} \cdot \mathbf{N} = 0$. From (2.23), since Gaussian curvature of a developable surface is zero,

$$K = \frac{LN - M^2}{EG - F^2} = \frac{-M^2}{EG - F^2} = 0 \quad (7.1)$$

and we have $M = 0$. Therefore, mean curvature as expressed by equation (2.24) reduces to

$$H = \frac{2FM - EN - GL}{2(EG - F^2)} = \frac{-GL}{2(EG - F^2)}. \quad (7.2)$$

Recall from (4.22) that the nonzero principal curvature is given by $\kappa^* = 2H$. When $L = 0$, H and κ^* become zero; otherwise, $\kappa^* = 2H \neq 0$.

Next, we will show that the $u = \text{const}$ parametric straight lines become the lines of zero curvature. This can be seen from the fact that

- the $u = \text{const}$ parametric straight lines have zero normal curvature, and
- no other direction has zero normal curvature.

The second fact comes from Euler's theorem (2.25),

$$\kappa_n = \kappa_1 \cos^2(\alpha) + \kappa_2 \sin^2(\alpha).$$

When $\kappa_2 = 0$, $\kappa_n = \kappa_1 \cos^2(\alpha)$, which becomes zero only when $\alpha = \frac{\pi}{2}$ or $\frac{3\pi}{2}$, corresponding to the direction of κ_2 . Similarly, when $\kappa_1 = 0$, $\kappa_n = 0$ only when $\alpha = 0$ or π , corresponding to the direction of κ_1 .

Theorem 7.2.1 *A developable surface does not possess generic isolated flat points¹ but rather may contain a line of non-generic flat points along a generator.*

Proof: From equation (7.2), L vanishes at a flat point (u_f, v_f) where $K = H = 0$. Therefore, from equation (2.14) we have

$$L(u_f, v_f) = -\mathbf{R}_u(u_f, v_f) \cdot \mathbf{N}_u(u_f, v_f) = 0. \quad (7.3)$$

From equation (7.1), $M = 0$ on a developable surface. Therefore, from (2.15) we have

$$M(u_f, v_f) = -\mathbf{R}_v(u_f, v_f) \cdot \mathbf{N}_u(u_f, v_f) = 0. \quad (7.4)$$

Since \mathbf{N} is a unit vector, we also have

$$\mathbf{N}(u_f, v_f) \cdot \mathbf{N}_u(u_f, v_f) = 0. \quad (7.5)$$

If \mathbf{N}_u is not zero, then from (7.3), (7.4) and (7.5) \mathbf{N}_u must be perpendicular to \mathbf{R}_u , \mathbf{R}_v and \mathbf{N} . This is impossible because \mathbf{N} is perpendicular to both \mathbf{R}_u and \mathbf{R}_v , and \mathbf{R}_u is not parallel to \mathbf{R}_v . Thus, $\mathbf{N}_u(u_f, v_f)$ must equal zero.

For developable surfaces, the unit normal vector \mathbf{N} is constant along a generator. Therefore, the rate of change of the unit normal vector in the u direction must also be constant along a generator. This leads us to the fact that \mathbf{N}_u is not only zero at (u_f, v_f) but also zero along the $u = u_f$ isoparametric line. Therefore, for a given $u = u_f$, equation (7.3) becomes

$$L(u_f, v) = -\mathbf{R}_{uu}(u_f, v) \cdot \mathbf{N}(u_f, v) = 0 \quad (7.6)$$

for $0 \leq v \leq 1$. Consequently, the entire generator consists of a line of flat points. ■

For a developable surface, the *inflection line* is a generator which consists of a line of flat points and coincides with a change in sign of the nonzero principal curvature. In other words, the nonzero principal curvature has a different sign on either side of an inflection line.

¹A developable surface can not possess spherical umbilics since one of the principal curvatures is always zero.

The inflection line can be detected by finding $u = u_f$ such that $L(u_f, v_n) = 0$ where v_n is an arbitrary constant between 0 and 1. $L(u, v_n) = 0$ can be written as

$$\mathbf{R}_{uu}(u, v_n) \cdot \frac{\mathbf{R}_u(u, v_n) \times \mathbf{R}_v(u, v_n)}{|\mathbf{R}_u(u, v_n) \times \mathbf{R}_v(u, v_n)|} = 0. \quad (7.7)$$

Since we are assuming a regular surface such that $|\mathbf{R}_u \times \mathbf{R}_v| \neq 0$, we need only set the numerator of equation (7.7) to zero. Thus,

$$|\mathbf{R}_{uu}(u, v_n) \quad \mathbf{R}_u(u, v_n) \quad \mathbf{R}_v(u, v_n)| = 0.$$

For a polynomial surface with degree n in the u direction, this results in a univariate polynomial equation of degree $(3n - 4)$ in u

$$(y_u z_v - z_u y_v)x_{uu} - (x_v z_u - x_u z_v)y_{uu} + (x_u y_v - x_v y_u)z_{uu} = 0. \quad (7.8)$$

If the surface is expressed in a piecewise polynomial form such as a B-spline representation, equation (7.8) must be applied to each polynomial segment separately. The univariate polynomial equation can be robustly and efficiently solved by the Interval Projected Polyhedron algorithm [24, 39]. Once we find the u value, we check if the nonzero principal curvature changes sign. If the sign does not change, the generator is not an inflection line. A simple example is given by $\mathbf{R}(u, v) = (u, v, u^4)$. Since

$$G = 1, \quad \mathbf{R}_{uu} = (0, 0, 12u^2) \quad \text{and} \quad \mathbf{N} = \frac{(-4u^3, 0, 1)}{\sqrt{16u^6 + 1}},$$

we have

$$\kappa^* = \frac{-12u^2}{\sqrt{16u^6 + 1}}.$$

It is apparent that κ^* becomes zero when $u = 0$; however κ^* does not change sign when u moves from $u < 0$ to $u > 0$. Therefore, $u = 0$ is not an inflection line.

At flat points the principal directions are indeterminate and the orthogonal net of lines of curvature may have singular properties. In the following we investigate the pattern of the lines of curvature near the line of non-generic flat points. Locally any surface is the graph of a differentiable function [8]. Given a point p of a surface S we can choose the coordinate axis so that the origin O of the coordinate is p and the z axis is directed along the positive normal of S at p ; thus, the xy plane coincides with the tangent plane of S at p . It follows that a neighborhood of p in S can be represented in the form $z = h(x, y)$ with $h(0, 0) = h_x(0, 0) = h_y(0, 0) = 0$.

By taking into consideration that $h(0, 0) = h_x(0, 0) = h_y(0, 0) = 0$, the Taylor expansion of the z component of the surface becomes

$$\begin{aligned} h(x, y) &= \frac{1}{2!}[x^2 h_{xx}(0, 0) + 2xy h_{xy}(0, 0) + y^2 h_{yy}(0, 0)] \\ &+ \frac{1}{3!}[x^3 h_{xxx}(0, 0) + 3x^2 y h_{xxy}(0, 0) + 3xy^2 h_{xyy}(0, 0) + y^3 h_{yyy}(0, 0)] \\ &+ R(x, y)(|x, y|^3) \end{aligned} \quad (7.9)$$

where $R(x, y)$ is a remainder term with $\lim_{x \rightarrow 0, y \rightarrow 0} R(x, y) = 0$ and $|x, y| = \sqrt{x^2 + y^2}$.

This local approximation will now be applied to developable surfaces.

Lemma 7.2.1 *A developable surface is, in general, locally a parabolic cylinder and becomes a cubic cylinder at the inflection line.*

Proof: Let us consider an orthogonal Cartesian reference frame attached to the surface at an arbitrary point (u_0, v_0) . We choose unit vectors $\frac{\mathbf{R}_v}{|\mathbf{R}_v|} \times \mathbf{N}$, $\frac{\mathbf{R}_v}{|\mathbf{R}_v|}$ and \mathbf{N} as the directions of x , y and z axes such that the y axis coincides with the generator $u = u_0$, the z axis coincides with the normal vector and the x axis is orthogonal to both axes. Equation (7.9) reduces to [32]

$$h(x, y) = \frac{1}{2}x^2 h_{xx}(0, 0) + \frac{1}{6}[x^3 h_{xxx}(0, 0) + 3x^2 y h_{xxy}(0, 0)] + R(x, y)(|x, y|^3). \quad (7.10)$$

Using the inverse function theorem, $h_{xx}(0, 0)$, $h_{xxx}(0, 0)$ and $h_{xxy}(0, 0)$ can be obtained as a function of u and v . At a the line of inflection, $h_{xx}(0, 0)$ and $h_{xxy}(0, 0)$ become zero [32], and equation (7.10) reduces to

$$h(x, y) = \frac{1}{6}(\mathbf{N} \cdot \mathbf{R}_{uuu}) \left(\sqrt{\frac{G}{EG - F^2}} \right)^3 x^3 + R(x, y)(|x, y|^3) \quad (7.11)$$

where the coefficient of x^3 is evaluated at (u_0, v_0) . From equation (7.10) it is apparent that for small x , the quadratic term dominates. From equation (7.11) it is apparent that at an inflection line, the surface is locally a cubic cylinder. ■

Theorem 7.2.2 *There is only one line of curvature that passes through each flat point on an inflection line, and that line of curvature is orthogonal to the direction of the generator.*

Proof: By Lemma 7.2.1 the developable surface is expressed locally as a cubic cylinder. If we rewrite the cubic term of equation (7.11) in terms of polar coordinates by substituting $x = r \cos \theta$ we obtain

$$h(\theta) = \frac{r^3}{6}(\mathbf{N} \cdot \mathbf{r}_{uuu}) \left(\sqrt{\frac{G}{EG - F^2}} \right)^3 \cos^3 \theta. \quad (7.12)$$

Since $h(\theta + \pi) = -h(\theta)$, $h(\theta)$ is an antisymmetric function of θ . The roots of $\frac{dh}{d\theta} = 0$ will give the angles where local maxima and minima of $h(\theta)$ may occur around the flat point. The equation can be restricted to the range $0 \leq \theta < 2\pi$ without loss of generality. The roots are easily computed as $\theta = 0, \frac{\pi}{2}, \pi$ and $\frac{3\pi}{2}$. Only $\theta = 0$ and $\theta = \pi$ (which coincide with the local x axis) give extrema, since

$$\frac{d^2 h \left(\frac{\pi}{2} \right)}{d\theta^2} = \frac{d^2 h \left(\frac{3\pi}{2} \right)}{d\theta^2} = 0$$

and thus $\theta = \frac{\pi}{2}$ and $\theta = \frac{3\pi}{2}$ (which coincide with the local y axis) provide neither a maximum nor a minimum. In other words, the inflection line is not a line of curvature. Consequently, there is only one line of curvature (minimum curvature where $\theta = 0$ and maximum curvature where $\theta = \pi$) that passes through the flat point. ■

Recall from Section 2.3 that the principal curvatures can be found by solving the two simultaneous equations (2.19) and (2.20),

$$\begin{aligned}(L + \kappa E)du + (M + \kappa F)dv &= 0 \\ (M + \kappa F)du + (N + \kappa G)dv &= 0,\end{aligned}$$

for κ . Since $M = N = 0$, equations (2.19) and (2.20) reduce to

$$(L + \kappa E)du + \kappa Fdv = 0 \quad \text{and} \quad (7.13)$$

$$\kappa Fdu + \kappa Gdv = 0. \quad (7.14)$$

We can trace the lines of curvature which pass through the flat points of an inflection line by providing the starting points and shifting outwards in the directions 0 and π from the flat points or, equivalently, along the positive and negative local x axis. The tracing can be carried out by integrating the initial value problem for the coupled ordinary differential equations (7.13) and (7.14).

Generic umbilics (including flat points) are stable with respect to small perturbations of the function representing the surface, while non-generic ones are unstable [32]. In generic cases umbilics are isolated [20]; thus the inflection line, which consists of line of flat points, is non-generic and therefore unstable. In the following we give a couple of numerical examples that demonstrate the instability of the line of flat points along the inflection line with respect to perturbations.

The example surface is a degree (3-1) integral Bézier patch which is constructed by the method described in Section 5.3, see Figure 7-1. The control points are shown in Table 7.1. The surface has an inflection line at $u = 0.5754$, which has been computed by solving the

$\mathbf{P}_{0,0}$	(0.0000, 0.0000, 0.0000)	$\mathbf{P}_{0,1}$	(0.5000, 0.0000, 2.0000)
$\mathbf{P}_{1,0}$	(1.8000, 3.0000, 0.0000)	$\mathbf{P}_{1,0}$	(1.8950, 2.3250, 2.0000)
$\mathbf{P}_{2,0}$	(3.3000,-2.0000, 1.5000)	$\mathbf{P}_{2,0}$	(3.0575,-1.5500, 3.1625)
$\mathbf{P}_{3,0}$	(4.0000, 0.0000, 0.0000)	$\mathbf{P}_{3,0}$	(3.6000, 0.0000, 2.0000)

Table 7.1: Control Points for a Degree (3,1) Developable Surface

degree 5 univariate polynomial equation (7.8). The inflection line is shown in Figure 7-1 with a dash dotted line. This surface has a net of lines of curvature which is shown in Figure 7-2(a). Solid lines represent the lines of maximum principal curvature, while dotted lines represent the lines of minimum principal curvature. The inflection line is depicted with a dash dotted line. Figure 7-2(b) shows a magnification near the inflection line. We can observe that there is only one line of curvature that passes through a flat point orthogonal to the inflection line.

We gradually perturb the control points of the surface and observe the behavior of the lines of curvature which pass through the inflection line. The control points are perturbed in the following manner. Since the example is a degree (3-1) patch, it has 8 control points. Each control point consists of three Cartesian coordinates x , y , z ; hence there are 24 components to be perturbed. A random number which varies from -1 to 1 is used to determine the perturbation of each component. Let us denote the randomly chosen numbers for each control point as $(e_{ij}^x, e_{ij}^y, e_{ij}^z)$, $0 \leq i, j \leq 3$. We normalize the vector and add it to each

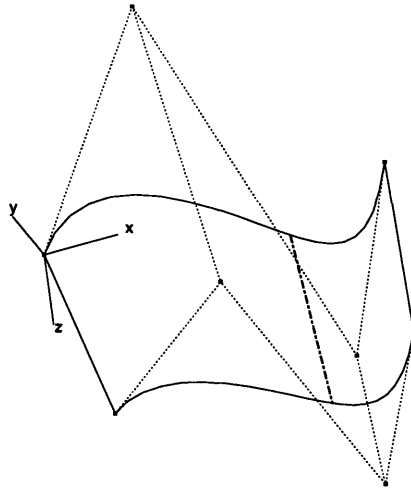


Figure 7-1: Developable surface and its control polyhedron with inflection line.

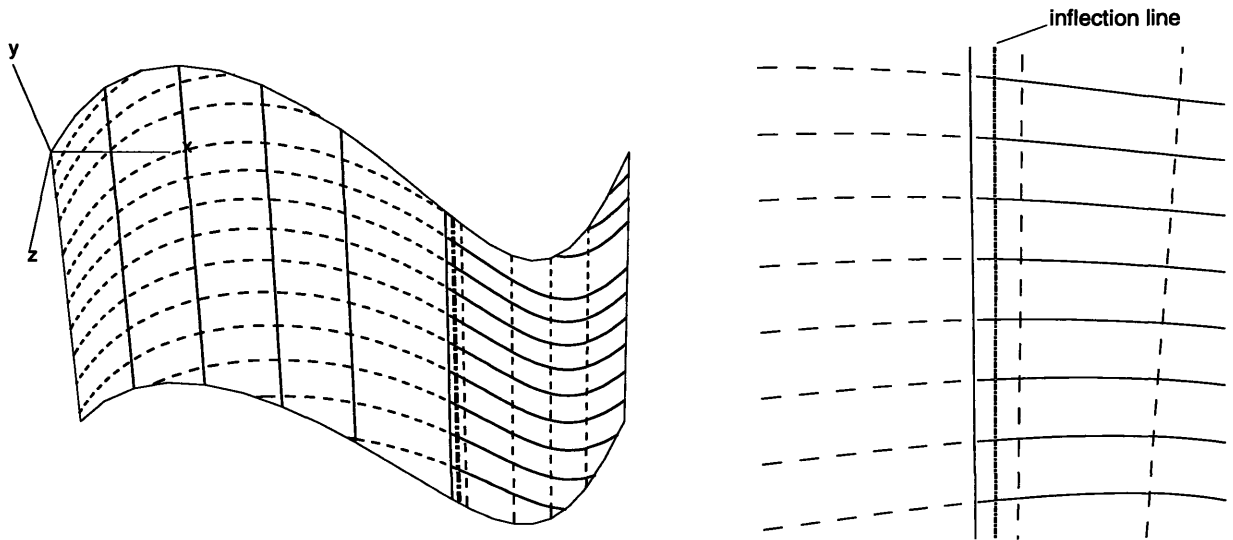


Figure 7-2: (a) Lines of curvature of developable surface with inflection. (b) Magnification near inflection line.

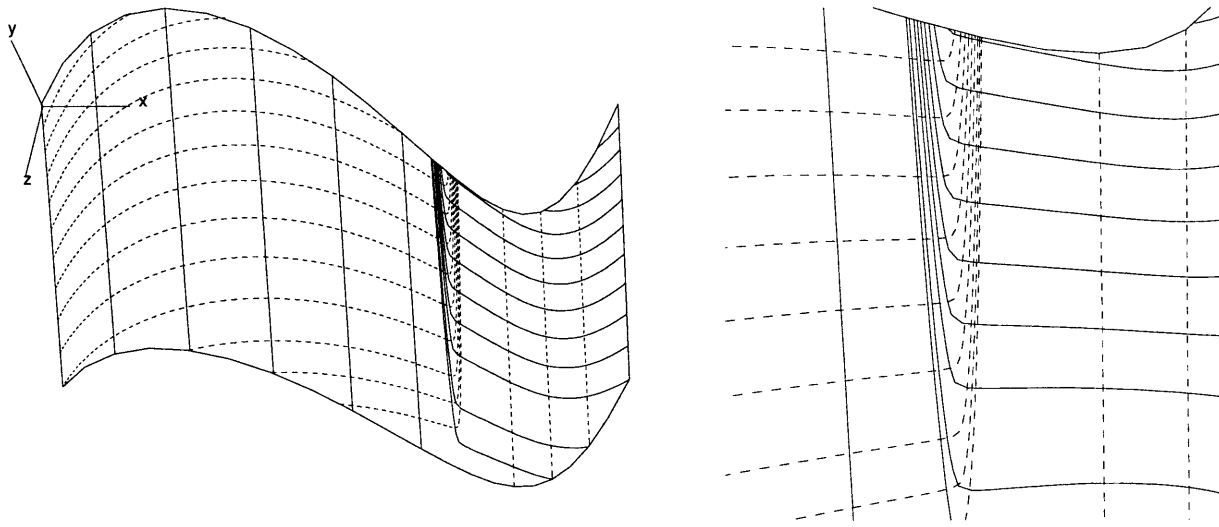


Figure 7-3: (a) Lines of curvature on perturbed surface $\zeta = 0.02$. (b) Magnification near $u=0.57$.

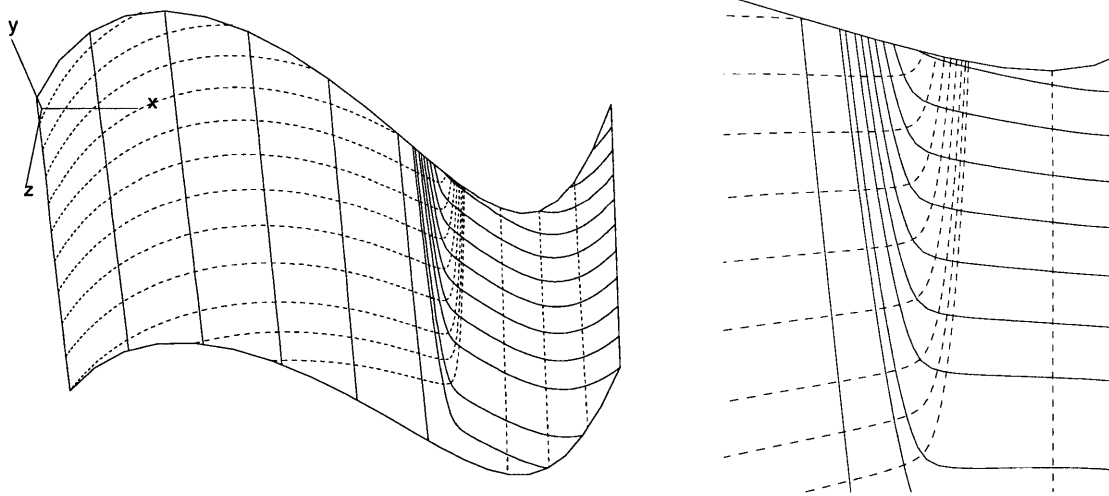


Figure 7-4: (a) Lines of curvature on perturbed surface $\zeta = 0.08$ (b) Magnification near $u=0.57$.

control point as follows:

$$\tilde{\mathbf{P}}_{ij} = \mathbf{P}_{ij} + \zeta \frac{[e_{ij}^x, e_{ij}^y, e_{ij}^z]}{\sqrt{e_{ij}^{x,2} + e_{ij}^{y,2} + e_{ij}^{z,2}}} \quad (7.15)$$

where $\zeta = 0.02$. We gradually increase the perturbation by increasing ζ from 0.02 to 0.08 in steps of 0.02.

Figures 7-3 and 7-4 illustrate the behavior of the lines of curvature when the control points are perturbed. We can see from the figures that the entire inflection line, which consists of a line of flat points, disappears. Hence there is no singularity in the net of lines of curvature when a perturbation is induced. The nonzero principal curvatures on both sides of the former inflection line ² meet at right angles near the former inflection line and make a very sharp change in direction (almost a right angle).

²Once the control points are perturbed both principal curvatures may not be nonzero, but here we are referring to the nonzero principal curvature before perturbation.

Chapter 8

Engineering Example

The final example is the design of a small boat using B-spline developable surfaces. The boat was designed with a hard chine which separates the bottom and side of the boat and demarks a tangent discontinuity in the hull of the boat. As an initial stage of the design, the following three curves, which define the desired characteristics of the hull, were determined using a model of a planing boat:

- sheer curve – the line that runs along the deck edge from bow to stern
- base curve – the line that runs along the keel of the boat (centerline from bow to stern)
- chine curve – the line that runs from the bow to the lower corner of the stern

Figure 8-1 shows the terminology used in this section. The coordinate system is located so that the origin is located on the baseline at the bow of the boat with the x axis pointing aft, the y axis pointing to starboard and the z axis pointing up. (Note that the baseline, a zero reference line, is different from the base curve defined above.) Due to the symmetry of the boat, we design only the starboard side and reflect those values across the plane of symmetry to obtain the port side. The cubic B-spline representation of the three curves is shown in Table 8.1.

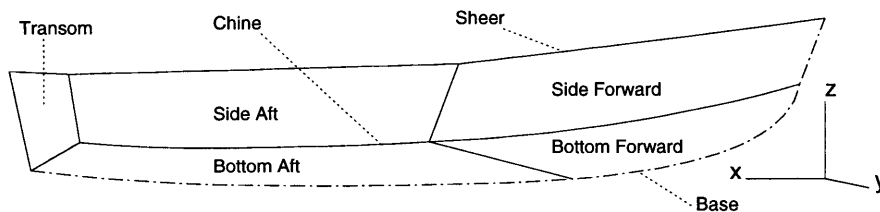


Figure 8-1: Planing Boat Terminology

Design Using 3D Directrices

Employing the design philosophy described in Chapter 5, the chine curve was designated as the design curve and the sheer and base curves as target curves, i.e. $\mathbf{r}_B(u)$, to construct

	Sheer Curve	Chine Curve	Base Curve
Control Points	(0.00, 0.00, 9.00)	(1.40, 0.00, 5.30)	(1.40, 0.00, 5.30)
	(6.86, 7.10, 8.22)	(10.5, 7.53, 1.93)	(2.26, 0.00, -0.21)
	(21.6, 8.93, 6.25)	(25.7, 7.85, 1.28)	(22.6, 0.00, -0.10)
	(36.9, 8.73, 5.86)	(40.4, 7.46, 1.27)	(36.3, 0.00, -0.10)
	(45.0, 7.65, 6.10)	(44.1, 7.20, 1.70)	(44.1, 0.00, 0.50)
Knot Vectors	0, 0, 0, 0, .5, 1, 1, 1, 1	0, 0, 0, 0, .75, 1, 1, 1, 1	0, 0, 0, 0, .5, 1, 1, 1, 1

Table 8.1: Target Curve Data

the side and bottom respectively. Initially, the endpoints of the sheer and base curves were used to construct the side and bottom of a single surface each; however, this resulted in a flat side and bottom. To remedy this situation, the chine was split into two B-spline curves at a parameter value of $u = 0.5$, and one additional knot was inserted at the midpoint of the forward B-spline curve. The resulting curves are shown in Table 8.2. Thus, the side and bottom are constructed of two surfaces each, allowing more flexibility in the design, but losing the C^2 continuity along the surface. The surfaces are, however, at least G^1 continuous between the forward and aft portions. Since the design curve was split into two curves that maintain C^2 continuity between them, the tangent at the connecting point is continuous. Since both patches are developable, both surfaces share the same tangent plane at the connecting generator. Hence, the patches are G^1 continuous.

Note that the forward and aft surfaces join along a generator which is a straight line. The planar transom (stern) joins the aft surfaces along generators as well.

The endpoints for the side and bottom surfaces were selected so as to force the resulting directrix as close to the target curves as possible while maintaining a maximum Gaussian curvature on the order of 10^{-5} . The data for each developable surface on the starboard side of the boat is listed in Table 8.2. Measurements are in feet. The port side of the boat has the same measurements, with a negative y value.

Patch	Design Curve Control Points	Knot Vector	Endpoints	Plane Definition Point	Gaussian Curvature
Forward Side	(1.40, 0.00, 5.30)	0, 0, 0, 0 0.5	(0.00, 0.00, 9.00)	(20.0, 0.00, 6.74)	8.18×10^{-5}
	(4.17, 2.32, 4.26)		(20.0, 8.30, 6.74)		
Forward Bottom	(10.7, 5.86, 2.56)	1, 1, 1, 1	(1.40, 0.00, 5.30)	(0.00, 0.00, 0.00)	0.00
	(18.2, 7.09, 1.87)		(14.0, 0.00, 0.00)		
	(21.9, 7.38, 1.66)				
Aft Side	(21.9, 7.38, 1.66)	0, 0, 0, 0 0.5	(20.0, 8.30, 6.74)	(45.0, 0.00, 6.10)	6.62×10^{-5}
	(25.6, 7.67, 1.44)		(45.0, 7.70, 6.10)		
Aft Bottom	(33.0, 7.66, 1.28)	1, 1, 1, 1	(14.0, 0.00, 0.00)	(0.00, 0.00, 0.00)	9.74×10^{-6}
	(40.4, 7.46, 1.27)		(44.1, 0.00, 0.50)		
	(44.1, 7.20, 1.70)				

Table 8.2: Developable Surface Data, Starboard Side

Constrained by Plane

All the second directrices were constrained so that they lie in a plane defined by the two designated endpoints of $\mathbf{r}_B(u)$ and a third point g provided by the user. This point g is termed the Plane Definition Point and is shown in Table 8.2. For the bottom surfaces, the constraining plane was the xz -plane which divides the boat into symmetric halves. For the side surfaces, the constraining plane was positioned so that a line in the plane and perpendicular to the x axis would be parallel to the xy plane.

Figure 8-2 shows the resulting developable surfaces with the design lines shown as dotted lines for reference. Note that the forward portion of the bottom of the boat is a triangular degenerate patch. Figure 8-3 is a bottom view of the boat. One side shows the rulings of the developable surfaces while the other side is a shaded view.

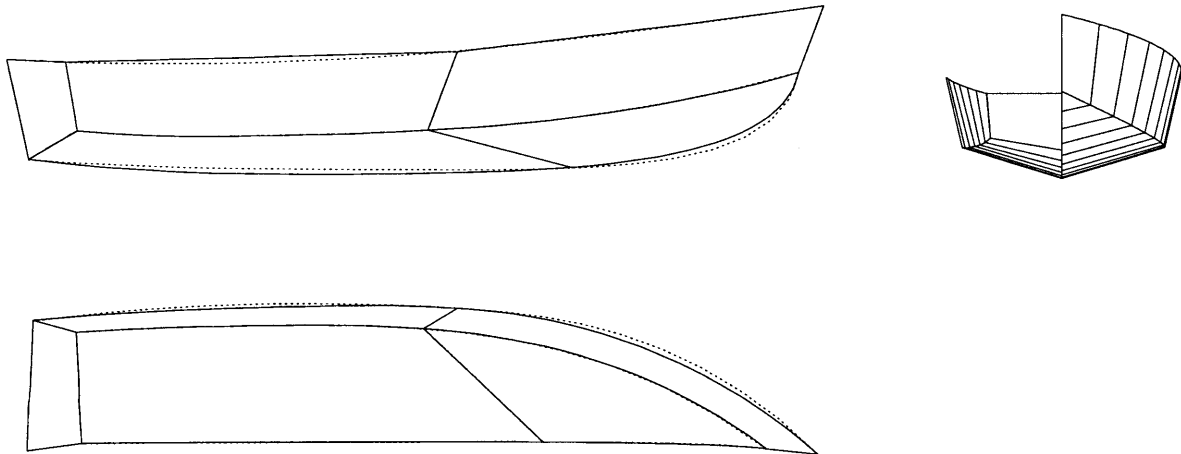


Figure 8-2: Boat Composed of Developable Degree (3-1) B-Spline Surfaces

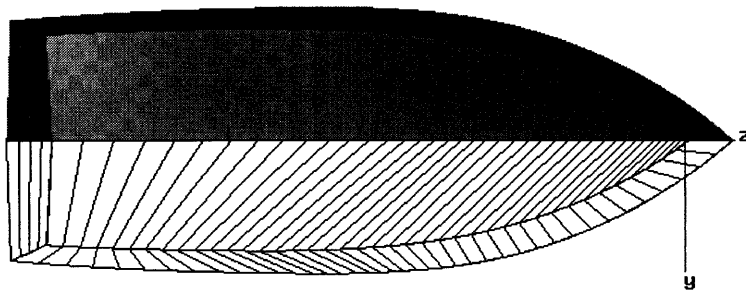


Figure 8-3: Boat Bottom View

Development

The plane development of each surface of the boat was computed, thus providing cutting information for the flat steel. Using the method described in Section 5.4, the planar surfaces shown in Figure 8-4 were constructed. All developments were within a tolerance of 10^{-6} .

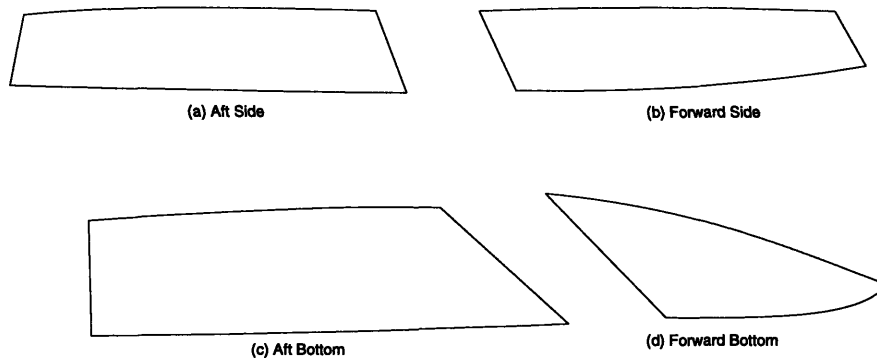


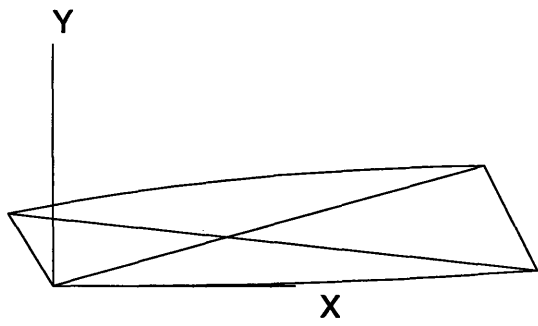
Figure 8-4: Boat Surfaces Developed onto a Plane

Geodesics

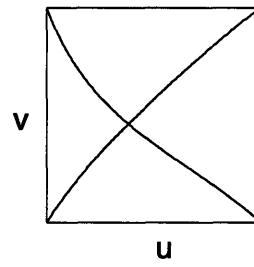
At the Electric Boat Corporation shipyard, many developable surfaces are used in the construction of submarines, since a large portion of the hull is cylindrical. When bending the steel into shape, accuracy is checked with detailed measurements of geodesics drawn on the surface. When the surface is flat, straight lines are drawn between the corners of the surface, forming an X as shown in Figure 8-5(a). The position of this line on the curved surface is easily computed using the method described in Chapter 6. As an example, the geodesics on the Forward Side section have been calculated. The uv parameter values are shown in Figure 8-5(b) and the geodesics on the developable surface are shown in Figure 8-5(c).

Lines of Curvature

These surfaces have no inflection lines, but the lines of curvature were calculated as described in Chapter 7 and are shown in Figure 8-6. The dashed lines represent lines of minimum curvature and the solid lines are lines of maximum curvature. Note that one set is always composed of straight lines that correspond to the generators.



(a) Surface Developed onto Plane



(b) uv Parametric Space



(c) Geodesic on 3D Surface

Figure 8-5: Geodesics on the Forward Side Section

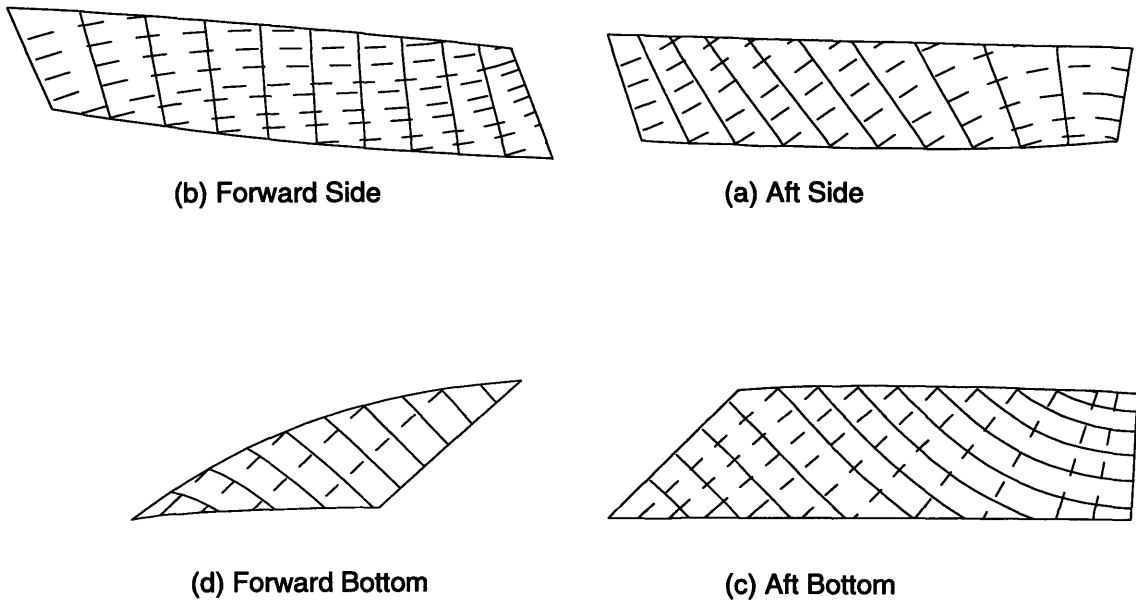


Figure 8-6: Lines of Curvature on Boat Surfaces (Solid Lines are Maximum Curvature Lines, Dashed Lines are Minimum Curvature Lines)

Chapter 9

Conclusions and Recommendations

9.1 Conclusions

In this thesis a novel method to design complex objects in terms of B-spline developable surfaces focusing on user friendliness is developed. The user only needs to specify the design B-spline curve and the two end rulings, and the developable surface in a B-spline representation is automatically generated. Although optimization techniques are relied upon, in most cases the computed results have a Gaussian curvature on the order of 10^{-5} or less unless the design of a very complex surface is attempted. The computational time for the design of all the examples in this thesis is on the order of a few tenths of seconds on a 100 MHz Silicon Graphics workstation.

In addition, two differential geometry properties of developable surfaces which have practical engineering applications were investigated. The first property was the definition of inflection lines on developable surfaces, which are critical in the manufacture of such surfaces. We proved that an inflection line on a developable surface occurs on a generator which consists of entirely flat points, and derived a single variable nonlinear polynomial equation to locate it. It was also found that for each flat point on an inflection line of a developable surface, there is only one line of curvature that passes through it, and that line of curvature is orthogonal to the direction of the generator.

The second differential geometry property investigated was the location of geodesics between two points on a developable surface. It was shown that the problem can always be converted from a boundary value problem to an initial value problem with a corresponding savings in time for the solution.

Finally, these techniques were applied to a boat model, a complex object that was represented entirely with B-spline approximate developable surfaces with cubic directrices. The Gaussian curvature was on the order of 10^{-5} . Geodesics and lines of curvature were calculated on these surfaces as well.

9.2 Future Work

The ultimate goal of this research is to be a useful tool in the design and manufacturing of ship hulls. Therefore, future research should take this work in that direction. Some specific areas of possible research are described below.

Approximation. The approximation of free form surfaces by developable surfaces would be extremely helpful in converting existing ship designs to ones including more developable

surfaces. Some preliminary research has been completed by Elber and Cohen [9] into representing surfaces as ruled surfaces, which could possibly be extended to include developable surfaces. In addition, research on approximation using developable surfaces was conducted by Hoschek and Pottmann [23] using the representation of developable surfaces as the envelope of a family of planes. Alternatively, Cho [6] discussed the approximate development of non-developable doubly curved surfaces onto a plane, which may also be useful in the above approximation problem.

Manufacturing. Once the surface is developed into a plane and the steel is cut to the correct size, it must be bent into the proper shape. Additional research should investigate the proper amount of curvature to be induced by rolling or pressing and instructions for the shop floor should be output. Although the lines of curvature are instrumental in this bending, mechanical considerations such as springback must be included in the design as well. Much research has been done in this area by Hardt et al [19, 18, 17]. The ultimate goal is for the engineer to design the ship hull and output information that is directly useful to the workers on the shop floor. To this end, the operating characteristics of bending equipment should be studied and properly accounted for.

Geometry. Several areas of interest remain for investigation within the differential geometry discussed in this thesis. First, a suitable non-dimensional Gaussian curvature expression should be developed to better judge the developability of surfaces designed using the minimization process described in Section 5.3.

Although strip surfaces of any degree can be handled by the computer programs developed during this research, the programs for the surfaces with arbitrary 3D directrices can handle only B-spline developable surfaces with cubic directrices. It may be beneficial to investigate higher degree surfaces which may include more flexibility and would be able to more closely approximate the desired output surface.

In addition, the surfaces in this thesis are all integral B-spline surfaces. Extension to include rational B-spline developable surfaces such as those investigated by Pottmann and Farin [37] and Lang and Röschel [29] would allow the representation of more complex surfaces.

One difficulty in designing surfaces using this method is that, for surfaces with 3d directrices, there is no method to determine in advance if the surface will include the edge of regression. Therefore, regular surfaces are achieved through trial and error, and hence regularity conditions should be investigated more fully.

Design. Much research has been conducted in design for producibility in ship hulls. For example, Lamb [27] shows a method to construct a bulbous bow from regular surfaces and discusses the simplification of bow and stern sections to include more developable surfaces. This should be expanded to investigate the design of an entire ship hull from developable surfaces. Once a ship hull is designed, it should be hydrodynamically tested to compare the performance to a similar hull that is not constructed of developable surfaces. The relative magnitude of the savings due to producibility and the losses due to performance should be compared.

Bibliography

- [1] G. Aumann. Interpolation with developable Bézier patches. *Computer Aided Geometric Design*, 8:409–420, 1991.
- [2] G. Aumann. A closer look at developable Bézier surfaces. *Journal of Theoretical Graphics and Computing*, 7:12–26, June 1994.
- [3] R. M. C. Bodduluri and B. Ravani. Design of developable surfaces using duality between plane and point geometries. *Computer Aided Design*, 25:621–632, 1993.
- [4] W. Boehm. Inserting new knots into B-spline curves. *Computer Aided Design*, 12(4):199–201, 1980.
- [5] W. Boehm. Subdividing multivariate splines. *Computer Aided Design*, 15(6):345–352, November 1983.
- [6] W. Cho. *Topologically Reliable Approximation of Curves and Surfaces*. PhD thesis, Massachusetts Institute of Technology, Cambridge, MA, January 1997.
- [7] J. C. Clements and L. J. Leon. A fast, accurate algorithm for the isometric mapping of a developable surface. *SIAM Journal of Mathematical Analysis*, 4:966–971, July 1987.
- [8] P. M. do Carmo. *Differential Geometry of Curves and Surfaces*. Prentice-Hall, Inc., Englewood Cliffs, New Jersey, 1976.
- [9] G. Elber and E. Cohen. Second-order surface analysis using hybrid symbolic and numeric operators. *ACM Transactions on Graphics*, 12(2):160–178, April 1993.
- [10] R. T. Farouki and V. T. Rajan. Algorithms for polynomials in Bernstein form. *Computer Aided Geometric Design*, 5:1–26, 1988.
- [11] I. D. Faux and M. J. Pratt. *Computational Geometry for Design and Manufacture*. Ellis Horwood, Chichester, England, 1981.
- [12] J. H. Ferziger. *Numerical Methods for Engineering Applications*. Wiley, 1981.
- [13] R. Fletcher. *Practical Methods of Optimization*. A Wiley-Interscience Publication, 1987. Second Edition.
- [14] W. H. Frey and D. Bindschadler. Computer-aided design of a class of developable Bézier surfaces. R&D Publication 8057, General Motors, September 1993.
- [15] P. E. Gill, W. Murray, and A. Wright. *Practical Optimization*. Academic Press, New York, 1981.

- [16] B. Gurunathan and S. G. Dhande. Algorithms for development of certain classes of ruled surfaces. *Computers and Graphics*, 11(2):105–112., 1987.
- [17] D. E. Hardt, M. C. Boyce, K. B. Ousterhour, and A. Karafillis. A flexible forming for sheet metal. Industrial Liaison Program LMP-91-058, Massachusetts Institute of Technology Laboratory for Manufacturing and Productivity, Cambridge, MA, March 1991.
- [18] D. E. Hardt and M. Hale. Closed loop control of a roll straightening process. *Annals of CIRP*, 1984.
- [19] D. E. Hardt, M. A. Roberts, and K. A. Stelson. Closed loop shape control of a roll bending process. *Transactions of ASME, Journal of Dynamic Systems*, 4:104, 1982.
- [20] D. Hilbert and S. Cohn-Vossen. *Geometry and the Imagination*. Chelsea, New York, 1952.
- [21] D. H. Hoitsma. Surface curvature analysis. In M. J. Wozny et al., editors, *IFIP TC5/WG5.2 Second Workshop on Geometric Modeling*, pages 21–38, New York, 1988. IFIP, North Holland.
- [22] J. Hoschek and D. Lasser. *Fundamentals of Computer Aided Geometric Design*. A. K. Peters, Wellesley, MA, 1993. Translated by L. L. Schumaker.
- [23] J. Hoschek and H. Pottmann. Interpolation and approximation with developable B-spline surfaces. In M. Daehlen et al., editors, *Mathematical Methods for Curves and Surfaces*. Vanderbilt University Press, Nashville, TN, 1995.
- [24] C.-Y. Hu, T. Maekawa, E. C. Sherbrooke, and N. M. Patrikalakis. Robust interval algorithm for curve intersections. *Computer Aided Design*, 28(6/7):495–506, June/July 1996.
- [25] H. B. Keller. *Numerical Methods for Two-Point Boundary Value Problems*. Blaisdell, 1968.
- [26] E. Kreyszig. *Differential Geometry*. University of Toronto Press, Toronto, 1959.
- [27] T. Lamb. *Engineering for Ship Production, NSRP #0219, UMTRI #72960*. 1986.
- [28] T. Lamb. Shell development computer aided lofting - is there a problem or not? *Journal of Ship Production*, 11(1):34–46, 1995.
- [29] J. Lang and O. Röschel. Developable (1,n) Bézier surfaces. *Computer Aided Geometric Design*, 9:291–298, 1992.
- [30] T. Maekawa. Computation of shortest paths on free-form parametric surfaces. *Journal of Mechanical Design, ASME Transactions*, 118(4):499–508, December 1996.
- [31] T. Maekawa and N. M. Patrikalakis. Interrogation of differential geometry properties for design and manufacture. *The Visual Computer*, 10(4):216–237, March 1994.
- [32] T. Maekawa, F.-E. Wolter, and N. M. Patrikalakis. Umbilics and lines of curvature for shape interrogation. *Computer Aided Geometric Design*, 13(2):133–161, March 1996.

- [33] F. C. Munchmeyer and R. Haw. Applications of differential geometry to ship design. In D. F. Rogers, B. C. Nehring, and C. Kuo, editors, *Proceedings of Computer Applications in the Automation of Shipyard Operation and Ship Design IV*, volume 9, pages 183–196, Annapolis, Maryland, USA, June 1982.
- [34] O. Nørskov-Lauritsen. Practical application of single curved hull definition - background, application, software and experience. In P. Banda and C. Kuo, editors, *Computer Applications in the Automation of Shipyard Operation and Design V*, volume 11, pages 485–491. Elsevier Science, North Holland, NY, September 1985.
- [35] Numerical Algorithms Group, Oxford, England. *NAG Fortran Library Manual, Mark 16, FLSG516D, Silicon Graphics (IRIX 5) Double Precision User's Notes*, 1994.
- [36] L. Piegl and W. Tiller. *The NURBS Book*. Springer, 1995.
- [37] H. Pottmann and G. Farin. Developable rational Bézier and B-spline surfaces. *Computer Aided Geometric Design*, 12(5):513, 1995.
- [38] W. H. Press et al. *Numerical Recipes in C*. Cambridge University Press, 1988.
- [39] E. C. Sherbrooke and N. M. Patrikalakis. Computation of the solutions of nonlinear polynomial systems. *Computer Aided Geometric Design*, 10(5):379–405, October 1993.
- [40] M. Spivak. *Calculus*. New York: W. A. Benjamin, Inc., 1967.
- [41] D. J. Struik. *Lectures on Classical Differential Geometry*. Addison-Wesley, Cambridge Mass., 1950.
- [42] W. Tiller. Knot-removal algorithms for NURBS curves and surfaces. *Computer Aided Design*, 24(8):445–453, August 1992.
- [43] F.-E. Wolter and S. T. Tuohy. Curvature computations for degenerate surface patches. *Computer Aided Geometric Design*, 9(4):241–270, September 1992.
- [44] F. Yamaguchi. *Curves and Surfaces in Computer Aided Geometric Design*. Springer-Verlag, NY, 1988.